

การรวมและการยัดติดยของวัสดุที่มีสมบัติการเปลี่ยนสีเพื่อใช้งานด้านการตรวจวัด

นายเจตพงษ์ กล้าหาญ

วิทยานิพนธ์นี้เป็นส่วนหนึ่งของการศึกษาตามหลักสูตรปริญญาวิทยาศาสตรมหาบัณฑิต
สาขาวิชาปิโตรเคมีและวิทยาศาสตร์พอลิเมอร์
คณะวิทยาศาสตร์ จุฬาลงกรณ์มหาวิทยาลัย
ปีการศึกษา 2556

ลิขสิทธิ์ของจุฬาลงกรณ์มหาวิทยาลัย
บทคัดย่อและแฟ้มข้อมูลฉบับเต็มของวิทยานิพนธ์ตั้งแต่ปีการศึกษา 2554 ที่ให้บริการในคลังปัญญาจุฬาฯ (CUIR)
เป็นแฟ้มข้อมูลของนิสิตเจ้าของวิทยานิพนธ์ที่ส่งผ่านทางบัณฑิตวิทยาลัย

The abstract and full text of theses from the academic year 2011 in Chulalongkorn University Intellectual Repository (CUIR)
are the thesis authors' files submitted through the Graduate School.

INCORPORATION AND DEPOSITION OF MATERIALS WITH CHROMISM
PROPERTIES FOR SENSING APPLICATIONS

Mr. Jadetapong Klahan

A Thesis Submitted in Partial Fulfillment of the Requirements
for the Degree of Master of Science Program in Petrochemistry and Polymer Science

Faculty of Science

Chulalongkorn University

Academic Year 2013

Copyright of Chulalongkorn University

Thesis Title INCORPORATION AND DEPOSITION OF MATERIALS
 WITH CHROMISM PROPERTIES FOR SENSING
 APPLICATIONS

By Mr. Jadetapong Klahan

Field of Study Petrochemistry and Polymer Science

Thesis Advisor Associate Professor Mongkol Sukwattanasinitt, Ph.D.

Thesis Co-advisor Assistant Professor Boonchoat Paosawatyanong, Ph.D.

Accepted by the Faculty of Science, Chulalongkorn University in Partial Fulfillment of
the Requirements for the Master's Degree

.....Dean of the Faculty of Science
(Professor Supot Hannongbua, Dr.rer.nat.)

THESIS COMMITTEE

.....Chairman
(Assistant Professor Warinthorn Chavasiri, Ph.D.)

.....Thesis Advisor
(Associate Professor Mongkol Sukwattanasinitt, Ph.D.)

.....Thesis Co-advisor
(Assistant Professor Boonchoat Paosawatyanong, Ph.D.)

.....Examiner
(Assistant Professor Varawut Tangpasuthadol, Ph.D.)

.....External Examiner
(Nakorn Niamnont, Ph.D.)

เจตพจน์ กล่าวหาญ : การรวมและการยึดติดของวัสดุที่มีสมบัติการเปลี่ยนสีเพื่อใช้งานด้านการตรวจวัด (INCORPORATION AND DEPOSITION OF MATERIALS WITH CHROMISM PROPERTIES FOR SENSING APPLICATIONS) อ.ที่ปรึกษาวิทยานิพนธ์หลัก : รศ.ดร.มงคล สุขวัฒนาศินินิทธิ, อ.ที่ปรึกษาวิทยานิพนธ์ร่วม : ผศ.ดร.บุญโชติ เผ่าสวัสดิ์ชัยรยง, 121 หน้า.

วิทยานิพนธ์ได้แบ่งเป็น 2 หัวข้อคือ 1) วิธีการยึดติดไดอะเซทิลีนและเทอร์มอโครมิกชนิดลิวโคบนพื้นผิว และ 2) เทคนิคการรวมพลาสติกกับเทอร์มอโครมิกชนิดลิวโค ได้รายงานถึงวิธีการยึดติดไดอะเซทิลีนและเทอร์มอโครมิกชนิดลิวโคบนพื้นผิวโดยใช้ 3 วิธีการ คือ วิธีการพิมพ์ติดด้วยเครื่องพิมพ์อิงค์เจท วิธีการพันติดด้วยแอร์บรัช และวิธีการเคลือบติดด้วยการจุ่มเคลือบ วิธีการทั้งสามนี้สามารถใช้ยึดติดไดอะเซทิลีนมอนอเมอร์ (PCDA และ TCDA) ลงบนพื้นผิวของแต่ละวัสดุด้วยลักษณะพิเศษของแต่ละเทคนิควิธี โดยเครื่องพิมพ์อิงค์เจทสามารถสร้างลวดลายไดอะเซทิลีนที่ผ่านการออกแบบด้วยคอมพิวเตอร์ลงบนพื้นผิวบนวัสดุแบบบางเช่นกระดาษได้เป็นอย่างดี วิธีการพันด้วยแอร์บรัชจะให้สีที่เข้มและเนื่องจากการใช้งานได้หลากหลาย ไม่ยุ่งยาก มีการใช้งานได้อย่างยืดหยุ่นและไม่จำเป็นต้องใช้สารละลายเข้าช่วย จึงเหมาะสมในการนำมาช่วยพัฒนาสร้างเป็นแถบบอกเวลาให้ตัวตรวจวัดความชื้น การจุ่มเคลือบถือเป็นวิธีการเคลือบสารลงบนวัสดุ ที่เรียบง่าย ไม่ซับซ้อน จึงนำมาประยุกต์ใช้ในบางขั้นตอนเพื่อพัฒนาตัวตรวจวัดความชื้น ในหัวข้อเทคนิคการรวมพลาสติกกับเทอร์มอโครมิกชนิดลิวโค ได้กล่าวถึง 3 กระบวนการวิธี คือ กระบวนการปั่นเส้นใยแบบหลอมเหลว กระบวนการอัด และกระบวนการบดผสมยางแบบสองลูกกลิ้ง ได้ทำการผสมเทอร์มอโครมิกชนิดลิวโค (Chameleon-T powder) ที่อัตราส่วนต่างๆ ลงในพอลิเมอร์ชนิดต่างๆ โดยใช้เทอร์มอโครมิกชนิดลิวโคปริมาณ 2% ผสมลงในพลาสติกชนิดพอลิโพรพิลีนด้วยกระบวนการปั่นเส้นใยแบบหลอมเหลว เทอร์มอโครมิกชนิดลิวโคปริมาณ 3% ผสมลงในพลาสติกชนิดพอลิเอทิลีนชนิดความหนาแน่นต่ำ พอลิโพรพิลีนและพอลิสไตรีน ด้วยกระบวนการอัด และเทอร์มอโครมิกชนิดลิวโคปริมาณ 5% ผสมลงในยางสังเคราะห์ ชนิดสไตรีนบิวตะไดอิน ด้วยกระบวนการบดผสมยางแบบสองลูกกลิ้งร่วมกับกระบวนการอัด พบว่าสมบัติในการเปลี่ยนสีโดยความร้อนของเทอร์มอโครมิกชนิดลิวโคยังคงอยู่ อย่างไรก็ตาม ยังคงมีความจำเป็นที่จะต้องศึกษาค้นคว้าถึงสภาวะต่าง ๆ ที่จะก่อให้เกิดประสิทธิภาพที่เหมาะสมที่สุดสำหรับแต่ละเทคนิคก่อนการนำไปใช้งาน เพื่อเตรียมเป็นผลิตภัณฑ์ตรวจวัดอุณหภูมิที่สามารถใช้งานได้จริงต่อไป

สาขาวิชา ปิโตรเคมีและวิทยาศาสตร์พอลิเมอร์ ลายมือชื่อนิสิต.....
 ปีการศึกษา.....2556..... ลายมือชื่อ อ.ที่ปรึกษาวิทยานิพนธ์หลัก.....
 ลายมือชื่อ อ.ที่ปรึกษาวิทยานิพนธ์ร่วม.....

5372487523 : MAJOR PETROCHEMISTRY AND POLYMER SCIENCE

KEYWORDS : POLYDIACETYLENE / LEUCO DYE / THERMOCHROMISM /
SOLVATOCHROMISM / HUMIDITY / RGB / AIRBRUSH / PRINTING

JADETAPONG KLAHAN : INCORPORATION AND DEPOSITION OF
MATERIALS WITH CHROMISM PROPERTIES FOR SENSING
APPLICATIONS. ADVISOR : ASSOC. PROF. MONGKOL
SUKWATTANASINITT, Ph.D., CO-ADVISOR : ASST. PROF.
BOONCHOAT PAOSAWATYANYONG , Ph.D., 121 pp.

This thesis deals with two topics: 1) surface deposition of diacetylene and leuco dye and 2) techniques for incorporation of leuco dyes into commercial polymers. For surface deposition, three techniques *i.e.* inkjet printing, airbrush painting and dip coating are evaluated. These three techniques can be used to deposit diacetylene monomers (PCDA and TCDA) onto surface of various solid materials with different advantages and limitations. While the ink-jet printing is good for deposition with computer-aided designed patterns on surfaces of thin sheet materials, the airbrush painting can give more intense color and more convenient to be used in the early development stage due to its greater operating flexibility and hassle-free ink formulation in comparison with the ink-jet technique. The dip coating is the most simple deposition technique to be used in the earliest step for the development of humidity indicators. With the subsequence use of airbrush painting, the time-humidity indicator prototypes are successfully developed. For the incorporation of leuco dyes into commercial polymers, three techniques *i.e.* melt spinning, compression molding and two roll mill processes can be used. The commercial thermochromic Chameleon-T powder is incorporated into several commercial polymers with retained reversible thermochromic properties. Various dye contents of 2, 3 and 5% can be incorporated into PP fiber filaments, LDPE, PP and PS plastic plates and SBR rubber plates by the melt spinning, compression molding and two roll mill combined with compression molding process, respectively. However, further investigation is required to optimize these incorporation techniques before they can be used in preparation of real temperature sensing plastic products.

Field of Study : Petrochemistry and Polymer Science Student's Signature

Academic Year : 2013 Advisor's Signature

Co-advisor's Signature

ACKNOWLEDGEMENTS

First of all, I would like to express my appreciation to my thesis advisor, Associated Professor Dr. Mongkol Sukwattanasinitt, and my co-advisor, Assistant Professor Dr. Boonchoat Paosawatanyong for their invaluable suggestion, generousness and extremely encouragement during the course of this research. This research is completely impossible to succeed without their helpfulness. Moreover, I have learned many things from my advisor such as attitude, creativeness, logic and kindness to students. He supported me to do the things that gave me the new experiences. I appreciate him and I try to remember to the things that he taught me for using in my life.

My appreciation is also given to Assistant Professor Warinthorn Chavasiri, and Assistant Professor Varawut Tangpasuthadol thesis defense committee, for their kind attention, valuable suggestion and recommendations. I also would like to thank my co-advisor for permission to use a plasma generator.

I would like to thank Dr. Nakorn Niamnont thesis defense committee from King Mongkut's University of Technology Thonburi for suggestions.

I would like to express my sincere gratitude to Assistant Professor Sommai Pivsa-art, Dr. Natee Srisawat and Dr. Sorapong Pavasupree from Department of Materials and Metallurgical Engineering, Faculty of Engineering, Rajamangala University of Technology Thanyaburi for allowing to launch activate and use objects on twin screw extruder, melt spinning fiber and compression molding machine.

Furthermore, I gratefully thank everyone in MAPS-group for a great friendships and encouragement, especially Dr. Watcharin Ngampeungpis for training and suggestion in this research; Dr. Warathip Siripornnoppakhun, Dr. Thirawat Sirijindalert, Miss Kanokthorn Boonkitpattarakul, Miss Pornpat Sam-ang, Miss Nattaporn Kimpitak, Miss Daranee Homrarueng, Mr. Natdanai Suta and Mr. Oral Pinrat for spirit, smile, good wish and their helps in everything.

I would like to thank Chulalongkorn University; Program in Petrochemistry and Polymer Science and Department of Chemistry, Faculty of Science,

Finally, I would like to express thankfulness to my family (The KLAHAN) for their love, care, encouragement and support throughout my study.

CONTENTS

	Page
ABSTRACT IN THAI	iv
ABSTRACT IN ENGLISH	v
ACKNOWLEDGEMENTS	vi
CONTENTS	vii
LIST OF TABLES	x
LIST OF FIGURES	xii
LIST OF SCHEMES	xxi
LIST OF ABBREVIATIONS	xxii
CHAPTER I INTRODUCTION	1
1.1 Overview	1
1.2 Theory.....	2
1.2.1 Polydiacetylene.....	2
1.2.2 Leuco dye.....	4
1.2.3 Colorimetric Response (CR).....	7
1.2.4 RGB color model.....	7
1.2.5 Humidity indicator.....	8
1.2.6 Ink-jet printing.....	9
1.2.7 Airbrush painting.....	11
1.2.8 Melt spinning.....	12
1.2.9 Two roll mill.....	13
1.3 Literature surveys.....	14
1.3.1 Forms of PDA	14
A. Vesicles.....	14
B. Films.....	15
C. Electrospun fibers.....	17
1.3.2 Deposition of PDA.....	18
A. Ink-jet printing.....	18
B. Airbrush painting.....	20
C. Dip coating.....	21

	Page
1.3.3 Colorimetric properties of PDA.....	23
A. Thermochromism.....	24
B. Solvatochromism.....	32
C. Alkalinochromism and acidochromism	38
1.3.4 Fabrication of thermochromic leuco dyes	41
1.4 Objectives and scope of the research.....	45
CHAPTER II EXPERIMENT.....	46
2.1 Surface deposition of diacetylene and leuco dye.....	46
Materials.....	46
Equipments.....	47
2.1.1 Photographic imaging and colorimetric analysis.....	47
2.1.2 Application techniques.....	48
Ink-jet printing.....	48
Airbrush painting.....	49
Multi-component sensing array.....	49
Dip coating.....	49
2.1.3 Paper-based polydiacetylene humidity indicators.....	50
Study of humidity sensitivity.....	51
Development of humidity indicator prototypes.....	52
2.2 Incorporation of leuco dye in commercial plastics.....	53
Materials and equipments.....	53
2.2.1 Thermal analysis of leuco dye.....	54
Thermogravimetric analysis (TGA) of leuco dye.....	54
Differential scanning calorimetry of leuco dye.....	54
2.2.2 Scanning electron microscopy (SEM).....	54
2.2.3 Study of thermal stability of Chameleon-T Powder.....	55
2.2.4 Melt-spinning of polypropylene/leuco dye.....	55
2.2.5 Compression molding of polymer/leuco dye.....	56
2.2.6 Two roll mill of rubber/leuco dye.....	56

CHAPTER III RESULTS AND DISCUSSION.....	57
3.1 Surface deposition of diacetylene and leuco dye.....	57
3.1.1 Ink-jet printing.....	58
3.1.2 Airbrush painting.....	63
3.1.3 Dip coating.....	66
3.1.4 Paper-based polydiacetylene humidity indicators.....	67
Fabrication and substrate selection.....	67
Selection of hydroscopic and basic salts.....	68
Development of humidity indicator prototypes.....	78
3.2 Techniques for incorporation of leuco dyes into commercial polymers..	80
Characterization of leuco dye.....	81
Scanning electron microscopy (SEM).....	85
3.2.1 Melt-spinning of polypropylene/leuco dye.....	85
3.2.2 Compression molding of polymer/leuco dye.....	87
3.2.3 Two roll mill of rubber/leuco dye.....	88
CHAPTER IV CONCLUSION.....	90
REFERENCES.....	92
APPENDICES.....	101
APPENDIX A Ink-jet printing.....	102
APPENDIX B Airbrush painting.....	105
APPENDIX C Dip coating.....	106
APPENDIX D Paper-based polydicetylene humidity indicators.....	107
APPENDIX E Melt-spinning of polypropylene/PCDA.....	119
APPENDIX F Award.....	120
VITAE.....	121

LIST OF TABLES

	Page
Table 3.1 Relative humidity over saturated salt solutions at specified temperatures.....	69
Table A1 RGB values of PCDA/ Brij [®] 58 P indicators at UV exposure times (3 independent experiments).....	102
Table A2 RGB values of PCDA/ Triton [®] X-100 indicators at UV exposure times (3 independent experiments).....	103
Table A3 RGB values of PCDA/ Tween [®] 20 indicators at UV exposure times (3 independent experiments).....	104
Table D1 RGB values of TCDA indicators without base after exposure at 63% RH for 24 hours (5 independent experiments).....	107
Table D2 RGB values of TCDA humidity indicators prepared with K ₂ CO ₃ alone at different incubation time under 63% RH for 24 hours (5 independent experiments).....	108
Table D3 RGB values of TCDA humidity indicators prepared with 4:1 mole ratio of K ₂ CO ₃ /NaOH mixed solution at different incubation time under 63% RH for 24 hours (5 independent experiments).....	109
Table D4 RGB values of TCDA humidity indicators prepared with 3:2 mole ratio of K ₂ CO ₃ /NaOH mixed solution at different incubation time under 63% RH for 24 hours (5 independent experiments).....	110
Table D5 RGB values of TCDA humidity indicators prepared with 2:3 mole ratio of K ₂ CO ₃ /NaOH mixed solution at different incubation time under 63% RH for 24 hours (5 independent experiments).....	111
Table D6 RGB values of TCDA humidity indicators prepared with 2 cm of K ₂ CO ₃ (50 %w/w) solution at different incubation time under 63% RH for 12 hours (5 independent experiments).....	112

	Page
Table D7 RGB values of TCDA humidity indicators prepared with 4 cm of K_2CO_3 (50 %w/w) solution at different incubation time under 63% RH for 12 hours (5 independent experiments).....	113
Table D8 RGB values of TCDA humidity indicators prepared with 4 cm of $K_2CO_3/NaOH$ (4:1 mole ratio) at different incubation time under 63% RH for 12 hours (5 independent experiments).....	114
Table D9 RGB values of TCDA humidity indicators prepared with 4 cm of $K_2CO_3/NaOH$ (4:1 mole ratio) at different incubation time under 36% RH for 24 hours (5 independent experiments).....	115

LIST OF FIGURES

	Page
Figure 1.1 Topopolymerization of diacetylene monomers.....	2
Figure 1.2 Structures of diacetylene monomers a) 10,12-Pentacosadiynoic acid (PCDA) and b) 10,12-Tricosadiynoic acid (TCDA).....	3
Figure 1.3 various color powder of leuco dye.....	5
Figure 1.4 Mechanism of reversible thermochromic process of crystal violet lactone via complex formation with bisphenol A in response to the phase change of solvent (e.g. 1-dodecanol).....	6
Figure 1.5 Images representation of the encapsulation of pigment material.....	6
Figure 1.6 The RGB color model.....	8
Figure 1.7 Images representation of the operation of the ink-jet printing with printheads using a) the piezoelectric crystals b) the high-pressure pump.....	10
Figure 1.8 Composition of airbrush.....	12
Figure 1.9 Melt spinning methods for producing polymer fibers.....	13
Figure 1.10 Images representation of the mastication on two roll mill.....	13
Figure 1.11 Structure and formation of a PDA lipid vesicle.....	14
Figure 1.12 Preparation of Langmuir Blodgett film a) floating of condensed monolayer film on the water subphase, b) film deposition, c) monolayer films on the substrate.....	15
Figure 1.13 a) Chemical structures of polycationic polymers, b) schematic preparation of PCDA vesicles, and c) illustration of layer-by-layer assembly on glass substrate.....	16
Figure 1.14 A schematic representation of the preparation of polymer fibers embedded with PDA supramolecules using the electrospinning technique, followed by irradiation with UV light.....	17
Figure 1.15 Schematic presentation of microemulsion conversion into nanoparticles by ink-jet printing.....	18

Figure 1.16	a) Structures of diacetylene monomers and b) surfactant molecules employed in this study. c) Schematic of a complex formed between diacetylene monomers and nonionic surfactants. d) SEM images of PCDA-Brij 78 composite and e) PCDA vesicles.....	19
Figure 1.17	Inactive development under white light (left) and its interaction with 350 nm UV light (right). Although it is difficult to discern, it is the white ridges which are fluorescing on the right.....	20
Figure 1.18	Array of cropped photographic images of PDAs on filter paper fabricated from PCDA and PCDA _S responding to various organic solvents.....	21
Figure 1.19	Photograph of PDA coated paper derived from primary amine (1% w/v) after being dipped in a solution of SDC, SDS, SDBS, TTAB, DTAB, HTAB, Tween 20, Brij®58P and Triton X-100 (500 mM).....	22
Figure 1.20	a) Structure of diacetylene monomers b) Scanned images of the paper-based PDA sensor array prepared from 1–8 exposed to various saturated vapors of volatile organic solvents.....	23
Figure 1.21	Structure of diacetylene monomers used in investigations of thermochromism in vesicles.....	25
Figure 1.22	Structures of diacetylene lipids investigated for thermochromism.....	26
Figure 1.23	Photographs of PCDA-EDEA embedded in PVA film and the PCDA-EDEA vesicle solution during heating process.....	27
Figure 1.24	Chemical structure of G _n and the optimized conformation of 24 mers of (upper) polyG ₃ and (lower) polyG ₄	27
Figure 1.25	Mechanism of chromic responses of irreversible PDAs.....	28
Figure 1.26	Color of PDA sols recorded by photography during the heating process displaying the variation of color transition temperature.....	29
Figure 1.27	Structure of diacetylene monomers, their color transition and reversibility in vesicles solution.....	30

Figure 1.28	Structure of investigated diacetylene monomers: symmetrical diyndiamides (Sx) and unsymmetrical diyndiamide monomers (Uy).....	31
Figure 1.29	Color photographs of the aqueous suspensions of (a) pure poly(PCDA), (b) poly(PCDA)/ZnO nanocomposite, (c) pure poly(TCDA), (d) poly(TCDA)/ZnO nanocomposite, and (e) poly(HDDA)/ZnO nanocomposite taken upon increasing temperature from 30 to 90 °C, followed by cooling to room temperature.....	31
Figure 1.30	Photographs of the PDA-embedded electrospun fiber mats prepared with diacetylene monomers 1-4 after exposure to organic solvent.....	32
Figure 1.31	Proposed side-chain movements in the chromic transitions of poly(PCDA) vesicles upon organic solvent.....	33
Figure 1.32	Schematic representation of the preparation of PDA-embedded electrospun microfibers and photographs of the polymerized PDA-embedded electrospun fiber mats after exposure to organic solvents at 25 °C for 30 s.....	34
Figure 1.33	photographs of the PDA-embedded polymer matrix films derived from TCDA, PCDA, PAPCDA and CNAPCDA after dipped in organic solvents at room temperature.....	35
Figure 1.34	Photographs of TTIs prepared from PCDA solution incorporated with Pluronic F127.....	35
Figure 1.35	Photographs of micelle dispersions in different water-solvent mixtures. At increasing solvent content, the color of (a) polyTDA and (b) polyAzoDA changes from blue to purple/red depending on type of solvent and its relative content, respectively.....	36
Figure 1.36	Colorimetric responses (CR) of a) poly(TCDA), b) poly(PCDA) vesicles in aqueous suspensions upon addition of linear alcohols with different chain lengths and c) the penetration of methanol and 1-butanol into the layers of poly(PCDA).....	37

Figure 1.37	a) Structure of the diacetylene lipid 10,12-pentacosadiynoic acid (1) and its derivatives: lipids 2-6, amino acids derivatives; lipid 7, 3-(dimethylamino)propylamine (DMAP) derivative. b) Schematic diagram of amino acid-derivatized polydiacetylene liposomes in a chromatic transition.....	38
Figure 1.38	Schematic representations of the polymerization behavior and colorimetric changes of the diacetylene hydrazides PHY and THY in the presence of HCl or NH ₃	39
Figure 1.39	a) The colorimetric responses (%CR) of the vesicles were plotted as a function of pH. Symbols are (O) poly(PCDA), (Δ) poly(TCDA) and (□) poly(AEPCDA). b) The charged species of head groups of poly(PCDA) in high pH region and poly(AEPCDA) in low pH region.....	40
Figure 1.40	Experimental equipment used for spinning fibers while measuring fiber diameter and temperature.....	41
Figure 1.41	SEM images of PEN fibers spun with LIB (a) surface and (b) cross section of undrawn fibers; (c) surface and (d) cross section of drawn fibers.....	42
Figure 1.42	From left: Photograph of the control alginate fiber (white), as-spun alginate fiber with PCDA liposome (blue), and alginate fiber with PCDA liposome after exposure to 60 °C for 45 s (red).....	43
Figure 1.43	Coaxial electrospinning setup used to produce thermochromic core-shell PMMA fibers.....	44
Figure 3.1	Structures of a) diacetylene monomer (PCDA), b) Triton [®] X-100, c) Brij [®] 58 P and d) Tween [®] 20.....	58
Figure 3.2	Color images of poly(PCDA) printed from PCDA/surfactant aqueous solutions using a) Brij [®] 58P b) Triton [®] X-100 c) Tween [®] 20 before (left) and after (right) heating at 90 °C for 10 sec.....	59

	Page
Figure 3.3 Color images of poly(PCDA) printed from PCDA/surfactant aqueous solutions using a) Brij [®] 58P b) Triton [®] X-100 c) Tween [®] 20 upon heating from 30 to 90 °C. The experiment was performed in three replicates.....	60
Figure 3.4 Plots of %R and %B against temperature, corresponding to the photographic images in Figure 3.3	60
Figure 3.5 SEM images of dry samples on glass substrate prepared from aqueous solutions of PCDA (13 mM, 7.5 mg/mL) in the absence and presence of surfactants (7.5 mg/mL): a) PCDA, b) with Brij [®] 58 P, c) with Triton [®] X-100 and d) with Tween [®] 20).....	62
Figure 3.6 Photographic images of PCDA/binder and orange leuco dye/binder solution airbrush-painted on various types of surfaces: (a) aluminum lid, (b) Thai cupernickel coins, (c) PE thin film, (d) paper, (e) PE plate, (f) cotton textile, (g) wood board, (h) PET bottle, (i) glass slide before and after heating.....	64
Figure 3.7 Photograph of multi-detector from airbrush painting technique co-operated with ink-jet printing.....	64
Figure 3.8 Photographic images of UV-irradiated paper printed with PCDA/surfactant after the exposure to water (control) and various organic solvents.....	65
Figure 3.9 Photographic images of PCDA coated polyester thread sewn to white polyester fabric pieces.....	66
Figure 3.10 Images of water droplet on a) printing paper b) drawing paper and c) filter paper in the water absorbing test.....	67
Figure 3.11 Time dependent color image of TCDA zone of the humidity indicators without salt, with MgCl ₂ , CaCl ₂ , K ₂ CO ₃ and LiCl incubated in a closed container with 75%RH. The pH values of the saturated salt solutions are shown in the right table.....	70

- Figure 3.12** Photographic images of the salt zone prepared from 7.81 molal aqueous solution of **a)** K_2CO_3 , and $K_2CO_3/NaOH$ mixed solution with **b)** 4:1, **c)** 3:2. and **d)** 2:3 mole ratio.....71
- Figure 3.13** **a)** Photographic images of TCDA zone of the humidity indicators prepared with K_2CO_3 alone at different incubation times, and **b)** Plots of %R (▲) and %B (■) of the TCDA zone in the humidity indicators versus exposure time under controlled %RH (●) by NaBr ($63\pm 3\%$)..... 72
- Figure 3.14** Photographic images of TCDA zone of the humidity indicators prepared with **a)** 4:1 **b)** 3:2 and **c)** 2:3 mole ratio of $K_2CO_3/NaOH$ mixed solution (7.81 molal) at different incubation times under $63\pm 3\%RH$ 73
- Figure 3.15** Plots of %R (▲) and %B (■) of the TCDA zone in the humidity indicators prepared with **a)** 4:1**b)** 3:2 and **c)** 2:3 mole ratio of $K_2CO_3/NaOH$ mixed solution (7.81 molal) versus exposure time under controlled %RH (●) by NaBr ($63\pm 3\%$).....74
- Figure 3.16** Humidity indicators with different zone lengths: **a)** initial design and **b)** expanded salt zone design. The dash square depicts the cropping area for the color analysis..... 75
- Figure 3.17** Color images of TCDA zone of the humidity indicators prepared with **a)** 2 cm and **b)** 4 cm of K_2CO_3 (50 %w/w) zone and their corresponding plots of %R (▲) and %B (■). The indicators were incubated under controlled RH of $63\pm 3\%$ (●).....76
- Figure 3.18** **a)** Color images of TCDA zone of the humidity indicators prepared with 4 cm of $K_2CO_3/NaOH$ (4:1 mol ratio) zone and **b)** their corresponding plots of %R (▲) and %B (■). The indicators were incubated under controlled RH of $63\pm 3\%$ (●).....77

- Figure 3.19** a) Color images of TCDA zone of the humidity indicators prepared with 4 cm of $K_2CO_3/NaOH$ (4:1 mol ratio) zone and b) their corresponding plots of %R (▲) and %B (■). The indicators were incubated under controlled RH of $36\pm 2\%$ (●).....78
- Figure 3.20** Plot of expanding distance of the red color in TCDA zone of humidity indicators versus moisture exposure time at $63\pm 3\%$ RH.....79
- Figure 3.21** Humidity indicator prototypes tested under controlled %RH of $63\pm 3\%$ and $36\pm 2\%$ for 24 hours.....80
- Figure 3.22** DSC thermogram (2nd heating) of commercial thermochromic leuco dye (Chameleon-T)..... 82
- Figure 3.23** TGA thermograms of commercial thermochromic leuco dye (Chameleon-T)..... 82
- Figure 3.24** Photo images of Chameleon-T powder samples before (left) and after (right) heating to 220 °C recorded a) at temperature 25 °C and b) during heating from 5 to 40 °C.....84
- Figure 3.25** SEM images (3,500x and 15,000x) of Chameleon-T powder..... 85
- Figure 3.26** Photographs of black Chameleon-T powder (1, 2 and 3% w/w) incorporated polypropylene fiber filament at a) 25 °C b) body temperature (hand touch) and c) warm temperature (blown with a hair dryer). The insets are the closed up pictures showing beads in the fiber filaments with 3% w/w of Chameleon-T powder....86
- Figure 3.27** Photographs of filter plate (105 μm) a) before and b) after melt spin processing of PP with % w/w of Chameleon-T powder.....86
- Figure 3.28** Photo images of 3% black Chameleon-T powder incorporated by compressing molding technique with a) LDPE at 150 °C, b) PP at 210 °C and c) PS at 250 °C, the image recorded at 25 °C (up) and warm temperature (blown with a hair dryer) (down)..... 88

Figure 3.29	Photographs of a) SBR plate containing 5% black Chameleon-T powder and b) cured SBR plate containing 5% black Chameleon-T powder at 25 °C (left), and at above 30 °C (blown with a hair dryer, right).....	89
Figure A1	Plots of %RGB value of 3 independent PCDA/ Brij [®] 58 P indicators against UV exposure times to determine the optimized time for exposure of PCDA.....	102
Figure A2	Plots of %RGB value of 3 independent PCDA/Triton [®] X-100 indicators against UV exposure times to determine the optimized time for exposure of PCDA.....	103
Figure A3	Plots of %RGB value of 3 independent PCDA/ Tween [®] 20 indicators against UV exposure times to determine the optimized time for exposure of PCDA.....	104
Figure B1	Cropped photographic images of solvent sensing arrays fabricated by a) airbrush painting and b) ink-jet printing technique of PCDA incorporated with Brij [®] 58 P, Triton [®] X-100 and Tween [®] 20 after the exposure to water (control) and 14 organic solvents.....	105
Figure B2	RGB histogram of colorimetric responses of PCDA incorporated with Brij [®] 58 P, Triton [®] X-100 and Tween [®] 20 in the present of water (control) and 14 organic solvents.....	105
Figure C1	Photo image of rubbing on polyester thread sewn to white polyester fabric pieces.....	106
Figure D10	the photo image of TCDA humidity indicators prepared with K ₂ CO ₃ alone deposit on a) filter paper Whatman No.1 and b) filter paper whatman No.3 of (5 independent experiments) at different incubation time under 63% RH for 24 hours.....	116
Figure D11	a) Color image of TCDA zone of the humidity indicators prepared without b) their corresponding plots of %R (▲) and %B (■). The indicators were incubated under controlled %RH of 63±3% (●) for 24 hours.....	117

	Page
Figure D12 Image of indicators fabricated by dip coating of TCDA and $K_2CO_3:NaOH$ mole ratio (4:1) a) before b) after exposed to UV lamp for 1 minute and c) after exposed to ambient humidity.....	118
Figure E1 Photo image of multi-filament of PP + 0.5 % PCDA a) after UV irradiated b) after heated.....	119
Figure F1 Winning the 2 nd award from 5 th Sci & Tech initiative and Sustainability Award by The Thai Institute of Chemical Engineering and Applied Chemistry, SCG Chemicals and Dow Chemical (From left to right : Mr. Jadetapong Klahan, Mr. Natdanai Suta, Mr. Pracharat Sa-ngadsup and Mr. Watcharin Ngampeungpis) (“System for real time monitoring of environmental parameters via optical responses”).....	120

LIST OF SCHEMES

	Page
Scheme 2.1 Method for the preparation of diacetylene ink solution from PCDA/surfactant.....	48
Scheme 2.2 Design of humidity paper indicator.....	50
Scheme 2.3 Preparation of humidity indicator prototypes.....	52
Scheme 3.1 Flow chart for preparation and study of humidity indicators.....	68

LIST OF ABBREVIATIONS

PDA	Polydiacetylene
PCDA	10,12-pentacosadiynoic acid
TCDA	10,12-tricosadiynoic acid
DSC	Differential scanning calorimetry
TGA	Thermogravimetric analysis
SEM	Scanning electron microscopy
°C	Degree Celsius
UV	Ultraviolet
g	Gram
mg	Milligram
mL	Millilitre
kW	Kilowatt
μW	Microwatt
μL	Microlitre
mM	Millimolar
m	Metre
nm	Nanometre
μm	Micrometre
min	Minute
Hr	Hour
%	Percent
cm	Centimeter
cm ²	Square centimeter
No.	Number
RGB	Red Green Blue
PP	Polypropylene
LDPE	Low-density polyethylene
GPPS	General-purpose polystyrene
CTT	Color transition temperature
RH	Relative humidity
rpm	Rounds per minute

CHAPTER I

INTRODUCTION

1.1 Overview

Materials that can change their colors in response to external stimuli such as temperature, pH, moisture, stress, and electric and magnetic fields have potential applications as signal transducers, sensors, indicators and detectors [1,2]. Leuco dye is the most commercially available thermochromic materials while polydiacetylene (PDA) is a research material which exhibit various kinds of chromism properties including thermochromism, solvatochromism, alkalinochromism, affinochromism and mechanochromism. Proper deposition techniques of these chromic materials onto surfaces of various objects can expand their utilization. The incorporation of these chromic materials into a commercial polymer is also desirable where the applications of the products can cause wear and tear. Interestingly, there have not been many studies reporting the fabrication techniques of this type of materials.

Since only some of the diacetylene monomers are commercially available in small quantity for research, they will be studied only in the surface deposition techniques as the examples for development of temperature, solvent and humidity indicators. The thermochromic leuco dye is commercially available in larger quantity, it is thus investigated for both surface deposition and incorporation techniques.

1.2 Theory

1.2.1 Polydiacetylene

A polydiacetylene (PDA) is an ene-yne conjugated polymer comprising of double and triple bonds in its backbone. It can be prepared by a topological 1,4-addition polymerization of diacetylene monomer by UV light or γ -irradiation of crystalline or semicrystalline states obtained from molecular self-assembled diacetylene (DA) monomer without the need for chemical initiators or catalysts as shown in **Figure 1.1**.

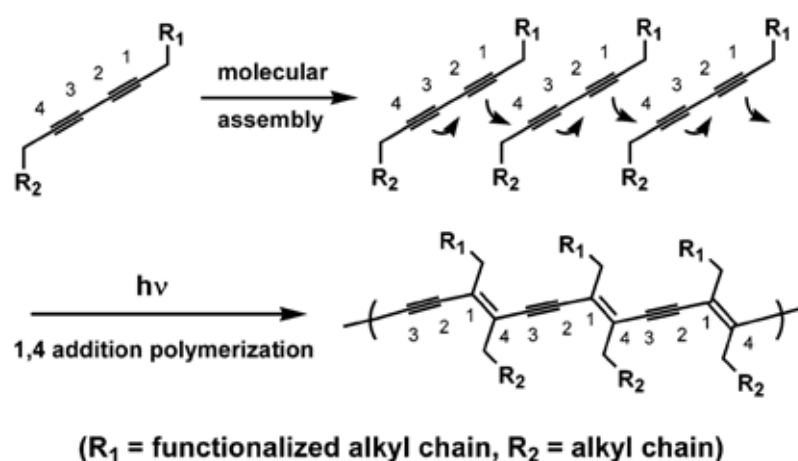


Figure 1.1 Topopolymerization of diacetylene monomers [3].

Topological polymerization is a polymerization which requires specific prealignment of the monomer usually found in solid state crystal [4]. For topological polymerization of diacetylenes, the distance (d) between the corresponding triple bonds of the adjacent monomers and the orientation angle (θ) relative to the translation axis should be $\sim 5 \text{ \AA}$ and $\sim 45^\circ$, respectively [5-6]. 10,12-Pentacosadiynoic acid (PCDA), 10,12-Tricosadiynoic acid (TCDA) are the most commonly used and widely studied diacetylene for chromic applications, Various types of stimuli such as temperature, organic solvent, mechanical stress, molecular recognition, pH and UV light can cause color change of PDAs. The color transition property can be tuned via rational design of supramolecular interactions among the polymeric side chains [7-9].

The structures of PCDA and TCDA as show in **Figure 1.2**. PDAs have also been prepared in the forms of various nanostructures such as vesicles, tubes, and ribbons [10-15]. The formation of nanovesicles allows the preparation of homogeneously dispersed PDA vesicle solutions resulting in several noteworthy chemical and biological sensing systems [16]. However, the aqueous sols have short shelf life and are not suitable for portable and tag-on applications. Fabrication of PDAs as solid state sensors or indicators in the form of gel [17] thin film [18,19] and electrospun fiber [20] have recently been reported. The preparation methods for these forms of PDAs generally require additional polymer matrix and equipment setup. Recently, white paper has been demonstrated as a very promising supporting material for portable and disposable multi-sensing devices because it is omnipresent, inexpensive and easy to be stored, transported and handled [21-22, 60]. In our research group, we have also recently reported the use of filter paper as a support for fabrication of PDA based colorimetric sensors of solvents, surfactants, VOCs [23-25, 78] and time-temperature chromatic sensor [74].

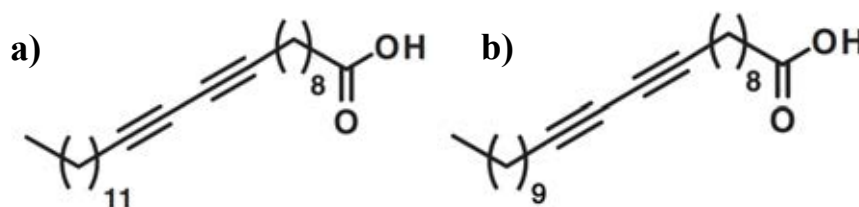


Figure 1.2 Structures of diacetylene monomers **a)** 10,12-Pentacosadiynoic acid (PCDA) and **b)** 10,12-Tricosadiynoic acid (TCDA).

UV-Vis absorption measurement is a common method for determination of colorimetric response percentage (%CR) for solution samples [13,19,26] but this technique does not generally give reliable values for opaque solid materials. CCD imaging technology has turned photography into a readily processable digital form [27]. The capability to capture wide area of image of digital imaging is also the advantage, in comparison with the reflective spectroscopic instrument, that produce more reliable color analysis of rough surface samples such as paper. For examples, it

has recently been used along with the RGB color system to record and evaluate colorimetric sensors [21] including PDA films [23-25, 28-29]. In this research, a utilization of webcam and RGB values to quantify the color transition PDAs on paper support along with mathematical formula to use RGB values in specifying the color transition of PDA paper based indicators [69]. The technique developed in this work should provide practical guidelines for systematic and comparison of chromic properties of PDAs toward the development of economical and reliable multi-purposed paper indicators from diacetylenes.

1.2.2 Leuco dye [81]

Leuco dye depend upon the difference in dipole moment of the solvatochromic color molecule between its ground state and excited state, there are two types of solvatochromism i.e. negative solvatochromism that corresponds to hypsochromic shift, positive solvatochromism that corresponds to bathochromic shift with increasing solvent polarity. 4,4'-bis(dimethylamino)fuchson (orange in nonpolar toluene, red in slightly polar acetone, and red-violet in more polar methanol) is a proper example of positive solvatochromism while the examples of negative solvatochromism include 2-(4'-hydroxystyryl)-*N*-methyl-quinolinium betaine (ink-blue in nonpolar chloroform and blood-red in polar water) and 4-(4'-hydroxystyryl)-*N*-methyl-pyridinium iodide (violet in *n*-butanol, red in 1-propanol, orange in methanol, and yellow in water).

Thermochromic dyes undergo a color change over a specific temperature range. The dyes currently available change from a particular color at low temperature to colorless at a high temperature (e.g. red at 29.5 °C and colorless at above 32 °C). The color change temperature can be controlled, such that the color-change can take place at different temperatures (e.g. just below a person's external body temperature so that a color change occurs in response to a human touch). The thermochromic dye manufacturers are able to manipulate the critical temperature for the color change [80].

Certain dyes undergo keto-enol type of tautomerism. Such tautomeric rearrangements can lead to an increase in the conjugation and formation of a new chromophore, leading to color development. Such rearrangements can be induced by a change of temperature, resulting in thermochromism. These dyes are extensively used for textile applications. The most common types are fluorans, crystal violet lactones (CVL), and spiro pyrans. All of these dyes undergo ring opening rearrangements. The equilibrium of crystal violet lactone is shown in **Figure 1.4**.

Leuco dye is a common coloring agent use in various commercial reversible thermochromic powders (**Figure 1.3**), which consist of three components i.e. thermochromic dye, a color developer and a phase-change medium [68].



Figure 1.3 various color powder of leuco dye.

Crystal violet lactone (CVL) is the most commonly used and widely studied leuco dye for thermochromic applications. Color developers are weak acids that act as proton donors to induce the colored state of the leuco dye components [76]. The phase-change medium, also referred to as the ‘solvent’, can be a fatty alcohol or ester. The melting and crystallization points of this ‘solvent’ largely control the temperatures of color change. The picture develops through the reaction of colorless leuco dye with acid component in polymer matrices as shown in **Figure 1.4**.

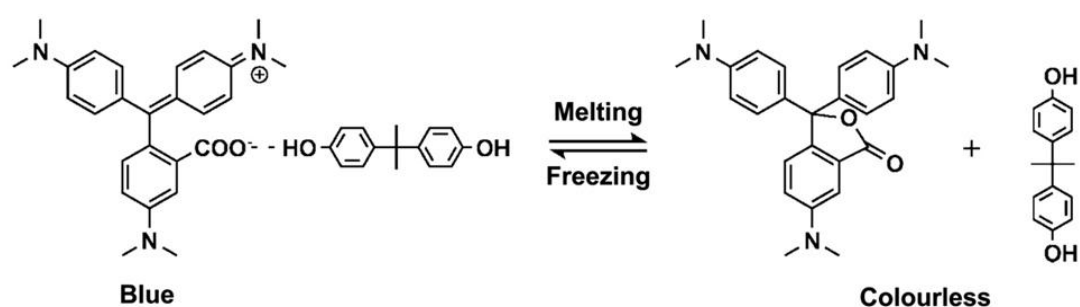


Figure 1.4 Mechanism of reversible thermochromic process of crystal violet lactone via complex formation with bisphenol A in response to the phase change of solvent (e.g. 1-dodecanol).

The components must be entrained together within a protective shell to allow reversibility of the thermochromic effect and to prevent loss of the ‘thermochromic composite’ due to fluidity after melting. Thermochromic materials are typically microencapsulated prior to application to textile and other substrates as shown in **Figure 1.5** [67].

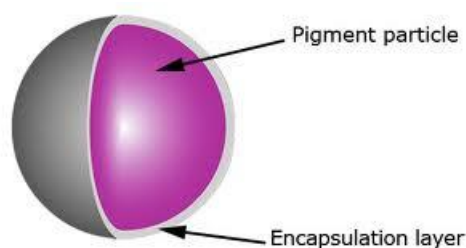


Figure 1.5 Image representation of the encapsulation of pigment material.

1.2.3 Colorimetric Response (CR)

The color transition of the polymerized vesicles was monitored by measuring the absorbance differences between the vesicles before and after stimulation by an interesting parameter. This information is often converted to a percentage, termed the Colorimetric Response (CR) [34].

A quantitative value for the extent of blue-to-red color transition is given by the colorimetric response (%CR) which is defined as

$$\%CR = (PB_0 - PB) / PB_0 \times 100$$

Where $PB = A_{\text{blue}} / (A_{\text{blue}} + A_{\text{red}})$, A_{blue} and A_{red} are the absorbance of the blue and the red phase at 630 and 540 nm, respectively. The visible absorbance was measured by a temperature controlled UV-vis spectrometer. PB_0 is the initial percent blue of the vesicle solution and film before heated. All blue-colored PDA vesicle solution and film samples were heated from 10 to 90 °C.

1.2.4 RGB color model

According to development of paper based colorimetric respond of polydiacetylene is a simple method and suitable to use as a sensors application, since evaluate the results into a quantitative analysis can be collected by using the RGB color model. The RGB color model is an additive color model in which red, green, blue color are added together in various component ratio to reproduce a broad array of colors as shown in **Figure 1.6**. The name of the model comes from the initials of the three additive primary colors, red, green, and blue. The main purpose of the RGB color model is for the sensing, representation, and display of images. The RGB color model was used to describe how much of each red, green, and blue color is included in the photographic images [35].

The basic of the RGB value, the color is black when the intensity of each component is zero (0, 0, 0) and the color is white when the intensity of each component is full (255, 255, 255). When the intensities are the same, the result is a shade of gray, darker or lighter depending on the intensity.

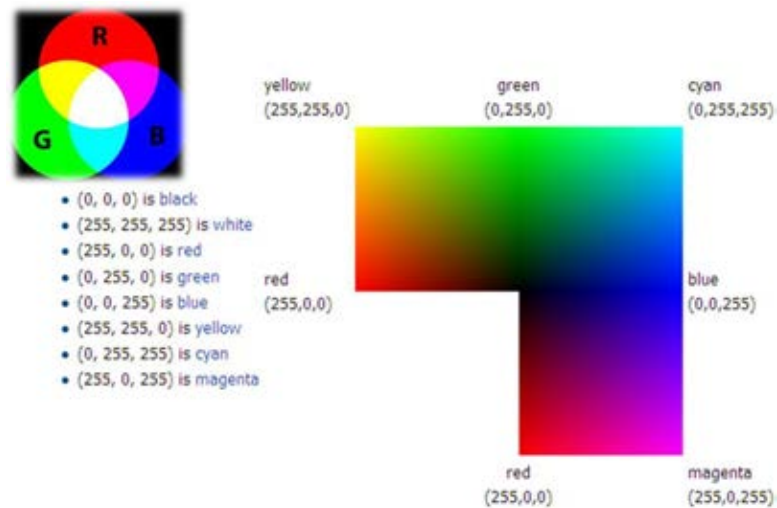


Figure 1.6 The RGB color model.

1.2.5 Humidity indicator [82]

Humidity is the amount of water vapor in the air. Water vapor is the gaseous state of water and is invisible. Humidity indicates the likelihood of precipitation, dew, or fog. Higher humidity reduces the effectiveness of sweating in cooling the body by reducing the rate of evaporation of moisture from the skin. This effect is calculated in a heat index table or humidex, used during summer weather.

There are three main measurements of humidity: absolute, relative and specific. Absolute humidity is the water content of air. Relative humidity, expressed as a percent, measures the current absolute humidity relative to the maximum for that temperature. Specific humidity is a ratio of the water vapor content of the mixture to the total air content on a mass basis.

Relative humidity is the ratio of the partial pressure of water vapor in the air–water mixture to the saturated vapor pressure of water at those conditions. The relative humidity of air is a function of both its water content and temperature.

The amount of water vapor in the air at any given time is usually less than that required to saturate the air. The relative humidity is the percent of saturation humidity, generally calculated in relation to saturated vapor density. The relative humidity was calculated from the following equations [83].

$$\text{Relative Humidity} = \frac{\text{actual vapor density}}{\text{saturation vapor density}} \times 100\%$$

Humidity is an important physical parameter for living, safety for food, drug and some industrial products. Therefore, the US Food and Drug Administration (FDA) had set a guideline to keep and store medicines and pharmaceutical products at 25 °C and $\leq 60\%$ RH to lower the chance of fungi and bacteria growth.

1.2.6 Ink-jet printing [84]

Inkjet printing is a type of computer printing that creates a digital image by propelling droplets of ink onto paper, plastic, or other substrates. Inkjet printers are the most commonly used type of printer, and range from small inexpensive consumer models to very large professional machines.

The emerging ink-jet material deposition market also uses inkjet technologies, typically printheads using piezoelectric crystals, to deposit materials directly on substrates. The continuous inkjet (CIJ) method is used commercially for marking and coding of products and packages. In CIJ technology, a high-pressure pump directs liquid ink from a reservoir through a gunbody and a microscopic nozzle, creating a continuous stream of ink droplets via the Plateau-Rayleigh instability. A piezoelectric crystal creates an acoustic wave as it vibrates within the gunbody and causes the stream of liquid to break into droplets at regular intervals: 64,000 to 165,000 droplets per second may be achieved. The ink droplets are subjected to an electrostatic field created by a charging electrode as they form; the field varies according to the degree of drop deflection desired (**Figure 1.7**). This results in a controlled, variable electrostatic charge on each droplet. Charged droplets are separated by one or more uncharged "guard droplets" to minimize electrostatic repulsion between neighbouring

droplets. The charged droplets pass through an electrostatic field and are directed (deflected) by electrostatic deflection plates to print on the receptor material (substrate), or allowed to continue on undeflected to a collection gutter for re-use. The more highly charged droplets are deflected to a greater degree. Only a small fraction of the droplets is used to print, the majority being recycled. CIJ is one of the oldest ink-jet technologies in use and is fairly mature. The major advantages are the very high velocity (~ 50 m/s) of the ink droplets, which allows for a relatively long distance between print head and substrate, and the very high drop ejection frequency, allowing for very high speed printing. Another advantage is freedom from nozzle clogging as the jet is always in use, therefore allowing volatile solvents such as ketones and alcohols to be employed, giving the ink the ability to "bite" into the substrate and dry quickly.

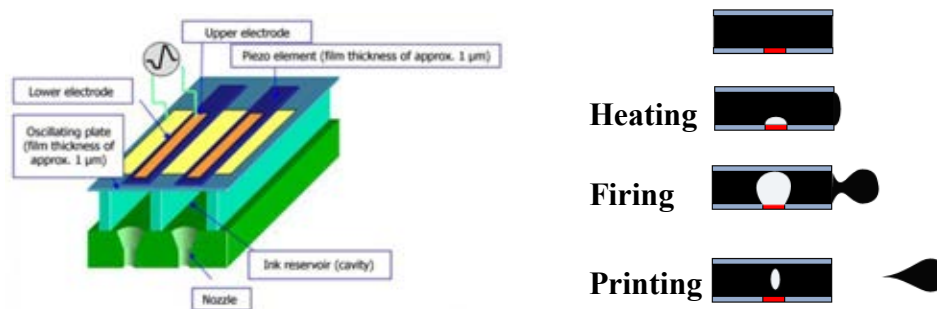


Figure 1.7 Images representation of the operation of the ink-jet printing with printheads using **a)** the piezoelectric crystals and **b)** the high-pressure pump.

The ink system requires active solvent regulation to counter solvent evaporation during the time of flight (time between nozzle ejection and gutter recycling), and from the venting process whereby air that is drawn into the gutter along with the unused drops is vented from the reservoir. Viscosity is monitored and a solvent (or solvent blend) is added to counteract solvent loss. The basic problem with inkjet inks is the conflicting requirements for a coloring agent that will stay on the surface vs. rapid dispersement of the carrier fluid. Desktop inkjet printers, as used in offices or at home, tend to use aqueous inks based on a mixture of water, glycol and dyes or pigments. These inks are inexpensive to manufacture, but

are difficult to control on the surface of media, often requiring specially coated media. Aqueous inks are mainly used in printers with thermal inkjet heads, as these heads require water to perform. While aqueous inks often provide the broadest color gamut and most vivid color, most are not waterproof without specialized coating or lamination after printing. Most dye-based inks, while usually the least expensive, are subject to rapid fading when exposed to light. Pigment-based aqueous inks are typically more costly but provide much better long-term durability and ultraviolet resistance.

1.2.7 Airbrush painting [85]

An airbrush is a small, air-operated tool that sprays various media including ink and dye, but most often paint by a process of nebulization. Spray guns were developed from the airbrush and are still considered a type of airbrush. An airbrush works by passing a stream of fast moving (compressed) air through a venturi, which creates a local reduction in air pressure (suction) that allows paint to be pulled from an interconnected reservoir at normal atmospheric pressure. The high velocity of the air atomizes the paint into very tiny droplets as it blows past a very fine paint-metering component. The paint is carried onto paper or other surface. The operator controls the amount of paint using a variable trigger which opens more or less a very fine tapered needle that is the control element of the paint-metering component. An extremely fine degree of atomization is what allows an artist to create such smooth blending effects using the airbrush (**Figure 1.8**). The technique allows for the blending of two or more colors in a seamless way, with one color slowly becoming another color. Freehand airbrushed images, without the aid of stencils or friskets, have a floating quality, with softly defined edges between colors, and between foreground and background colors. A well skilled airbrush artist can produce paintings of photographic realism or can simulate almost any painting medium. Painting at this skill level involves supplementary tools, such as masks and friskets, and very careful planning.

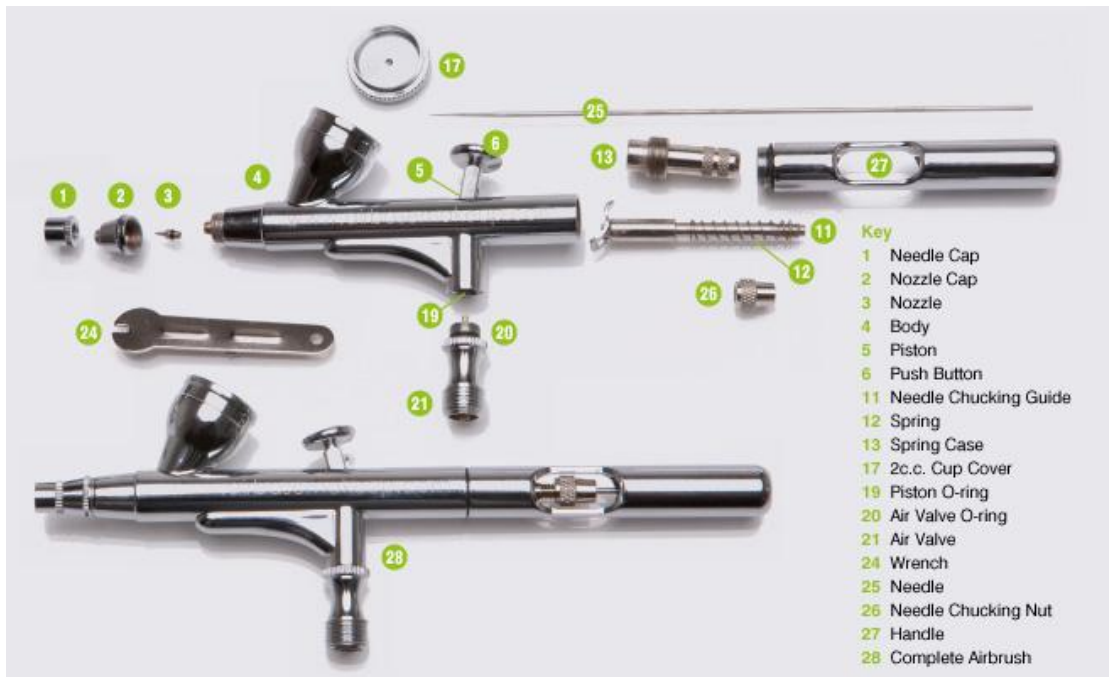


Figure 1.8 Composition of airbrush.

Some airbrushes use pressures as low as 20 psi (1.38 bar) while others use pressures in the region of 30-35 psi (2-2.4 bar). Larger "spray guns" as used for automobile spray-painting need 100 psi (6.8 bar) or more to adequately atomize a thicker paint using less solvent. They are capable of delivering a heavier coating more rapidly over a wide area.

1.2.8 Melt spinning [86]

Melt spinning is used for polymers that can be melted. Pellets or granules of the solid polymer are fed into an extruder. The pellets are compressed, heated and melted by an extrusion screw, then fed to a spinning pump and into the spinneret. The polymer solidifies by cooling after being extruded from the spinneret. Nylon, olefin, polyester, saran and sulfur are produced via this process. The picture of melt spinning processes as shown in **Figure 1.9**.

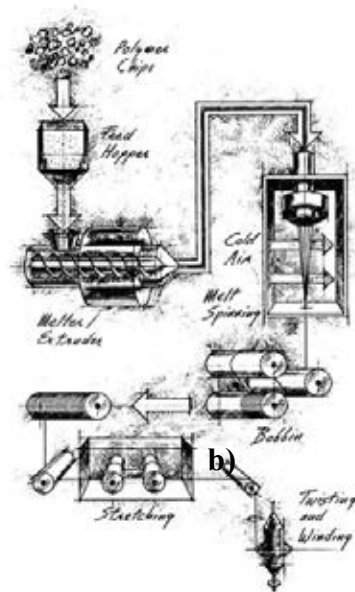


Figure 1.9 Melt spinning processes for producing polymer fibers.

1.2.9 Two roll mill [87]

Method for mastication rubber like mixing, calendaring, extrusion, all processes being essential to bring crude rubber into a state suitable for shaping the final product. The former breaks down the polymer chains, and lowers their molecular mass so that viscosity is low enough for further processing. After this has been achieved, various additions can be made to the material ready for cross-linking. Rubber may be masticated on a two-roll mill (**Figure 1.10**) or in an industrial mixer, which come in different types. Rubber is first compounded with additives like sulphur, carbon black and accelerators. It is converted into a dough-like mixture which is called "compound" then milled into sheets of desired thickness. Rubber may then be extruded or molded before being cured.

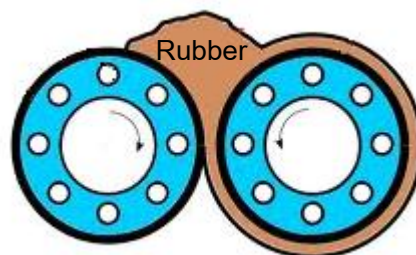


Figure 1.10 Image representation of the mastication on two roll mill.

1.3 Literature survey

1.3.1 Forms of PDA

PDA have been prepared in numerous forms: bulk single crystal, Langmuir monolayer film, multilayer film, nanotube and vesicle. These forms of PDA are closely related to the molecular self-assemblies of the corresponding diacetylene monomers.

A. Vesicles

The vesicle is one of the most widely used forms of polydiacetylene for sensor applications [13]. It is water filled spherical assembly of lipid bilayer. The formation of vesicle is thermodynamically driven so that the hydrophobic surface of the lipid molecules is not exposed to water. Only the hydrophilic head group of the lipid is exposed to water inside and outside of the bilayer membrane. A number of lipids containing diyne unit can self assemble into vesicle that have the right packing parameters for topological polymerization to form PDA vesicles (**Figure 1.11**). In the form of vesicle, PDA can be homogeneously dispersed in an aqueous media to form a sol type colloid, which is convenient for further characterization, fabrication and applications. The most studied diacetylene lipids are 10,12-pentacosadiynoic acid (PCDA). The interest in these lipid vesicles is mainly related to the development into bio- [30] and chemosensors [31].

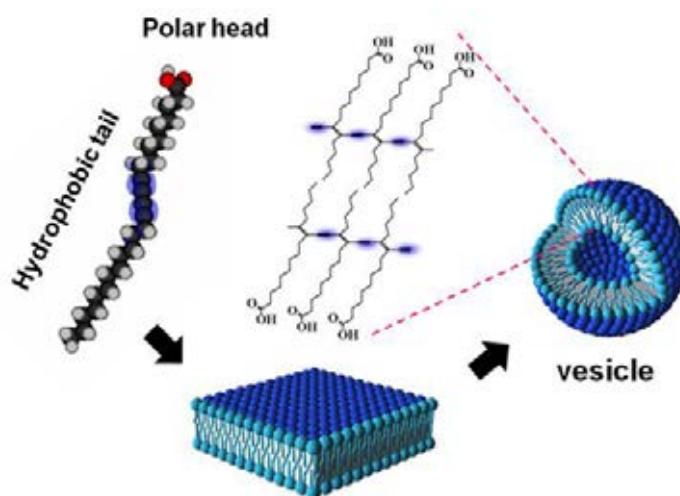


Figure 1.11 Structure and formation of a PDA lipid vesicle.

B. Films

Several techniques have been utilized for making different types of thin films on the surface of substrates. Langmuir-Blodgett film can generate an ideal highly ordered monolayer assembly of lipid molecules at water/air interface. The monolayer can be transferred onto solid substrate by horizontal or vertical deposition (**Figure 1.12**). The monolayer Langmuir-Blodgett film is however often fragile and difficult to prepare in large area. The number of layers can be increased by repeating the transferring process with a newly generated monolayer. Hence, it can be quite bothersome to prepare a multilayer film as the preparation of each new monolayer requires a slow surface compression and the transferring step needs adroit attention. This type of PDA film is one of the most interesting forms of PDA in research but the development of the technique for practical mass production remains elusive [32].

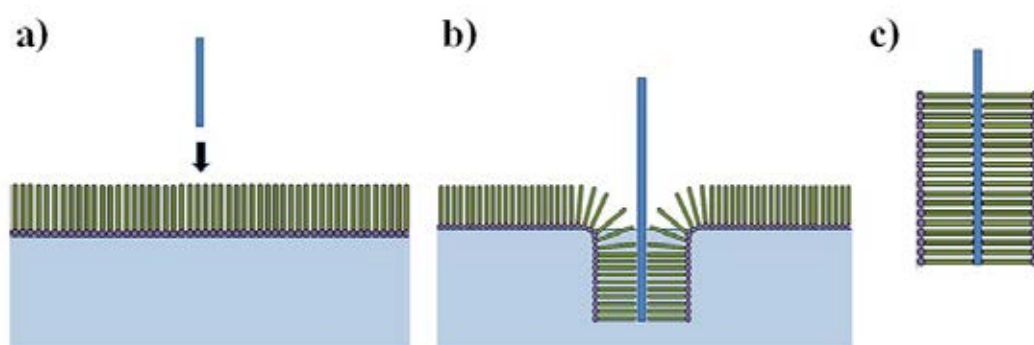


Figure 1.12 Preparation of Langmuir Blodgett film **a)** floating of condensed monolayer film on the water subphase, **b)** film deposition, **c)** monolayer films on the substrate.

The polyelectrolyte multilayers (PEM) technique is an alternative method for the preparation of multilayer thin film (**Figure 1.13**). Although based on a very simple adsorption process, PEM assembly has proven to be a very powerful method for immobilizing charged species onto a substrate. In this technique, oppositely charged polyelectrolytes (polyanions and polycations) are assembled into thin films by sequential dipping of a substrate into polyelectrolyte solutions followed by rinsing steps. The electrostatic interaction between the adsorbed layer on the substrate and the oppositely charged polyelectrolytes in the solution leads to the adsorption of another

polyelectrolyte layer and the reversal of the surface charge, allowing the deposition of the next layer. The PEM technique is well suited for the preparation of thin films on objects with various types of surface and shape. The thickness of the film can also be easily controlled by choosing the appropriate number of layers deposited, which is convenient for preparation of colorimetric sensing devices detectable by naked eyes. Early use of the PEM technique to assemble diacetylene monomers or polydiacetylene chains with polyallylamine (PAH) resulted in thin films with an irreversible red color, which excluded them from being colorimetric sensors [42]. It is important to emphasize here that in order for polydiacetylene vesicles to be usable in sensing applications, the characteristic blue color of the vesicles must be maintained during the film preparation process [62-63].

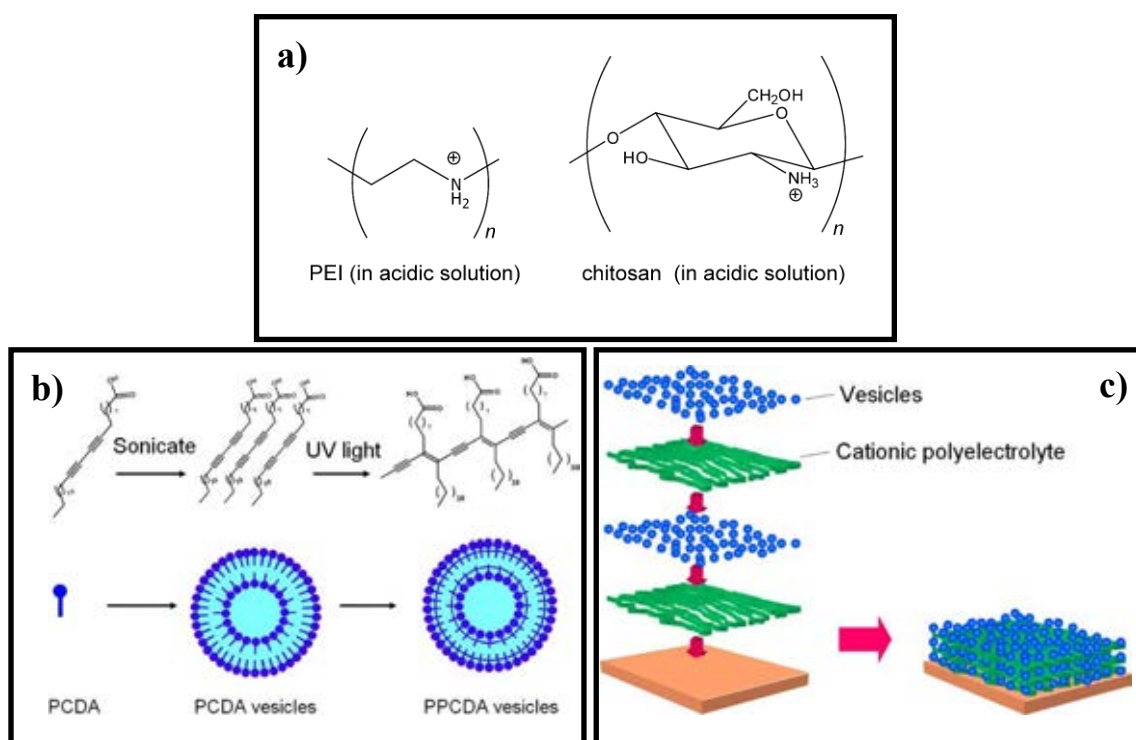


Figure 1.13 a) Chemical structures of polycationic polymers, b) schematic preparation of PCDA vesicles, and c) illustration of layer-by-layer assembly on glass substrate.

C. Electrospun fibers

Electrospinning has proved to be an efficient method for forming long polymer fibers with diameters in the range from nanometers to several micrometers [77]. In this technique, a high voltage is applied to a conductive capillary attached to a reservoir containing a polymer solution as shown in **Figure 1.14**. A charged polymer jet is ejected from the surface of the polymer solution when the charge imbalance exceeds the surface tension of the polymer solution. Polymer fibers are formed when the jet stream, driven by the electrostatic force, moves to the grounded screen collector [33].

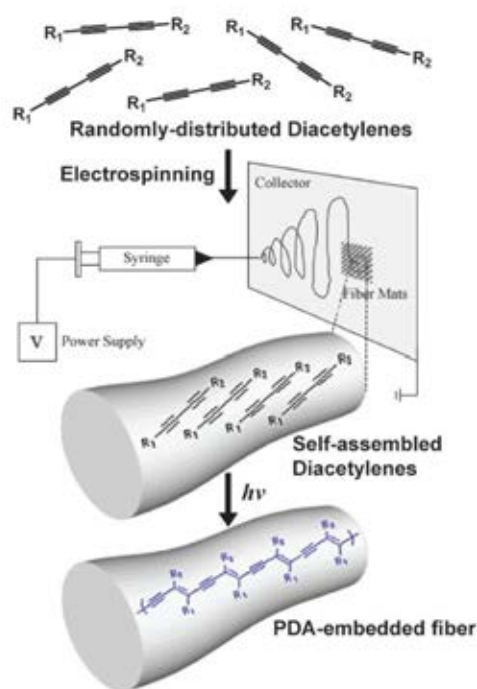


Figure 1.14 A schematic representation of the preparation of polymer fibers embedded with PDA supramolecules using the electrospinning technique, followed by irradiation with UV light.

1.3.2 Deposition of PDA

There are different techniques for fabricating the PDA onto various surface materials: ink-jet printing, airbrush painting technique, dip coating technique.

A. Ink-jet printing

In 2002, Magdassi, s. *et al.* [66] demonstrated new route for low-cost fabrication of various products that require fine patterning of functional molecules. The organic nanoparticles could be patterned, by printing of an oil-in-water microemulsion, in which the organic functional molecules are initially dissolved within the internal phase of the microemulsion. It was expected that the concept can be applied to a variety of organic molecules, including polymers, without the need for complex preparation processes prior to pattern printing by ink-jet printers (**Figure 1.15**).

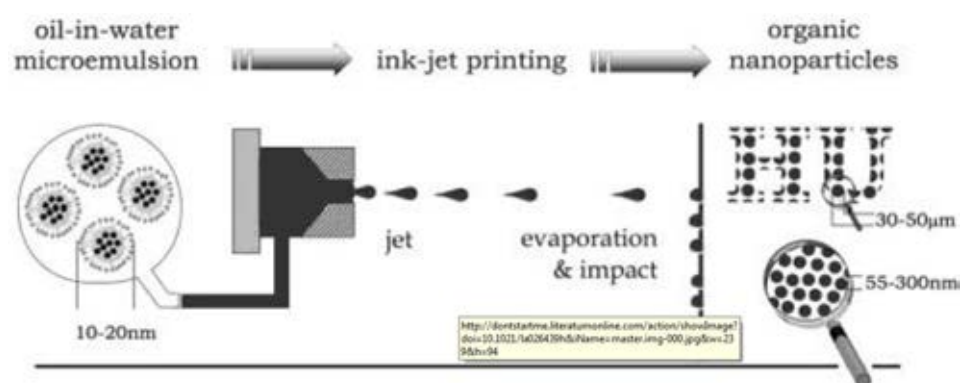


Figure 1.15 Schematic presentation of microemulsion conversion into nanoparticles by ink-jet printing.

In 2011, Yoon, B. *et al.* [56] generated printable ink solution to fabricate four diacetylene (DA) monomers, i.e. 10,12-Pentacosadiynoic acid (PCDA), *N*-(2-(2-(2-aminoethoxy)ethoxy)ethyl)pentacosyl-10,12-diyndamide (PCDA-EDEA), *N*-(2-(2-hydroxyethoxy)ethyl)pentacosyl-10,12-diyndamide (PCDA-AEE) and 3-pentacosyl-10,12-diyndamidobenzoic acid (PCDA-mBzA) on paper by printer technique [57-58] that can be used for daily life applications such as displays, sensors, solar cells, and memory devices. Nonionic surfactants (Brij® 78) was found to be compatible with all

of the DA monomers investigated and these composites enabled generation of reasonably high quality PDA images with a precursor concentration of about 13 mM suspended in an aqueous solution. **Figure 1.6c** shows a schematic representation of a supramolecular complex formed between DA monomers and nonionic surfactant. In the complex the hydrophobic alkyl chain of the surfactant molecule is embedded in the hydrophobic part of DA assembly and the hydrophilic ethylene oxide moieties favor the polar aqueous environment. Inspection of scanning electron microscopic (SEM) images, displayed in **Figure 1.6d**, reveals that a nanorod-like morphology of PCDA-Brij 78 composite exists and that the shape of the nanostructures are strikingly different from those obtained using pure PCDA (**Figure 1.16e**). The ink suspension was found to be stable for at least for three months at room temperature and could be used after a prolonged storage in a refrigerator about 6 months.

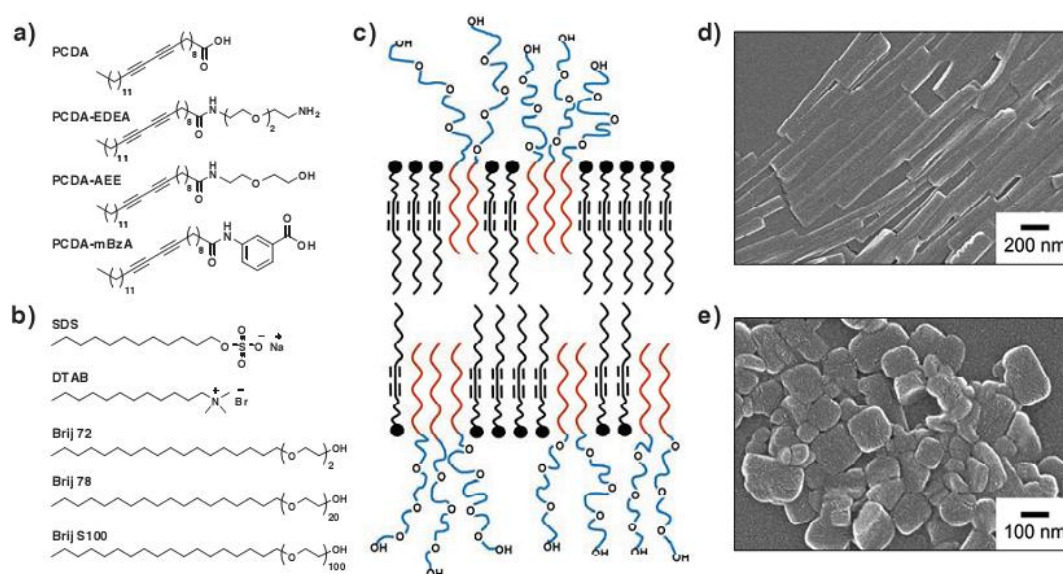


Figure 1.16 a) Structures of diacetylene monomers and b) surfactant molecules employed in this study. c) Schematic of a complex formed between diacetylene monomers and nonionic surfactants. d) SEM images of PCDA-Brij 78 composite and e) PCDA vesicles.

B. Airbrush painting

In 2012, Adrian, A. D. *et al.* [59] showed solution containing two diacetylene monomers, 2,4-hexadiyne-1,6-bis(phenylurethane) (HDDPU) and 2,4-hexadiyne-1,6-bis(*p*-chlorophenylurethane) (HDDCPU) (HDDPU:HDDCPU 10:1, in acetone solution) was used to the detection latent fingermarks on various surfaces such as, polymer banknotes, paper, non-porous surfaces (including glass, aluminum foil, coins), plastics (including fluorescent acrylic sheets, transparency sheets, parafilm and polyethylene bags) and infrared-reflective (metal-oxide coated) glass slides to develop fingermarks on a wide variety of surface, both non-porous and porous, including paper. An airbrush system was optimized for the application of the reagent solution. Once the solution evaporates on a surface, the monomers co-crystallize in different ways, depending upon a number of factors, including the surface residue. “Active” co-crystallization leads (with heat or radiation) to the formation of purple polymer, while “inactive” crystallization results in a non-polymerizable white deposit (**Figure 1.17**. Finger mark contrast was achieved as a result of active co-crystallization (giving purple polymer) in either the ridges or the furrows, depending upon the surface and other factors. A general observation (supported by spot tests with linseed oil, salt and amino acid solutions) was that on paper, oily materials are more likely to lead to the formation of the purple polymer, while the presence of water inhibits polymerization. An interesting observation was the development of fingermarks deposited on paper that had already been treated with the diacetylene reagent.

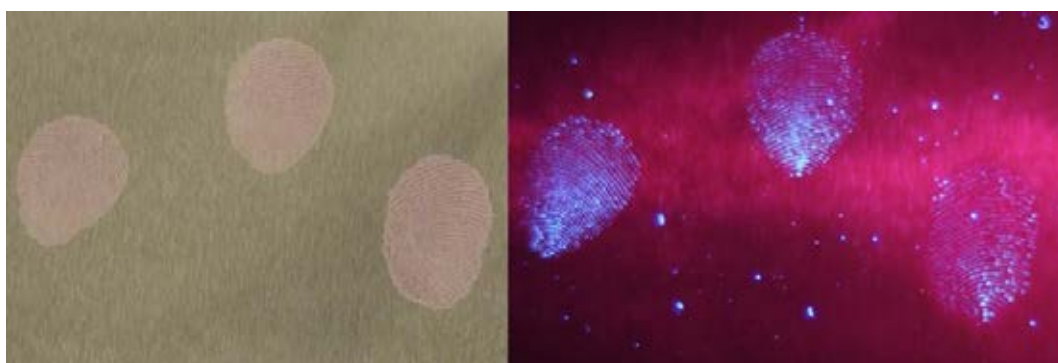


Figure 1.17 Inactive development under white light (left) and its interaction with 350 nm UV light (right). Although it is difficult to discern, it is the white ridges which are fluorescing on the right.

C. Dip coating

In 2011, Puntang, S. *et al.* [23] reported the synthesis of a novel series of diacetylene acids from the condensation of pentacos-10,12-diynylamine (PCDAmine) and dicarboxylic acid or its anhydrides. One of these diacetylene lipids, 4-(pentacos-10,12-diynylamino)-4-oxobutanoic acid (PCDAS), is used in combination with pentacos-10,12-diynoic acid (PCDA) for dropcasting on pieces of filter paper which are consequently irradiated by UV light to generate a paper based sensor array for solvent detection and identification. Upon the exposure to various types of organic solvents, the blue colored sensors colorimetrically respond to give different shades of colors between blue to red (**Figure 1.18**). The color patterns of the sensor array are recorded as RedGreenBlue (RGB) values and statistically analyzed by principal component analysis (PCA). The PCA score plot reveals that the array is capable of identifying eleven common organic solvents.

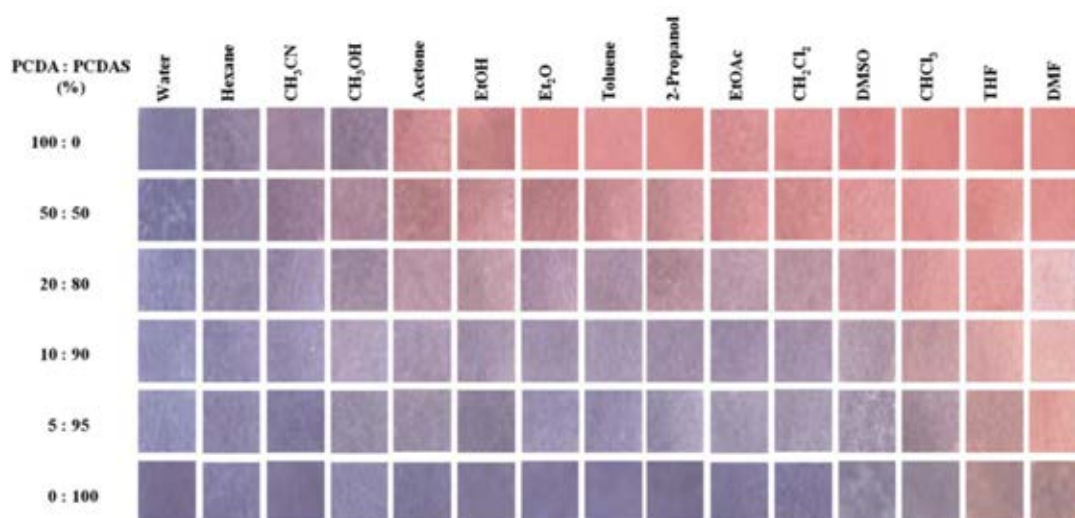


Figure 1.18 Array of cropped photographic images of PDAs on filter paper fabricated from PCDA and PCDAS responding to various organic solvents.

In 2011, Thongmalai, W. *et al.* [71] reported the synthesis and fabrication of PDA on filter paper for anionic surfactants from DAs containing primary amino, secondary amino and ammonium polar groups and preparation of the colorimetric sensors. From **Figure 1.19**, the blue to pink colorimetric transition of polymerized DAs in the presence of anionic surfactants such as sodium dodecanoate (SDC), sodium dodecyl sulphate (SDS), and sodium dodecyl benzene sulphate (SDBS) are observed by the naked eye.

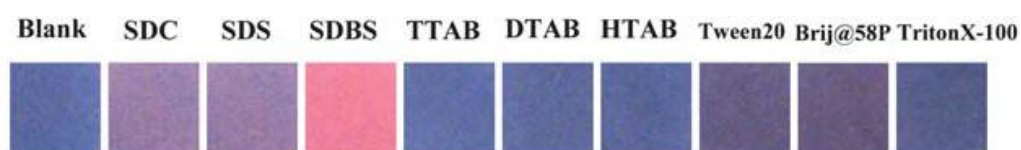


Figure 1.19 Photograph of PDA coated paper derived from primary amine (1% w/v) after being dipped in a solution of SDC, SDS, SDBS, TTAB, DTAB, HTAB, Tween 20, Brij@58P and Triton X-100 (500 mM).

In 2012, Eaidkong, T. *et al.* [25] reported detection and identification of VOCs by paper-based polydiacetylene (PDA) colorimetric sensor array. They were prepared from eight diacetylene monomers, six of which are amphiphilic and the other two are bola-amphiphilic. To fabricate the sensors, monomers are coated onto a filter paper surface using the drop-casting technique and converted to PDAs by UV irradiation. The PDA sensors show solvent induced irreversible color transition upon exposure to VOC vapors as shown in **Figure 1.20**. When combined into a sensing array, the color change pattern as measured by RGB values and statistically analyzed by principal component analysis (PCA) is capable of distinguishing 18 distinct VOCs in the vapor phase. The PCA score and loading plots also allow the reduction of the sensing elements in the array from eight to three PDAs that are capable of classifying 18 VOCs.

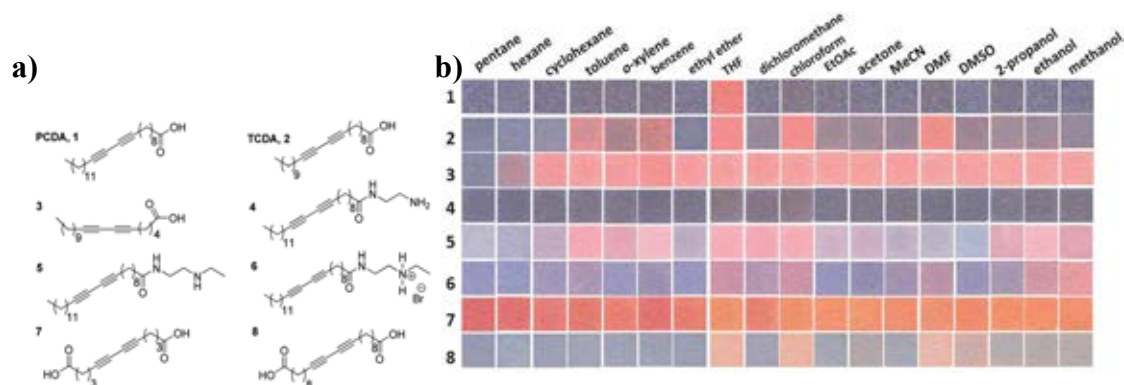


Figure 1.20 a) Structure of diacetylene monomers b) Scanned images of the paper-based PDA sensor array prepared from 1–8 exposed to various saturated vapors of volatile organic solvents.

1.3.3 Colorimetric properties of PDA

PDA usually appear as deep colored materials that exhibit interesting colorimetric properties. Optical absorption in polydiacetylene occurs via an electronic $\pi \rightarrow \pi^*$ transition within the linear π -conjugated polymer backbone. Upon polymerization, frequently the first chromogenically interesting state of PDA appears blue in color. The exposure of PDA to environmental perturbations, such as temperature, UV light, pH, solvent, mechanical stress and ligand-receptor interactions [75], induce a significant shift in absorption from low to high energy bands of the visible spectrum, so the polydiacetylene transforms from blue ($\lambda_{\max} \sim 630$ nm) to red ($\lambda_{\max} \sim 540$ nm) [8-9]. These perturbations alter the polymer side chain orientation that in turn change the backbone strain and torsion, thus changing the electronic states and the corresponding optical absorption. The most investigated PDAs are those having blue color, which can change their color to red corresponding to the shift of the maximum absorption peak from as a result of reduction of the effective conjugation length. The color transition can be induced by several external stimuli.

For plots of %B and %R as a function of temperature or time, the crossing point between %B and %R curves can be assigned as the color transition temperature or time. The percentages of the red (%R), green (%G) and blue (%B) colors can calculate by the following equations [69].

$$\%R = \frac{R}{R+G+B} \times 100 \quad (1)$$

$$\%G = \frac{G}{R+G+B} \times 100 \quad (2)$$

$$\%B = \frac{B}{R+G+B} \times 100 \quad (3)$$

A. Thermochromism

Thermochromism, the color transition upon the increase of temperature, is one of the interesting chromic properties of polydiacetylenes both for its applications and fundamental understanding [79]. Thermochromism in polydiacetylenes arises from the conformational changes of the conjugated backbone from planar to non-planar due to movement of the side chains. The color transition is thus resulted from the increase of energy gap between the HOMO and LUMO level. The color transition of polydiacetylenes is driven by the relief of mechanical strain in their structures [36].

For polydiacetylene vesicles, hydrogen bonding between the head groups of the lipid monomers is usually responsible for the planarity of the conjugated backbone. Thermal energy can break or weaken the hydrogen bonding between the head groups resulting in random movement of the side chains and lower the planarity of the backbone and hence the average conjugation length of π -electrons along the polymer backbone inducing the color change from blue to red.

In 1998, Okada, S. *et al.* [13]. studied the self-assembly in vesicles form of diacetylene containing carboxylic in hydrophilic head group and its derivatives which various alkyl chain length within the chain and between diacetylene and carboxyl group (**Figure 1.21**) in water media. Then polymerized by UV-irradiation 254 nm and studied the thermochromic properties monitoring by UV-vis spectrometer. It was found that polydiacetylene which have the short alkyl chain length between diacetylene and carboxyl group (compound 3 and 4) were more sensitive to the thermal changes than long alkyl chain length (compound 1 and 2).

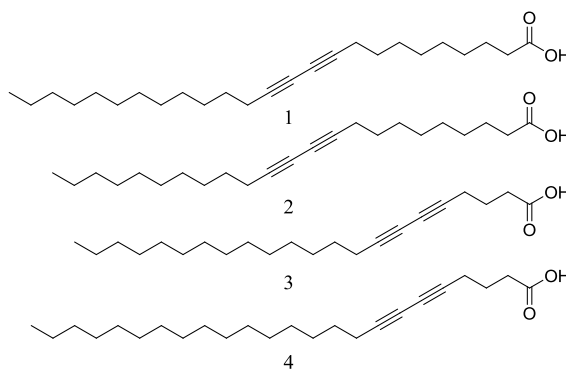


Figure 1.21 Structure of diacetylene monomers used in investigations of thermochromism in vesicles.

In 2005, Kim, J. M. *et al.* [3] reported the colorimetric reversibility of polydiacetylene supramolecules, derived from a variety of functionalized diacetylenic lipids as shown in **Figure 1.22**. Polydiacetylene vesicles prepared from PCDA-mBzA 1, bearing terminal *m*-carboxyphenylamido groups. They studied the effects of (1) internal amide groups, (2) headgroup aromatic interactions, (3) lengths of the hydrophobic alkyl chains, and (4) terminal carboxylic groups on the colorimetric reversibility of polydiacetylene. The results demonstrate that well developed hydrogen-bonding and aromatic interactions between headgroups are essential for complete recovery of the length of the conjugated π -electron chain following thermal stimulus.

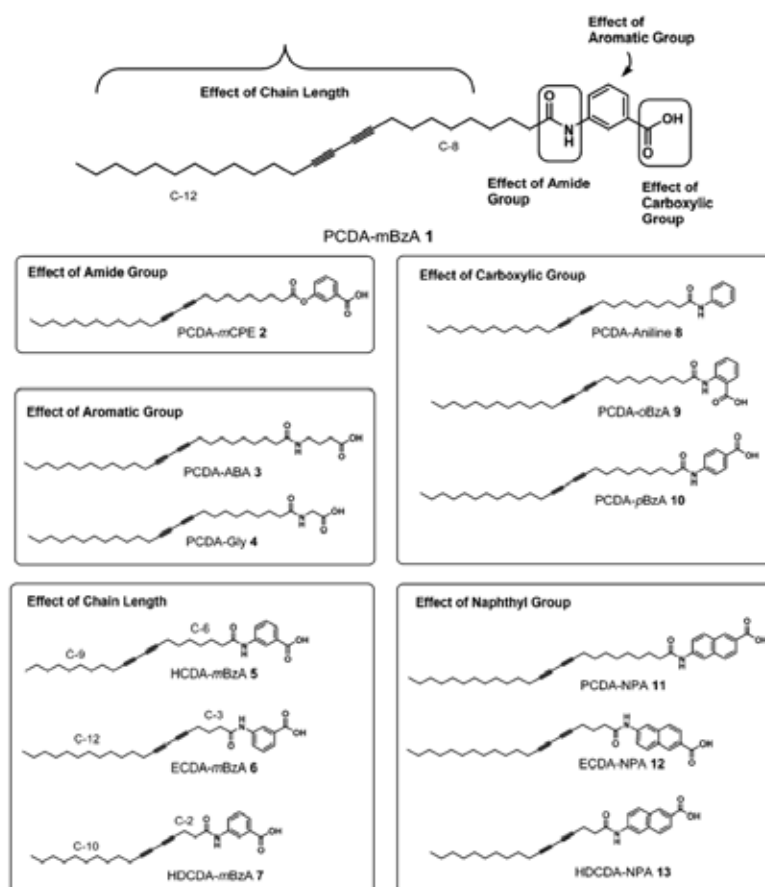


Figure 1.22 Structures of diacetylene lipids investigated for thermochromism.

In 2006, Kim, J. M. *et al.* [72] investigated blue-to-red color transition of PDA film, prepared from 10,12-pentacosadiynoic acid-2,2-(ethylenedioxy) bis(ethylamin) (PCDA-EDEA) embedded in Poly(vinyl alcohol) (PVA) reported the preparation of DA monomer (PCDA-EDEA) embedded in Poly(vinyl alcohol) film by mixing-drying process. The blue film obtained after UV irradiation and applied as thermal sensor. The author reported that the PCDA-EDEA thin film required higher temperature to induce a complete color transition from blue to red compared to the PCDA-EDEA in aqueous solution due to less mobility of PDA molecules in solid state as shown in **figure 1.23**.

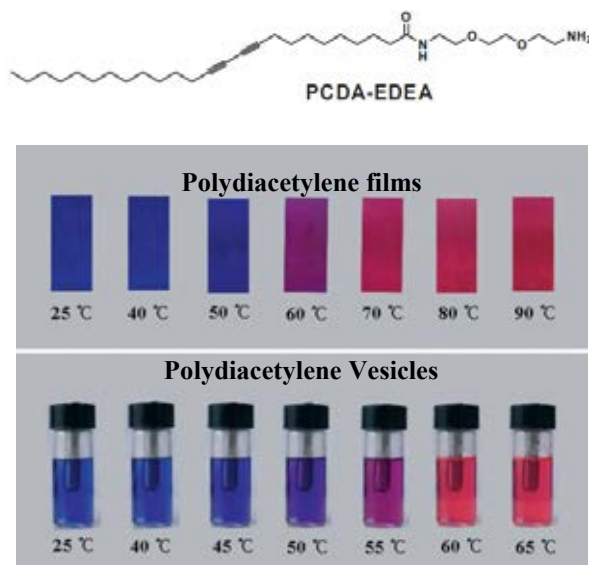


Figure 1.23 Photographs of PCDA-EDEA embedded in PVA film and the PCDA-EDEA vesicle solution during heating process.

In 2007, Fujita, N. *et al.* [37] proposed that molecular modeling to seek a stable conformation of PDA prepared from G_n s in the gel state which is useful in predicting the effective conjugation length (ECL) in PDA where the odd-even number of alkyl chains (n) is a key factor for determining the blue and red phases of the PDAs (See in **Figure 1.24**).

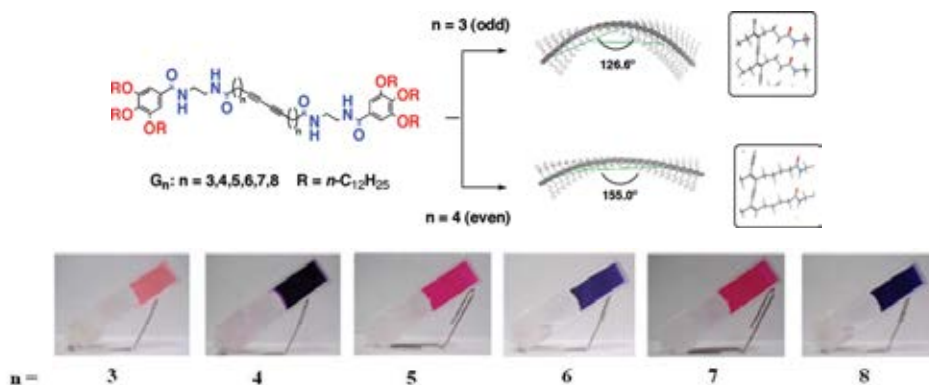


Figure 1.24 Chemical structure of G_n and the optimized conformation of 24 mers of (upper) poly G_3 and (lower) poly G_4 .

In 2009, Ahn, D. J. *et al.* [2] proposed the mechanism of the color transition from blue to red of PDA (**Figure 1.25**). The authors suggested that headgroup interactions (hydrogen bonding, aromatic interactions, etc.) play significant roles in leading the orientation of methylene sidechains of PDAs to a distorted state during the polymerization process. The distortion results in mechanical strain in the PDA backbone. In the case of color irreversible PDA system, head group interactions are relatively weak. Thus, the release of mechanical strain upon thermal stimulation results in C-C bond rotation of polymer backbone and weakening of headgroup hydrogen bonding interaction.

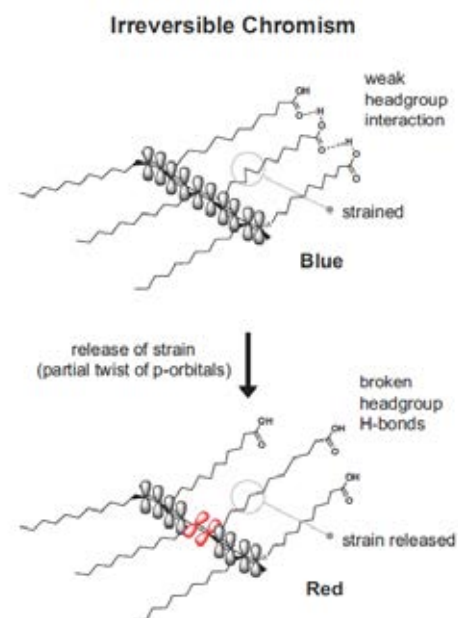


Figure 1.25 Mechanism of chromic responses of irreversible PDAs.

In 2010, Wacharasindhu, S. *et al.* [8] synthesized Mono- and diamides derivatives of 10, 12-pentacosadiynoic acid (PCDA) from condensation of PCDA with various aliphatic and aromatic diamines. The color transition temperatures and thermochromic reversibility of the polymers are varied depending on the number of amide groups and the structure of the aliphatic and aromatic linkers. The phenylenediamide and polymethylenediamide PCDA derivatives give polydiacetylenes with complete thermochromic reversibility, while the polydiacetylenes obtained from 1,2-cyclohexylene and glycolic chain diamide derivatives exhibited irreversible thermochromism, whereas the polymers attained

from the aromatic monoamide analogues are partially reversible. The variation of the linkers also allows the color transition temperature of the polydiacetylene to be tuned in the range of 20 °C to over 90 °C (See in **Figure 1.26**).

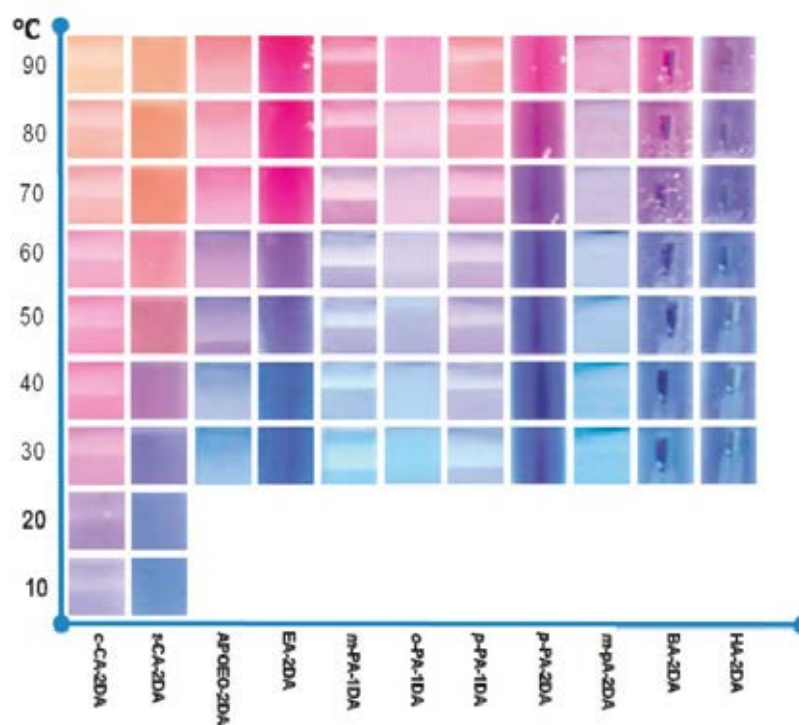


Figure 1.26 Color of PDA sols recorded by photography during the heating process displaying the variation of color transition temperature.

In 2010, Phollookin, C. *et al.* [9] investigated a series of bisdiynamide lipids containing various lengths of methylene spacer ($m=2, 3$ and 4) between the diynes and the diamide headgroup and number of methylene units ($n = 6$ and 9) in their hydrophobic tails are synthesized. The color transitions from blue to red during heating-cooling cycles of the PDA sols are photographically recorded and monitored by UV-vis absorption spectroscopy. The bisdiynamide PDAs exhibit excellent thermochromic reversibility and the color transition temperature can be tuned between 25-55 °C by the variation of m and n values as shown in **Figure 1.27**. The decrease of n value enhances the thermal sensitivity resulting in lower color transition temperature, the effect of m value is not as straightforward. Moreover, temperature indicators can be obtained by applying a screen printing ink formulated from the

bisdiynamide monomer on plastic substrates followed by UV irradiation to generate desired patterns of thermochromically reversible PDAs.

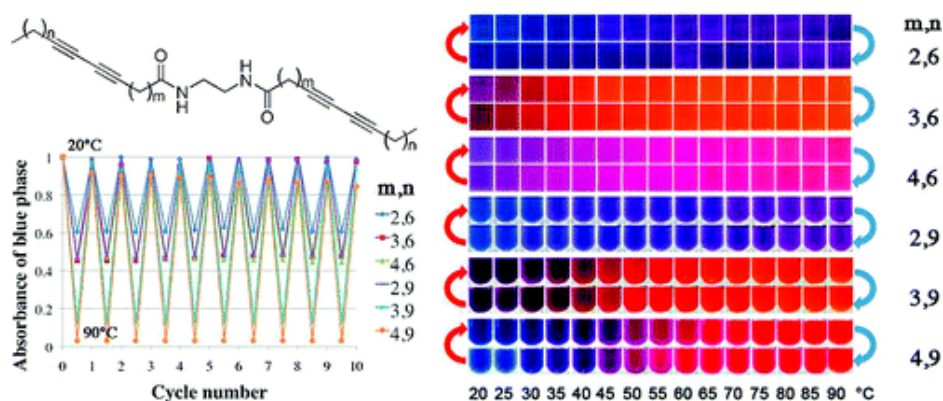


Figure 1.27 Structure of diacetylene monomers, their color transition and reversibility in vesicles solution.

In 2012, Ampornpun, S. *et al.* [38] reported that two series of symmetrical (S_x) and unsymmetrical (U_y) diacetylene monomers containing diamide groups with different methylene units are successfully prepared (See in **Figure 1.28**). Photopolymerization of their nanovesicles dispersed in water is carried out by irradiation at 254 nm affording blue sols of the corresponding PDAs. The degree of thermochromic reversibility (%DR) of the PDA sols are determined using UV-vis spectroscopy in order to probe effects of the number of the methylene units, x and y , within the linker and hydrophobic tail, respectively. The complete color reversibility (%DR > 89%) is observed only when x is an even number while partially reversible or irreversible thermochromism (%DR < 65%) is displayed in the case of odd x number. For the U_y series, the color recovering ability within the heating and cooling process increases along with the y number; %DR = 3, 62, and 90% for $y = 0, 4$, and 16, respectively. This work is the first direct demonstration of the roles of number of methylene units within the diacetylene monomers on the thermochromic reversibility of their PDAs that provide additional dimensions for rational molecular design in the development of PDA thermal sensors.

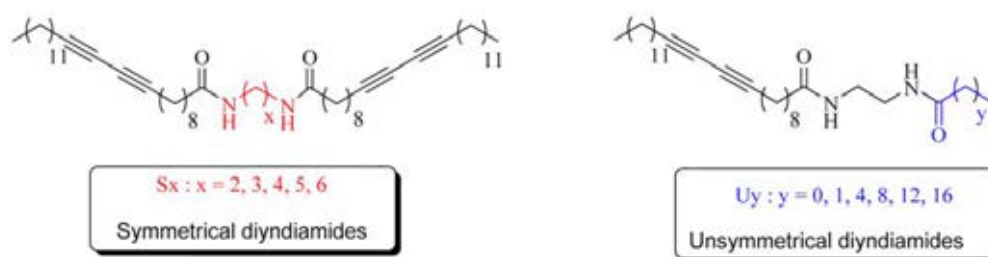


Figure 1.28 Structure of investigated diacetylene monomers: symmetrical diyndiamides (S_x) and unsymmetrical diyndiamide monomers (U_y).

In 2013, Chanakul, A. *et al.* [39] reported polydiacetylene (PDA)/ZnO nanocomposites are prepared by using three types of monomers with different alkyl chain length, 5, 7-hexadecadiynoic acid, 10, 12-tricosadiynoic acid, and 10,12-pentacosadiynoic acid. The monomers dispersed in aqueous medium spontaneously assemble onto the surface of ZnO nanoparticles, enhanced by strong interfacial interactions. All nanocomposites show reversible blue/purple color transition upon multiple heating/cooling cycles, while the irreversible blue/red color transition is observed in the systems of pure PDAs (**Figure 1.29**). The shortening of alkyl side chain in PDA/ZnO nanocomposites leads to a systematic decrease in their color transition temperatures.

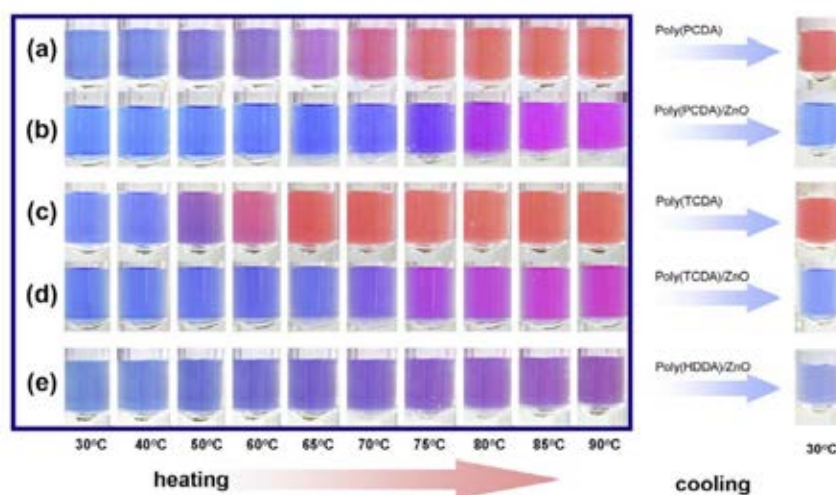


Figure 1.29 Color photographs of the aqueous suspensions of (a) pure poly(PCDA), (b) poly(PCDA)/ZnO nanocomposite, (c) pure poly(TCDA), (d) poly(TCDA)/ZnO nanocomposite, and (e) poly(HDDA)/ZnO nanocomposite taken upon increasing temperature from 30 to 90 °C, followed by cooling to room temperature.

B. Solvatochromism

Solvatochromism is the ability of a chemical substance to change color due to a change in solvent polarity. The molecularly ordered states of supramolecular PDAs can be influenced also by the presence of organic solvents as investigated by many researchers.

In 2007, Yoon, J. *et al.* [31] have developed the efficient sensors for the detection of volatile organic compounds (VOCs) based on conjugated polymer-embedded electrospun fibers. The observation of an organic solvent induced, blue-to-red color transition of PDA embedded electrospun fibers suggests that the colorimetric response might vary in an organic solvent-dependent manner on the structure of diacetylene monomer. They show different colorimetric responses upon exposure to the 4 organic solvents such as chloroform, tetrahydrofuran (THF), ethyl acetate (EA), or *n*-hexane as illustrated in **Figure 1.30**.

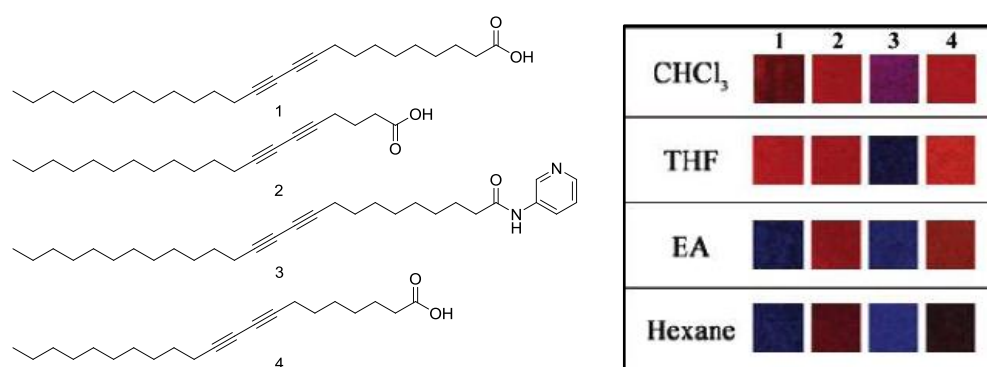


Figure 1.30 Photographs of the PDA-embedded electrospun fiber mats prepared with diacetylene monomers 1-4 after exposure to organic solvent.

In 2008, Potisatityuenyong, A. *et al.* [7] conducted extensively investigation poly-10,12-pentacosadiynoic acid (poly(PCDA)) vesicle solution in the aspect of thermochromism, solvatochromism and alkalinochromism. In the case of solvatochromic and alkalinochromic experiment, UV-vis absorption and observation by eye show the similar pattern, blue to red color transformation. The decreasing and increasing in absorbance of red and blue phase without peak shifting indicate directly to quantitative conversion between blue and red vesicle. Solvatochromism and alkalinochromism involve hydrogen bond breaking turning the blue vesicle into red color. The author proposed the mechanism of color transition of PCDA as shown in **Figure 1.31**.

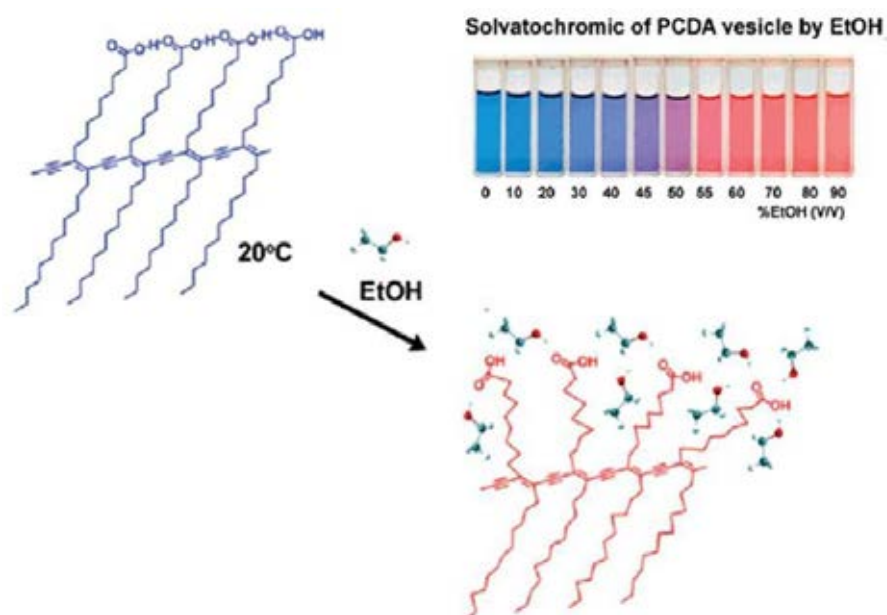


Figure 1.31 Proposed side-chain movements in the chromic transitions of poly(PCDA) vesicles upon organic solvent.

In 2009, Yoon, J. *et al.* [48] have generated the electrospun fiber mats from PDA-embedded polymer matrix that can be used to detect volatile organic compounds (VOCs). The results display the different color patterns of the fiber mats derived from different combinations of PDA-ABA 1 and PCDA-AN 2 as illustrated in **Figure 1.32**.

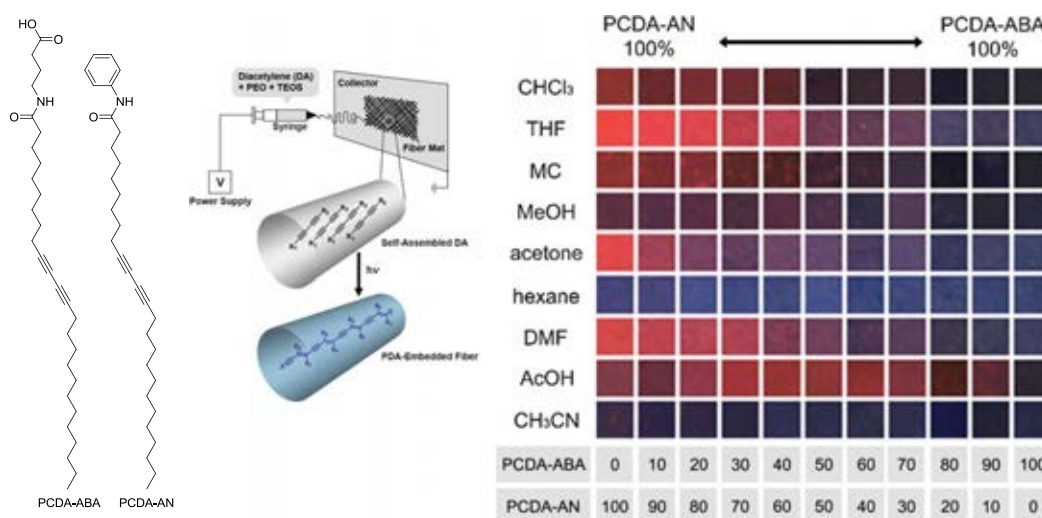


Figure 1.32 Schematic representation of the preparation of PDA-embedded electrospun microfibers and photographs of the polymerized PDA-embedded electrospun fiber mats after exposure to organic solvents at 25 °C for 30 s.

In 2010, Jiang, H. *et al.* [49] have also reported the development of a novel polydiacetylene (PDA)-based sensitive colorimetric microarray sensor for the detection and identification of volatile organic compounds. PDA-embedded polymer matrix films as the multi-layer PDA-based micro patterns (**Figure 1.33**) could be prepared by the spin-coating method combined with the sol-gel process. Polydimethylsiloxane Sylgard 184 (PDMS) was employed to enhance the stability of the PDA films when dipped in VOCs, especially chlorinated solvent.

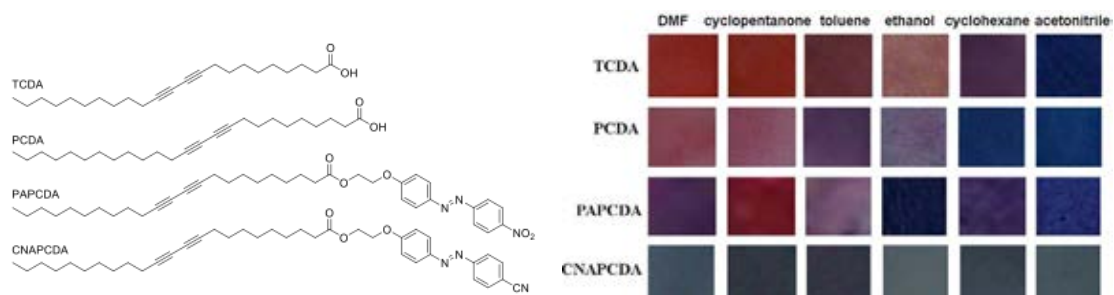


Figure 1.33 photographs of the PDA-embedded polymer matrix films derived from TCDA, PCDA, PAPCDA and CNAPCDA after dipped in organic solvents at room temperature.

In 2010, Gou, M. *et al.* [70] demonstrated time–temperature chromatic sensor based on PDA vesicle and amphiphilic polymer. In presence of amphiphilic polymers (*i.e.* Pluronic F127, F68 and L35 and Tween-20), PDA vesicles could gradually transit from blue to red, which was irreversible and depended on the temperature, time, and properties of amphiphilic polymer (**Figure 1.34**). The authors suggested that the hydrophobic segment of amphiphilic polymer were gradually inserted into vesicles due to hydrophobic interaction. This work provides Time-temperature chromatic sensor based on PDA vesicles and amphiphilic polymers and use as time-temperature indicator.

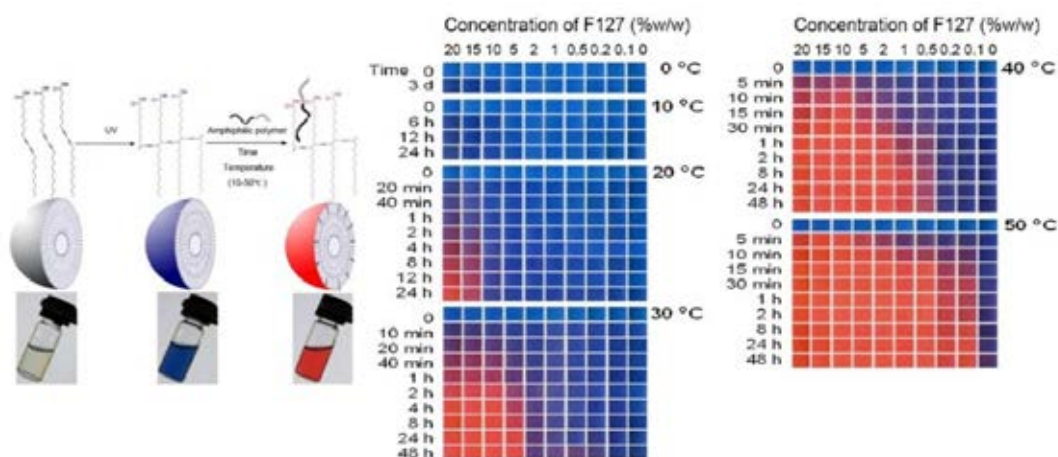


Figure 1.34 Photographs of TTIs prepared from PCDA solution incorporated with Pluronic F127.

In 2010, Wu, S. *et al.* [50] investigated the effects of solvents on structure of micelle-like assemblies of an azo chromophore-functionalized polydiacetylene (polyAzoDA) and polymerized tricoso-10,12-diynoic acid (polyTDA). They used the mixtures of water with glycol, DMSO, ethanol and THF to observe blue-to-red color changes of polydiacetylenes. They found that the colors of polyTDA and polyAzoDA change at certain contents of organic solvents. The results in **Figure 1.35** exhibit the strength of the polyTDA-solvent interaction in the following order: THF>ethanol>DMSO>glycol. According to the results, THF is a solvent which can effected on blue-to-red color transitions of polyAzoDA in THF/water mixtures. However, they do not observe color transitions in the other solvents/water mixtures. The authors have proposed that the stability to several solvents of polyAzoDA caused by the H- and J-like aggregates of azo chromophores in polyAzoDA.

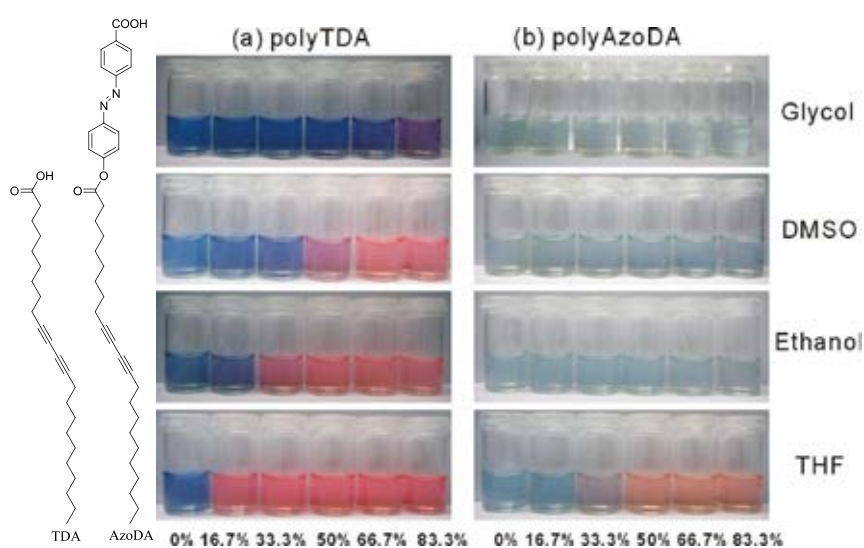


Figure 1.35 Photographs of micelle dispersions in different water-solvent mixtures. At increasing solvent content, the color of (a) polyTDA and (b) polyAzoDA changes from blue to purple/red depending on type of solvent and its relative content, respectively.

In 2012, Pattanatornchai, T. *et al.* [73] investigated the color transition behavior of PDA using different alcohol (i.e. molecule size, length, shape, polarity and charge)(linear and branched alcohol). In the case of linear alcohol, the longer alkyl chain causes easier colorimetric response (**Figure 1.36a** and **1.36b**). The author suggested that the driving force for the alcohols to penetrate into the hydrophobic layers of the PDAs increases with increasing the alkyl length. The longer alcohols can also penetrate into the deeper region of PDA layers. Therefore, it requires lesser amount of long chain alcohols to induce segmental rearrangement and hence color transition of the PDAs (**Figure 1.36c**).

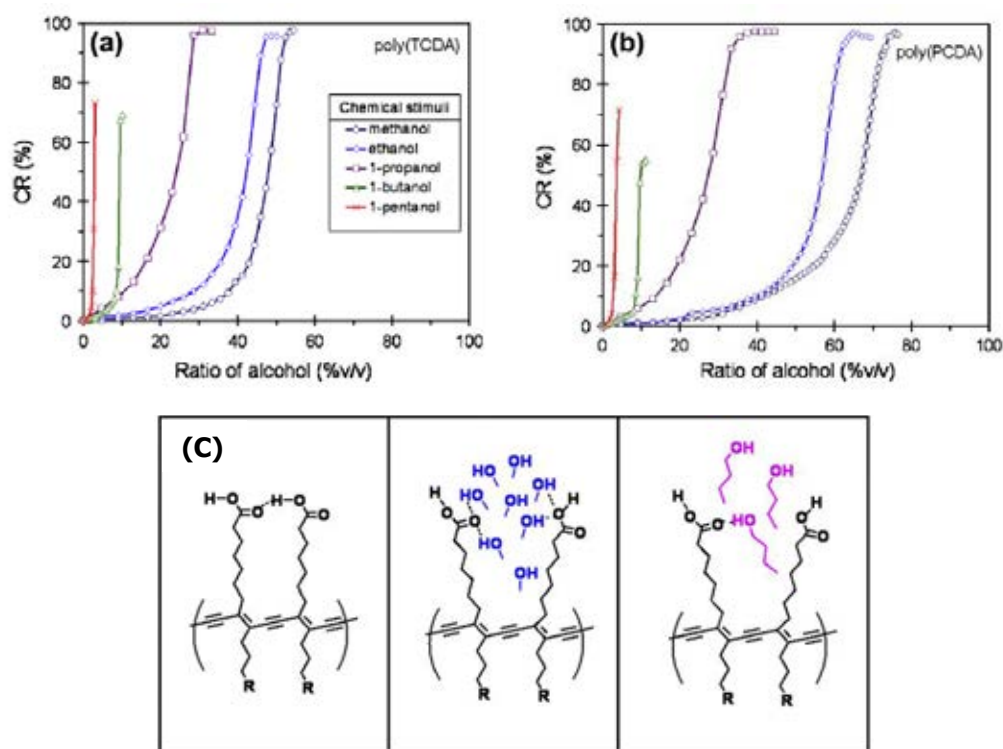


Figure 1.36 Colorimetric responses (CR) of **a**) poly(TCDA), **b**) poly(PCDA) vesicles in aqueous suspensions upon addition of linear alcohols with different chain lengths and **c**) the penetration of methanol and 1-butanol into the layers of poly(PCDA).

C. Alkalinochromism and Acidochromism

Alkalinochromism and acidochromism were chromic properties that material can change color by deprotonation in case of alkalinochromism and protonation in case of acidochromism. Either alkalinochromism or acidochromism, the role of head group of diacetylene monomer had directly impact on the colorimetric transition as reported by several researchers.

In 1998, Cheng, Q. *et al.* [51] had been synthesized and studied the colorimetric response in various pH solutions of a series of amino acid-derivatized 10,12-pentacosadiynoic acid. The result showed a different colorimetric response based on type of head groups. For example, Glu-PDA which has dicarboxylic head group changed the color from blue to red at pH 6 by deprotonation of the carboxylic group. The protonation of the tertiary amine head group of DMAP-PDA changed its color at pH 5. His-PDA which has both of carboxylic and imidazole changed the color at pH below 0 and pH 8-9 (**Figure 1.37**).

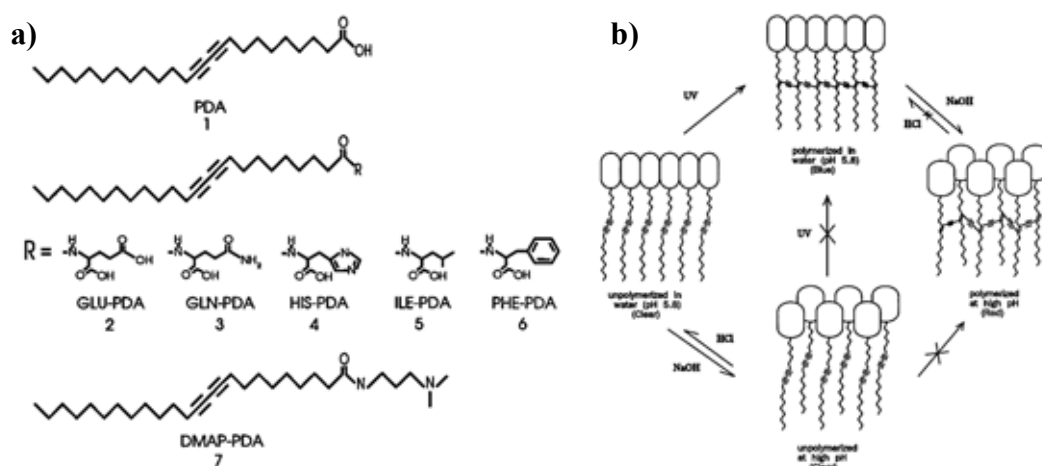


Figure 1.37 a) Structure of the diacetylene lipid 10,12-pentacosadiynoic acid (1) and its derivatives: lipids 2-6, amino acids derivatives; lipid 7, 3-(dimethylamino) propylamine (DMAP) derivative. b) Schematic diagram of amino acid-derivatized polydiacetylene liposomes in a chromatic transition.

In 1999, Jonas, U. *et al.* [15] studied a novel system based on hydrazide derivatives of single chain diacetylene lipids which are 10,12-Tricosadiynohydrazide (THY) and 10,12-Pentacosadiynohydrazide (PHY). These materials showed an unusual aggregation and polymerization behavior in organic solution, in contrast to the parent carboxylic acids. In addition, these hydrazide lipids undergo an unprecedented reversible color change (blue/red) in polymerized vesicles when the pH of the surrounding aqueous medium is cycled between acidic and basic conditions. This unusual behavior is attributed to the unique hydrogen-bonding pattern of the hydrazide head group (**Figure 1.38**).

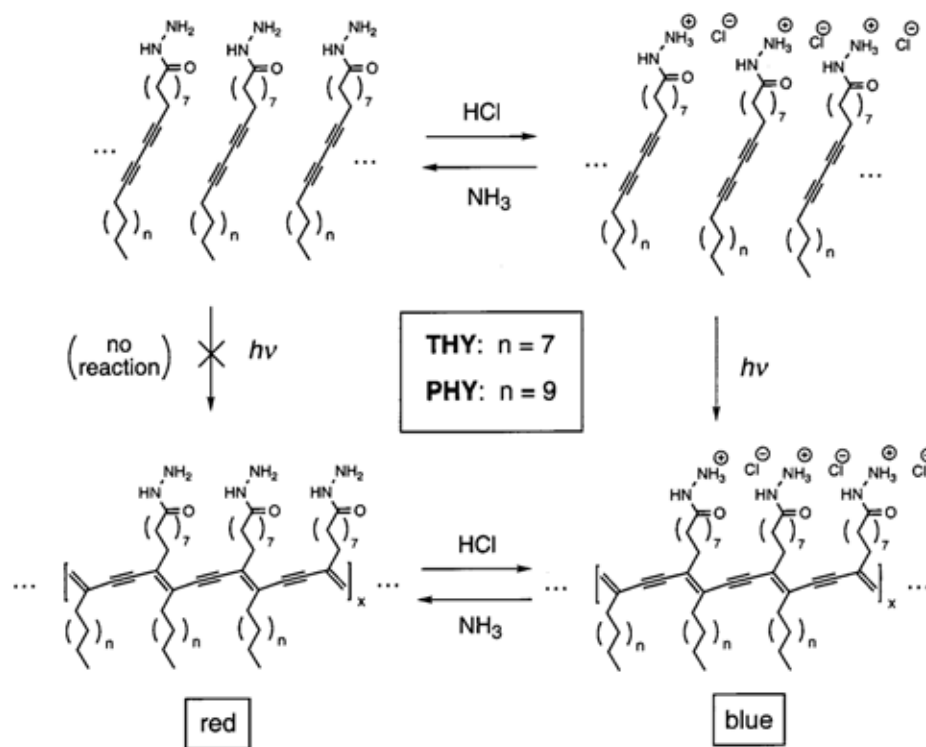


Figure 1.38 Schematic representations of the polymerization behavior and colorimetric changes of the diacetylene hydrazides PHY and THY in the presence of HCl or NH₃.

In 2011, Charoenthai, N. *et al.* [52] investigated that the colorimetric response of the polydiacetylene (PDA) vesicles prepared by 10,12-tricosadiynoic acid (TCDA), 10,12-pentacosadiynoic acid (PCDA) and N-(2-aminoethyl)pentacosadiynoic acid (AEPCDA) were stimulated by temperature, ethanol and pH. They found that a shorter side chain of poly(TCDA) yields weaker inter- and intra-chain dispersion interactions in the bilayers compared to the system of poly(PCDA). The color transition of poly(TCDA) and poly(PCDA) vesicles occurred when increasing of pH to ~ 9 and ~ 10 , respectively (**Figure 1.39**). The poly(AEPCDA) vesicles, on the other hand, change color upon decreasing pH to ~ 0 .

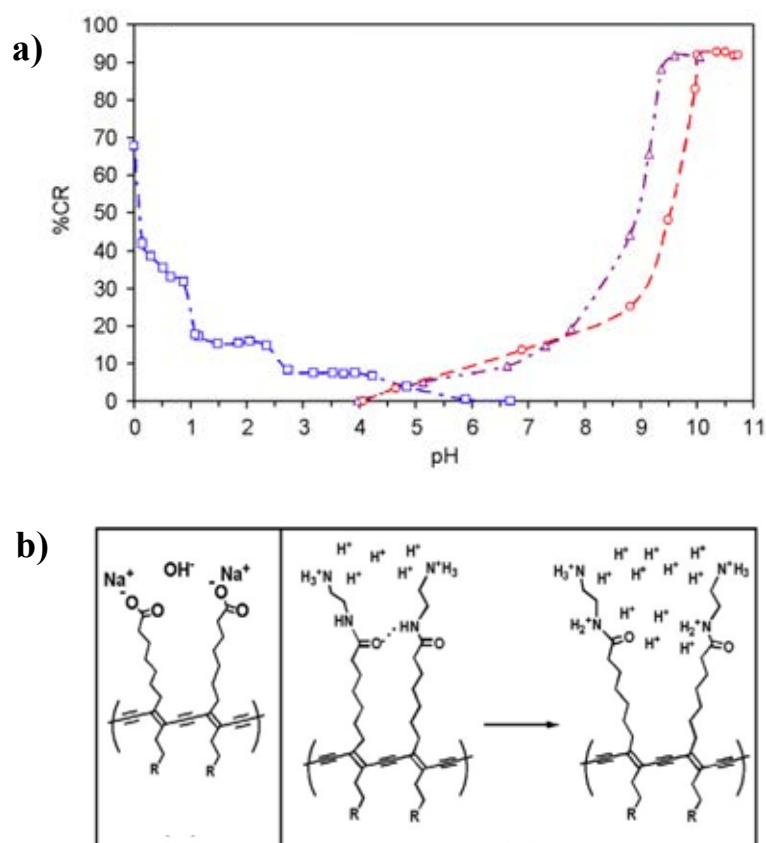


Figure 1.39 a) The colorimetric responses (%CR) of the vesicles were plotted as a function of pH. Symbols are (○) poly(PCDA), (△) poly(TCDA) and (□) poly(AEPCDA). b) The charged species of head groups of poly(PCDA) in high pH region and poly(AEPCDA) in low pH region.

1.3.4 Fabrication of thermochromic leuco dyes

In 2009, Marla, V. *et al.* [64] investigated online measurements of fiber temperature and diameters were made for both the melt-spinning and the meltblowing processes. The fiber temperature was determined by infrared thermography, and the fiber diameter was determined by high-speed photography (**Figure 1.40**). These measurements were then compared with predictions made with mathematical models for melt spinning and melt blowing. In melt spinning, the fibers seemed to cool slightly faster with an increase in spinning speed for both polypropylene (PP) and polybutylene (PB). When the heat in melt blowing, the fiber temperature at any downstream location showed a slight increase with an increase in the mass studied. The predictions of the fiber diameter profile from the melt-blowing model compared favorably with experimental data obtained from high-speed flash photography. The choice of heat transfer correlation did not show a strong effect on the predicted diameter profile obtained from the melt blowing model. There was good agreement between the models and the experimental results, and the agreement was best when heat-transfer correlations developed specifically for fine fibers (cylinders) were used.

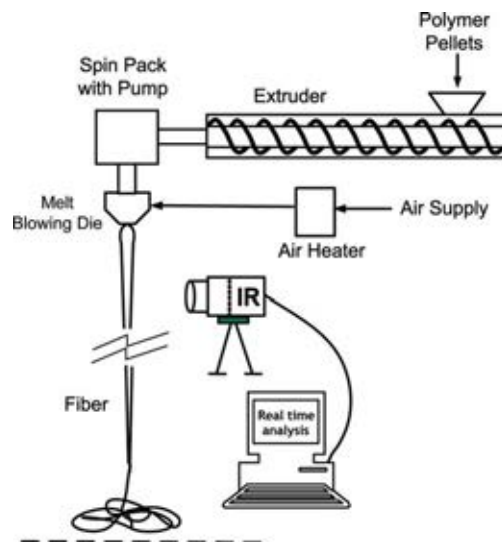


Figure 1.40 Equipment used for spinning fibers while measuring fibers diameter and temperature.

In 2009, Chen *et al.* [65] investigated the initial example of producing fibers with improved properties by the well-controlled generation of the precursor morphology using the practicable melt-spinning process. Poly(ethylene terephthalate) (PET) and poly(ethylene naphthalate) (PEN) fibers with unique precursor morphology were directly produced in the melt-spinning process via a liquid isothermal bath (LIB). The fibers, which were white in color, were amorphous but oriented, as measured by WAXD. SEM observations revealed a banded structure and microvoids in the white fibers (**Figure 1.41**). After hot drawing, the white color of the fibers faded, accompanied by the transformation of the banded structure into a highly crystallized fibrillar structure. As a result, fibers with improved properties were produced by applying a low draw ratio.

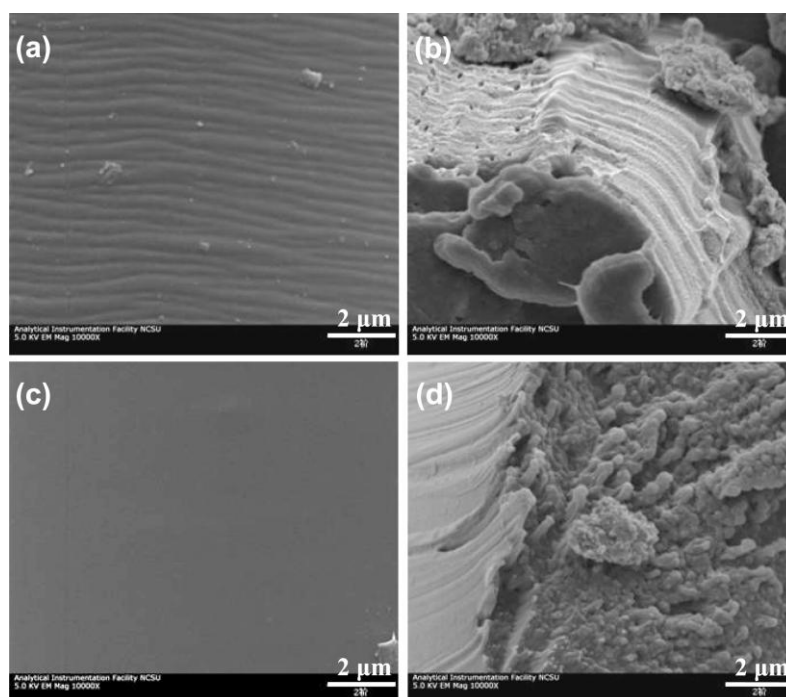


Figure 1.41 SEM images of PEN fibers spun with LIB (a) surface and (b) cross section of undrawn fibers; (c) surface and (d) cross section of drawn fibers.

In 2009, Kauffman, J *et al.* [61] created polydiacetylene (PDA)-doped calcium alginate fibers by the solution blending of polymerized 10,12- pentacosadiynoic acid liposomes with sodium alginate in water prior to extrusion. The liposomes maintained their blue color during wet spinning and drying of the fibers but changed to red with exposure to specific external stimuli (heat, solvent, and chemical) (**Figure 1.42**). In the latter case, the color change only occurred when the fibers were sufficiently permeable for the reacting species to reach the interior. A parameter termed the “Raman response” (RR) has been developed to quantify the amount of PDA liposomes in each of two critical conformations within the fibers. The RR attributes a quantitative measure of PDA response to individual stimuli. This method provides advantages over the commonly used “colorimetric response” in systems where sample limitations and chromophore activity make UV-vis spectroscopic measurements difficult or inaccurate. PDA liposomes are shown to effectively add a versatile sensing component to alginate fibers.

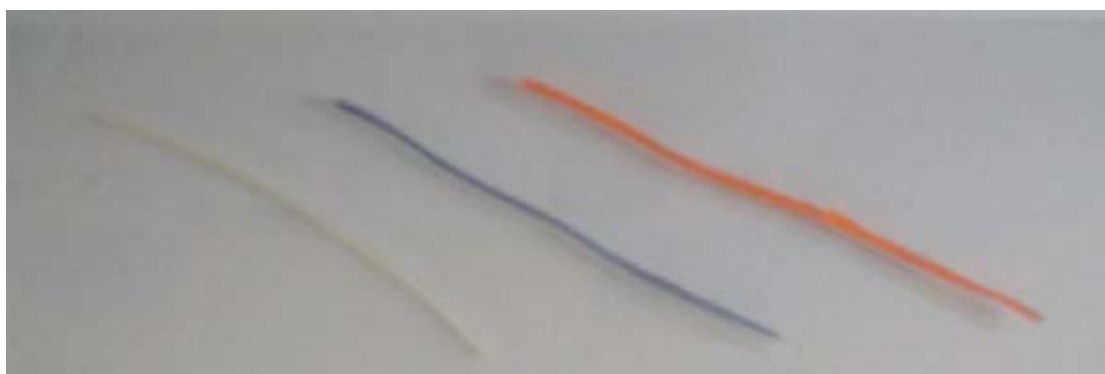


Figure 1.42 From left: Photograph of the control alginate fiber (white), as-spun alginate fiber with PCDA liposome (blue), and alginate fiber with PCDA liposome after exposure to 60 °C for 45 s (red).

In 2010, Malherbe *et al.* [68] demonstrated a ‘solvent facilitated’ coaxial electrospinning process was used to produce reversible narrow temperature gap thermochromic, core-shell fibers (**Figure 1.43**). A thermochromic composite composed of crystal violet lactone (the leuco dye), bisphenol A (the developer) and 1-dodecanol (the phase-change solvent) was entrained as core material inside poly(methyl methacrylate) shells. A mutual core and shell solvent (chloroform) was used to obtain low interfacial tension between the core and shell spinning solutions. This enabled room temperature entrainment of the low molecular weight, low viscosity core fluid. In order to minimize the effect of light scattering and subsequently produce fibers with visible color transitions, the fibers were produced with external diameters of 3-8 mm and core diameters of 1.7-5.7 mm. In order to produce core-shell fibers with repeated, reversibly thermochromic behaviour and a stable color developed state, it was necessary to entrain a dye composite that contained an excess developer, essentially making this composite non-thermochromic prior to entrainment. The fibers were analyzed using SEM and DSC.

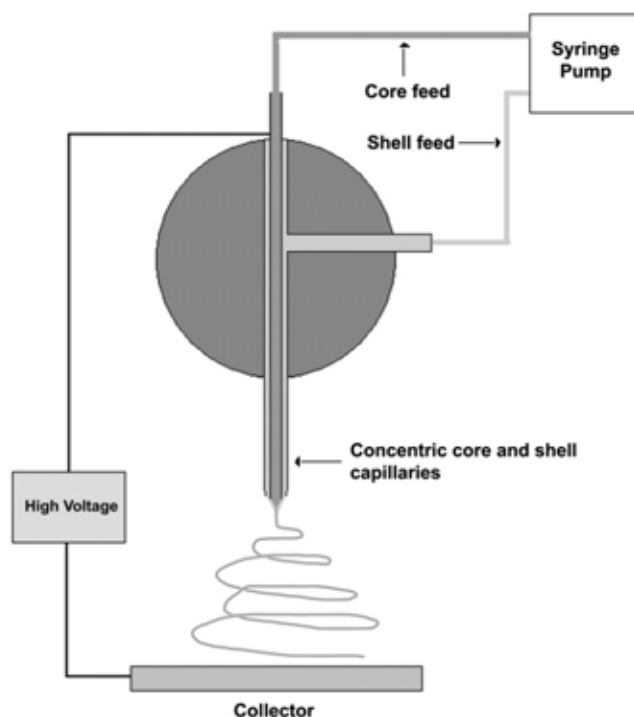


Figure 1.43 Coaxial electrospinning setup used to produce thermochromic core-shell PMMA fibers.

1.4 Objectives and scope of the research

The main goal of this thesis is to develop a practical colorimetric indicator from chromic materials i.e. diacetylene and leuco dyes by studying various surface deposition and incorporation techniques. To achieve this goal, the following working scopes are set:

1. To study the surface deposition techniques i.e. ink-jet printing, airbrush painting and dip coating of diacetylene lipids and leuco dyes on various materials.
2. To evaluate the colorimetric responses of diacetylene and leuco dye coated materials.
3. To study incorporation techniques i.e. melt spinning, compression molding and two roll mill of leuco dyes into various commercial polymers.
4. To evaluate the colorimetric responses of leuco dye incorporated polymers.
5. To select the suitable deposition or incorporation techniques to be used in the development of at least one indicator prototype.

CHAPTER II

EXPERIMENTAL

2.1 Surface deposition of diacetylene and leuco dye

Materials :

- 10,12-Pentacosadiynoic acid (PCDA), GFS Chemicals, USA
- 10,12-Tricosadiynoic acid (TCDA), GFS Chemicals, USA
- Brij[®] 58 P, Fluka
- Triton[®] X-100, Fluka
- Tween[®] 20, Fluka
- Sodium hydroxide (NaOH), Merck, Germany
- Potassium carbonate anhydrous (K₂CO₃), Fluka, France
- Magnesium chloride (MgCl₂), Sigma-Aldrich, USA
- Lithium chloride anhydrous (LiCl), Fluka
- Calcium chloride dehydrated (CaCl₂), Fluka
- Dimethyl sulfoxide, RCI Labscan
- Thinner, Ocean Rota Co., Ltd, Thailand
- Lacquer (TOA T-5000), TOA PAINT (THAILAND) CO.,LTD, Thailand

Equipments :

- Rotary evaporator, R200, Buchi , Switzerland
- Ultrasonicator, Elma, Germany
- UV Lamp, TUV 15W/G15 T18 lamp, Philips, Holland
- Webcam, ICON228, 14M pixels
- Airbrush ,HKX HB-3G, Hongkong
- Printer, HP Deskjet K109g
- Ink cartridge, HP 703
- Laptop, Lenovo Thinkpad E435, Malaysia
- pH meter, UB-10, Denver Instrument
- Magnetic stirrer, Fisher Scientific, USA
- Hot plated magnetic stirrer, IKA, Germany
- Syringe filter, Verticlean, PTFE, 13 mm, 0.45 μm

2.1.1 Photographic imaging and colorimetric analysis

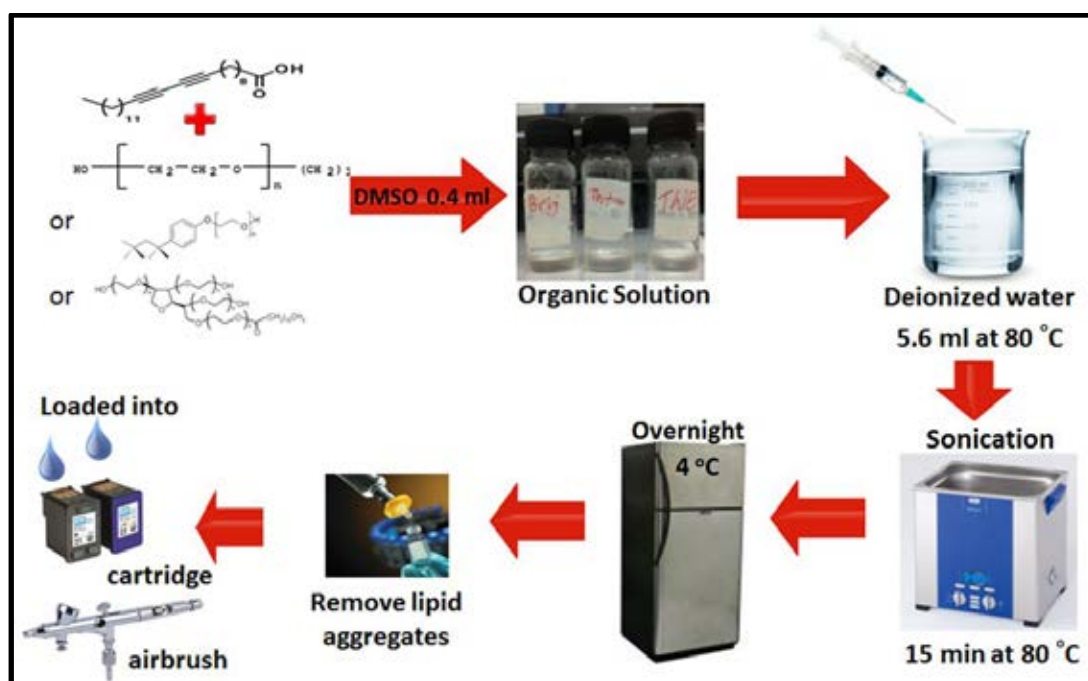
The images on thin substrates were obtained by a scanner (Epson Perfection V33). For real time monitoring, a commercial webcam (ICON228, 14M pixels) was used. The color pictures of thick or 3-D substrates were captured by a Digital SLR camera (Nikon D40X with a Nikon Nikkor lens 18–55 mm) fixed to a camera stand at the nearest distance from the object for possible focus.

The colors of the images were evaluated into RGB values by an image processing program (Adobe Photoshop CS6). The percentages of red (%R), green (%G) and blue (%B) colors were calculated and plotted as a function of a variable parameter i.e. temperature and time [69].

2.1.2 Application techniques

Ink-jet printing

A typical method for the preparation of diacetylene ink suspension is as follows. PCDA (30 mg) and nonionic surfactant (Brij[®] 58 P or Triton[®] X-100 or Tween[®] 20) (30 mg) were dissolved in 0.30 mL of dimethyl sulfoxide (DMSO), and the organic solution was slowly dropped into 3.7 mL of DI-water at 80 °C. The resulting suspension was sonicated (Elma S40H Elmasonic) for 30 min at 80 °C. Following the sonication, the suspension was kept at 4 °C overnight and filtered to remove large lipid aggregates using sintering glass (4-5 μm) and syringe filter (0.8 μm), respectively, to obtain the desired diacetylene ink. A commercial inkjet cartridge (HP703 black) was emptied, thoroughly washed with water and methanol, respectively, and dried at 100 °C for 2 hours. Then, the diacetylene ink (4 mL) was loaded into the clean cartridge before it was installed into a printer (HP Deskjet Ink Advantage K109a-z) (**Scheme 2.1**).



Scheme 2.1 Method for the preparation of diacetylene ink solution from PCDA/surfactant.

Airbrush painting

A thermochromic dye i.e. PCDA and leuco dye (30 mg) was dissolved in a binder solution (4 mL) made from a 1:2 (v/v) mixture of a commercial lacquer (TOA T-5000, TOA PAINT) and thinner (Ocean Rota). The ink solution loaded into an airbrush tank (HKX HB-3G, 6 mL). The solution was sprayed onto the tested surface by nitrogen gas pressurization at 2 bar via a regulator (Sunny tool, Taiwan). The surfaces used in this study included a clean aluminum lid, Thai coppernickel 1 baht coin, PET bottle, PE sheet, PE plate, 80 g/m² paper (A4, Double A), wood board, white cotton textile and glass slide.

Multi-component sensing array

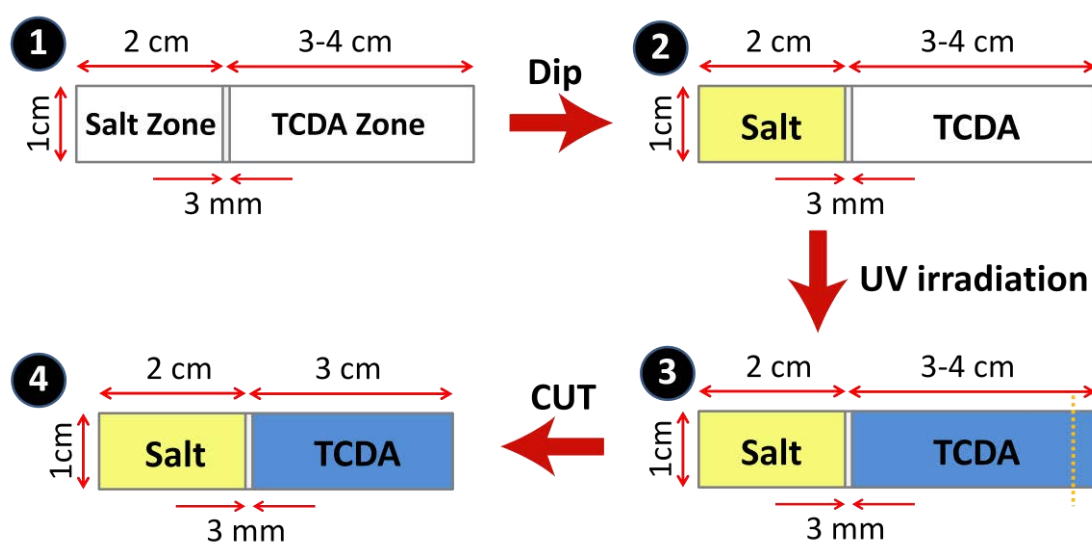
Multi-component, The array was designed to contain 3- striped pattern of PCDA/surfactant i.e. Brij[®] 58 P, Triton[®] X-100 and Tween[®] 20 sensing array was conveniently fabricated by load ink each ink component into a airbrush tank and then spray for each the ink solution onto paper when the paper ejected from feed slot of printer, under control similar condition (pressure, object distance and volume size of spray nozzle), repeated this method for other ink solution on same paper to obtained multi-detector on single substrate.

Dip coating

White polyester thread (1 m) was dipped into a PCDA solution in CH₂Cl₂ (10 mM) for 1 hours. The soaked thread was allowed to dry in the air for 5 minutes. The PCDA coated thread was sew into white polyester textile by sewing machine and irradiated by UV lamp (254 nm) to create a blue pattern.

2.1.3 Paper-based polydiacetylene humidity indicators

A paper strip ($1 \times 6 \text{ cm}^2$) was divided into 2 zones with 2 cm and 4 cm lengths (**Scheme 2.2**). The 2 cm zone was dipped into a salt solution and dried at $100 \text{ }^\circ\text{C}$ for 30 min. The 4 cm zone was dipped into a TCDA solution in CH_2Cl_2 , allowed for air dry. The dipping process was performed with care to make sure that these two zones are separated by 3 mm. The end of the strip was cut to leave 3 cm of TCDA zone and kept in a desiccator for at least 30 min before further study. The coated paper was irradiated with 254 nm UV light to generate a humidity indicator with blue PDA zone on one end and off-white zone of the salt on the other end.



Scheme 2.2 Design of humidity paper indicator.

Three types of paper i.e. printing paper (Double A, 80 grams), drawing paper (80 and 100 grams) and filter paper (Whatman No. 1 and No. 3) were tested as the indicator substrate. At least five pieces of replicate samples were prepared for each indicator.

Five types of salts i.e. calcium chloride (CaCl_2), magnesium chloride (MgCl_2), lithium chloride (LiCl), potassium carbonate (K_2CO_3) and sodium hydroxide (NaOH) and their combinations were tested as moisture absorbing and chromism inducing agents for poly(TCDA).

Study of humidity sensitivity

To test the humidity sensitivity, the blue indicator samples were placed in a closed transparent Poly(methyl methacrylate) container ($26 \times 12 \times 14 \text{ cm}^3$) of which relative humidity was controlled at 60%RH by a saturated NaBr solution (15 mL). The color images of the indicators were recorded by a webcam (1.4 Mpixel). The %RH within the container was monitored with a hygrometer which showed relatively constant humidity of 63 ± 2 %RH at 28 ± 2 °C throughout the entire experimental period of 24 h. The color image of the blue zone was cropped into a $1 \times 1 \text{ cm}^2$ square and the RGB values were read by an image processing software (Adobe Photoshop CS6). The percentages of red (%R), green (%G) and blue (%B) colors were calculated from the following equations.

$$\%R = \frac{R}{R+G+B} \times 100 \quad (1)$$

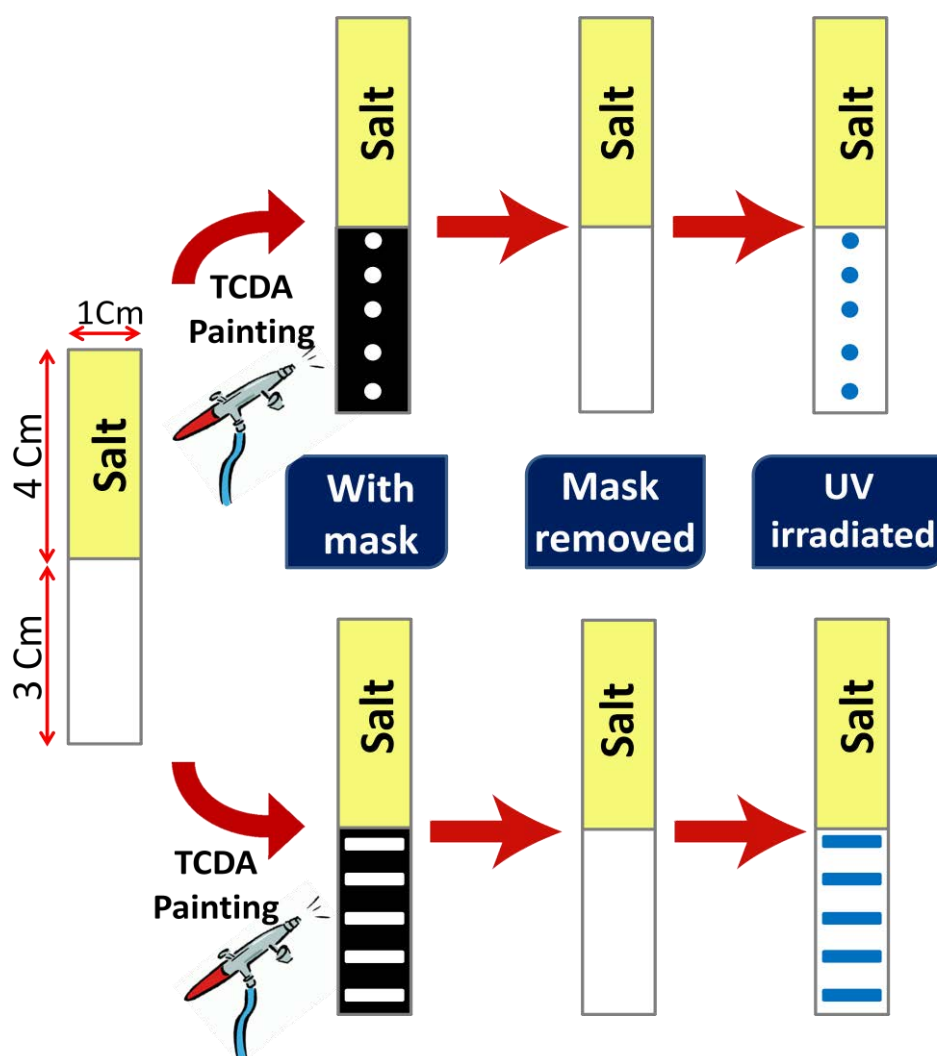
$$\%G = \frac{G}{R+G+B} \times 100 \quad (2)$$

$$\%B = \frac{B}{R+G+B} \times 100 \quad (3)$$

At each %RH, the %B and %R were plotted as a function of time. The time required for the intersection between the %B and %R curves was assigned as a color transition time that used to evaluate the sensor sensitivity.

Development of humidity indicator prototypes

The humidity indicator was developed by using a mixture of K_2CO_3 and NaOH (4:1 mole ratio) as moisture absorbing and chromism inducing agents for poly(TCDA). The salt zone lengths were 2 and 4 cm. The TCDA zone was created by an airbrush painting technique to form periodic patterns using the corresponding masks (**Scheme 2.3**). The TCDA periodic patterns were designed to achieve a more evocative time dependent humidity indicators.



Scheme 2.3 Preparation of humidity indicator prototypes.

2.2 Incorporation of leuco dyes in commercial plastics

Material and equipments :

- Leuco dye (Chameleon-T Powder), Polychrom.Co.Ltd, Korea
- Differential scanning calorimetry (DSC), NETZSCH, DSC 204 F1Phoenix.
- Thermogravimetric analysis (TGA), NETZSCH STA 409 C/CD
- Scanning electron microscopy (SEM), JEOL, Japan (model JSM-5410LV)
- Compression machine, Yong Fong Machinery Co., Ltd. (Model YFY HM 100T with main motor 7.5 kW)
- Two roll mill machine, Yong Fong Machinery Co., Ltd. (Model YF R-8 F8” 18”L with main motor 7.5 kW)
- Melt spinning machine (ThermoHaake[®] PolyDrive)
- Polypropylene (PP, 561R grade, Thai Polypropylene, SCG)
- Low-density polyethylene (LDPE, ExxonMobil™ LDPE LD 100 Series)
- General-purpose polystyrene (GPPS, PORENE, Thai ABS Co., LTD)
- Styrene butadiene rubber (sbr 1502 r)
- Airbrush, HKX HB-3G, Hongkong
- Thinner (Ocean Rota Co., Ltd, Thailand)
- Lacquer (TOA T-5000, TOA PAINT Co.,Ltd, Thailand)

2.2.1 Thermal analysis of leuco dye

Thermogravimetric analysis (TGA) of leuco dye

Thermogravimetric analysis was performed on a NETZSCH STA 409 C/CD under nitrogen gas flow at a rate of 50 mL/min. A leuco dye sample (6 mg) was placed in a platinum pan. Starting at 25 °C, the sample was heated to 800 °C at a ramp rate of 10 °C/min. The decomposition temperature and percent weight loss of the sample were determined by using TA Instrument Universal Analysis 2000 program.

Differential scanning calorimetry of leuco dye

Differential scanning calorimetry was performed on a NETZSCH, DSC 204 F1Phoenix. A leuco dye sample (5 mg) was placed in an aluminum pan and the pan was sealed. The sealed sample was heated in a DSC cell under helium flow (20 mL/min) from 25 °C to 380 °C (10 °C/min) and then cooled to -70 °C (-10 °C/min) with liquid nitrogen at a rate of 50 mL/min. The DSC thermogram was recorded on the second heating with the same rate.

2.2.2 Scanning electron microscopy (SEM)

The scanning electron microscopy (SEM) was used to determine the particle size of the leuco dye samples. A leuco dye powder sample was spread on a SEM stub and coated with gold by sputtering technique. The image was acquired using a JEOL, Japan (model JSM-5410LV) electron microscope equipped with a CCD camera. The measurement was operated at 15 kV.

2.2.3 Study of thermal stability of Chameleon-T Powder

The Chameleon-T Powder was placed in a watch glass and then heated to 220 °C in a laboratory calcined furnace for 5 min. The heated Chameleon-T Powder was filled into test tubes and then immersed onto a water beaker (500 mL) and were then warmed up from 5 to 40 °C. The color images of the Chameleon-T Powder at different temperatures were recorded by a digital camera (Nikon D40X with a Nikon Nikkor lens 18–55 mm).

2.2.4 Melt spinning of polypropylene/leuco dye

Fiber filaments of polypropylene (PP, 561 R grade, Thai polypropylene, SCG) blended with 1,2 and 3% (w/w) Chameleon-T powder (Polychrom.Co.Ltd, Korea) were created by a single screw extruder (ThermoHaake[®] PolyDrive) equipped with a spinneret with five 0.3 mm holes and a 105µm filter plate. The temperatures of the 1st-5th extruder zones were set at 180, 190 , 200, 212 and 220 °C, respectively. The mixture of PP/Chameleon-T powder (0.5 kg) was loaded to the extruder with the screw speed of 4 rpm. The operating pressure range was controlled within 2-100 bar. The fiber filament samples were collected from the spinneret on a 8.5 cm roll at the speed of 57-59 rpm.

2.2.5 Compression molding of polymer/leuco dye

A flat plastic plate of polymer/Chameleon-T powder (3% w/w) blend was fabricated by compression molding (Yong Fong Machinery Co., Ltd. Model YFY HM 100T with main motor 7.5 kW). Chameleon-T powder (1.65 g) and the commercial polymer pellet (\varnothing 5 mm \times 2 mm, 55 g) i.e. polystyrene (PS, PORENE, Thai ABS Co., LTD), polypropylene (PP) and low-density polyethylene (LDPE, ExxonMobil™ LDPE LD 100 Series) were thoroughly mixed in a shaking bag. The mixture was filled into an aluminum mold plate (20 cm \times 20 cm \times 2 mm) and the upper and lower plates were heated at the processing temperature of 150, 210 and 250 °C for LDPE, PP and PS, respectively. The molding process included a preheating time of 3 min, venting time of 3 sec, full-pressing time of 6 min and cooling time of 5 min, respectively.

2.2.6 Two roll mill of rubber/leuco dye

The Chameleon-T powder (5% w/w) and additives such as sulfur (curing agent, 2 phr), N-cyclohexyl-2-benzothiazole sulfonamide (CBS, accelerator, 1.3 phr), stearic (activator, 1 phr) and paraffinic oil (softener, 5 phr) were masticated with styrene butadiene rubber (sbr 1502 r) by a two roll mill machine (Yong Fong Machinery Co., Ltd. Model YF R-8 F8'' 18''L with main motor 7.5 kW). The resulted rubber compound was cured and compressed in an aluminum mold plate (12 cm \times 12 cm \times 5 mm) at 95 °C with a preheating time of 3 min and full-pressing time of 9 min.

CHAPTER III

RESULTS AND DISCUSSION

This thesis deals with the surface deposition and incorporation of 2 types of chromic materials, *i.e.* polydiacetylenes (PDAs) and leuco dyes, and their applications as colorimetric sensors or indicators. The results and discussion in this chapter is thus divided into 2 sections. The first section involves the study of deposition of PDA and leuco dye on solid surfaces using ink-jet printing, airbrush painting and dip coating techniques. The end of the first section devotes extensively to the development of PDA humidity indicators on paper substrates. The second section describes the attempt to incorporate thermochromic leuco dyes into various commercial polymers starting from the thermal and morphology characterization of the commercial dyes (Chameleon-T, Polychrom Co., Ltd. Korea) followed by the incorporation techniques.

3.1 Surface deposition of diacetylene and leuco dye

For colorimetric sensing applications, especially for naked eye detection, deposition of an appropriate chromic material on solid substrates is very economical and reasonable because it can produce high detection area per material mass. In majority of this section, PDA generated from a commercially available diacetylene monomers *i.e.* 10, 12-pentacosadiynoic acid (PCDA) and 10,12-tricosadiynoic acid (TCDA) were used as a model of chromic materials for the study of fabrication techniques on various solid substrates. Three techniques *i.e.* inkjet printing, airbrush painting and dip coating were evaluated. The commercial leuco dye was also tested in the airbrush painting techniques. The dye coated substrates were tested for colorimetric properties. The results and discussion of these studies are elaborated in details as follows.

3.1.1 Ink-jet printing

To fully utilize PDAs in sensing applications, fabricating and patterning techniques are of importance. Ink-jet printing allowed ability to create designed patterns with noncontact operation on surface in low-cost, especially for custom made or low volume manufacture. In this work, a commercial office ink-jet printer (HP Deskjet K109g) was used. The aqueous solution of PCDA monomer (20 mM) containing a nonionic surfactant (Brij[®] 58 P, Triton[®] X-100 and Tween[®] 20) (as shown in **Figure 3.1**) was used as the printing ink (see section 2.1.3 for the preparation details). The surfactant was required to produce a high concentration solution by inducing the formation of stable diacetylene/surfactant rod-shaped aggregates in nanometer size [56]. The printing results were evaluated by comparing the color depth and uniformity after the UV irradiation.

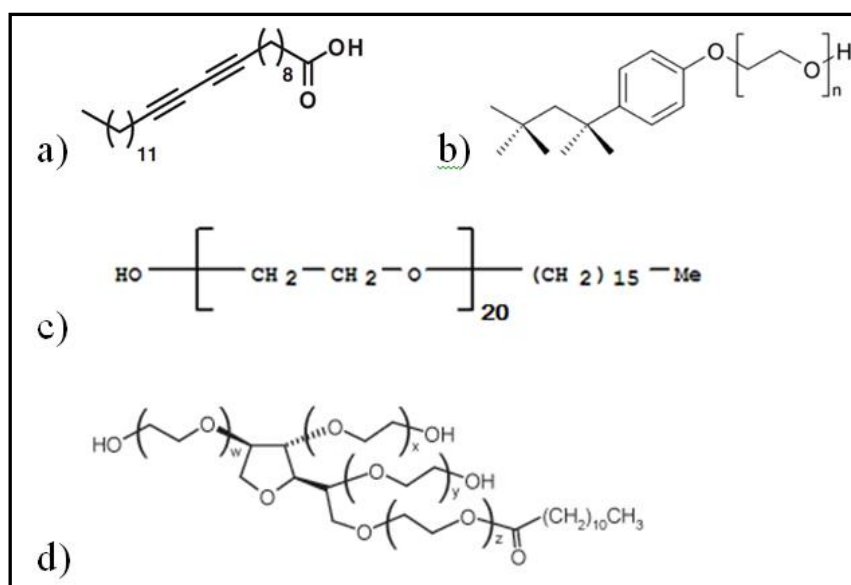


Figure 3.1 Structures of **a)** diacetylene monomer (PCDA), **b)** Triton[®] X-100, **c)** Brij[®] 58 P and **d)** Tween[®] 20.

The diacetylene ink was printed on printing paper (80 grams) by an ink-jet printer. The printed paper was allowed for air dry for 2 hours and stored in the dark. The dry printed paper was irradiated at 254 nm UV light (1400 $\mu\text{W}/\text{cm}^2$) for 2 minutes. As shown in **Figure 3.2**, among three nonionic surfactants used, Brij[®] 58 P provided the highest contrast blue image of poly(PCDA) after the irradiation. The

image turned to red color upon heating at 90 °C for 10 sec indicating that the PCDA/surfactant mixtures retained the thermochromic properties of poly(PCDA). It is important to mention here that the aqueous solution of PCDA without the surfactant can be prepared with a significantly lower concentration of only 5 mM that produce only fade color printing images. The results found in this work are in good agreement with the previously reported literature work that the Brij[®] nonionic surfactants can increase the concentration of PCDA stabilized in water suspension [56]. As described above, Brij[®] 58 P was also found here to give better color depth for the printing images comparing with Triton[®] X-100 and Tween[®] 20.



Figure 3.2 Color images of poly(PCDA) printed from PCDA/surfactant aqueous solutions using a) Brij[®] 58P b) Triton[®] X-100 c) Tween[®] 20 before (left) and after (right) heating at 90 °C for 10 sec.

The poly(PCDA) printed paper was studied for the thermochromism properties by gradual heating from 30 to 95 °C on the wall of a beaker filled with water (450 mL). The color images of the printed paper captured by a commercial webcam are shown in **Figure 3.3**. The images show blue-to-red color transition around 60-70 °C for all PCDA/surfactant combinations.

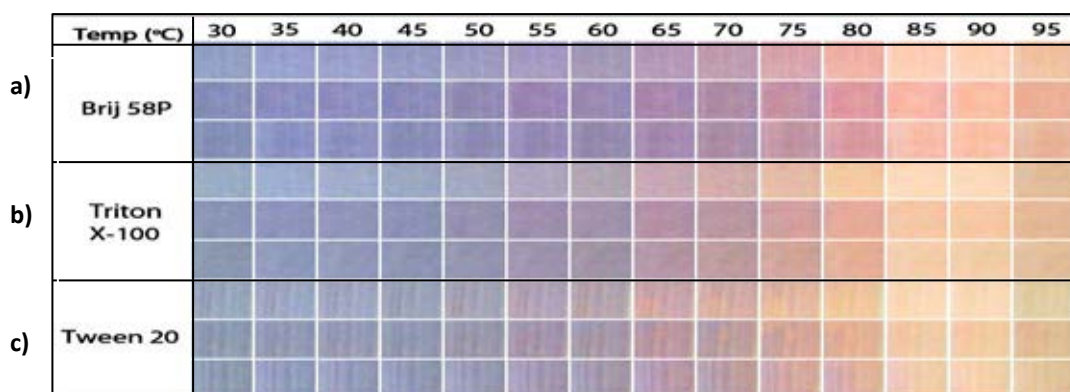


Figure 3.3 Color images of poly(PCDA) printed from PCDA/surfactant aqueous solutions using a) Brij[®] 58P b) Triton[®] X-100 c) Tween[®] 20 upon heating from 30 to 90 °C. The experiment was performed in three replicates.

The images of poly(PCDA) printed on A4 paper were converted to %R, %G and %B values in the RGB system by an image processing software (see section 2.1.2 for experimental details). The plots of %B and %R against temperature gave two curves with the intersection assigned as the color transition point (**Figure 3.4**) [69].

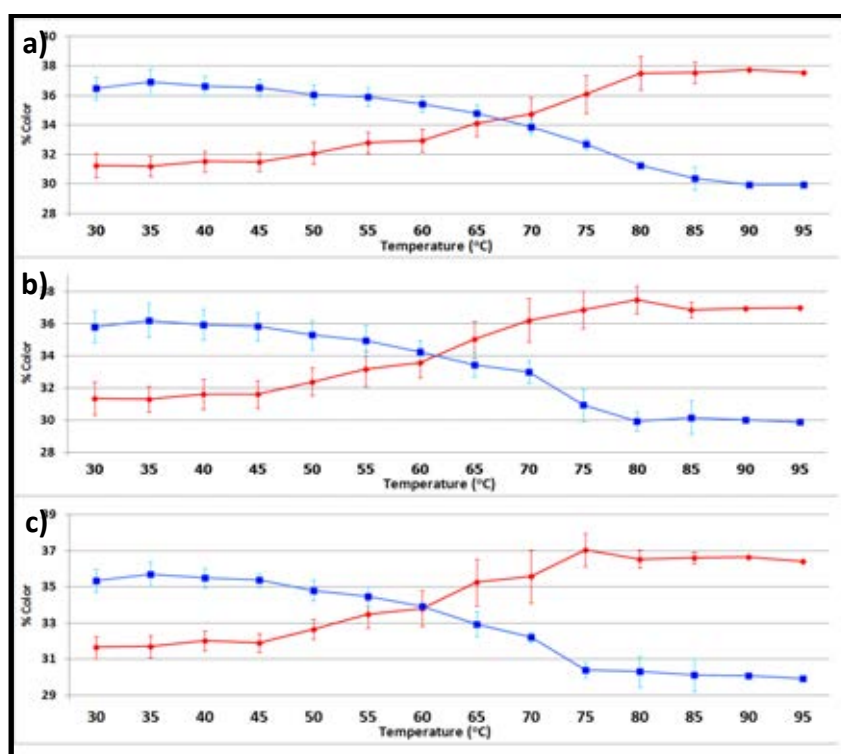


Figure 3.4 Plots of %R and %B against temperature, corresponding to the photographic images in **Figure 3.3**.

From this assignment, the blue to red color transition temperature of poly(PCDA) incorporated with Brij[®] 58 P, Triton[®] X-100 and Tween[®] 20 were determined as 68, 63 and 60 °C, respectively. Thus, it is discovered here that the surfactants not only help stabilizing the PCDA nanoassembly but also provide a mean to tune down the color transition temperature of poly(PCDA) (70 °C).

The morphology of PCDA/surfactant aqueous solutions in the presence of Brij[®] 58P, Triton[®] X-100 and Tween[®] 20 were studied by scanning electron microscopy (SEM). The morphologies of the lipid assembly clearly changed with the presence of the surfactants. However it was not clear to justify the change of their sizes. PCDA itself showed pellet shape with various sizes (**Figure 3.5a left**). These pellets tended to highly aggregate (**Figure 3.5a right**). The mixture of PCDA/Brij[®] 58P had a rod shape (**Figure 3.5b left**). These rods seemed to be more stable with less tendency to form aggregates (**Figure 3.5b right**). The morphology of PCDA/Triton[®] X-100 mixture was a spherical droplet shape (**Figure 3.5c left**). The individual droplet assembly also seemed to be more stable comparing with the surfactant-free PCDA. The mixture of PCDA/Tween[®] 20 had a rice grain shape (**Figure 3.5d left**). This mixture also showed some aggregation of the assemblies with relatively larger size (**Figure 3.5d right**). The SEM images confirmed that the nonionic surfactants, especially for Brij[®] 58P and Triton[®] X-100, could stabilize the molecular self-assembly of PCDA preventing them from aggregation that allow the formulation of the high concentration of PCDA ink solution for the ink-jet printing of which nozzle usually contains 20 µm outlets.

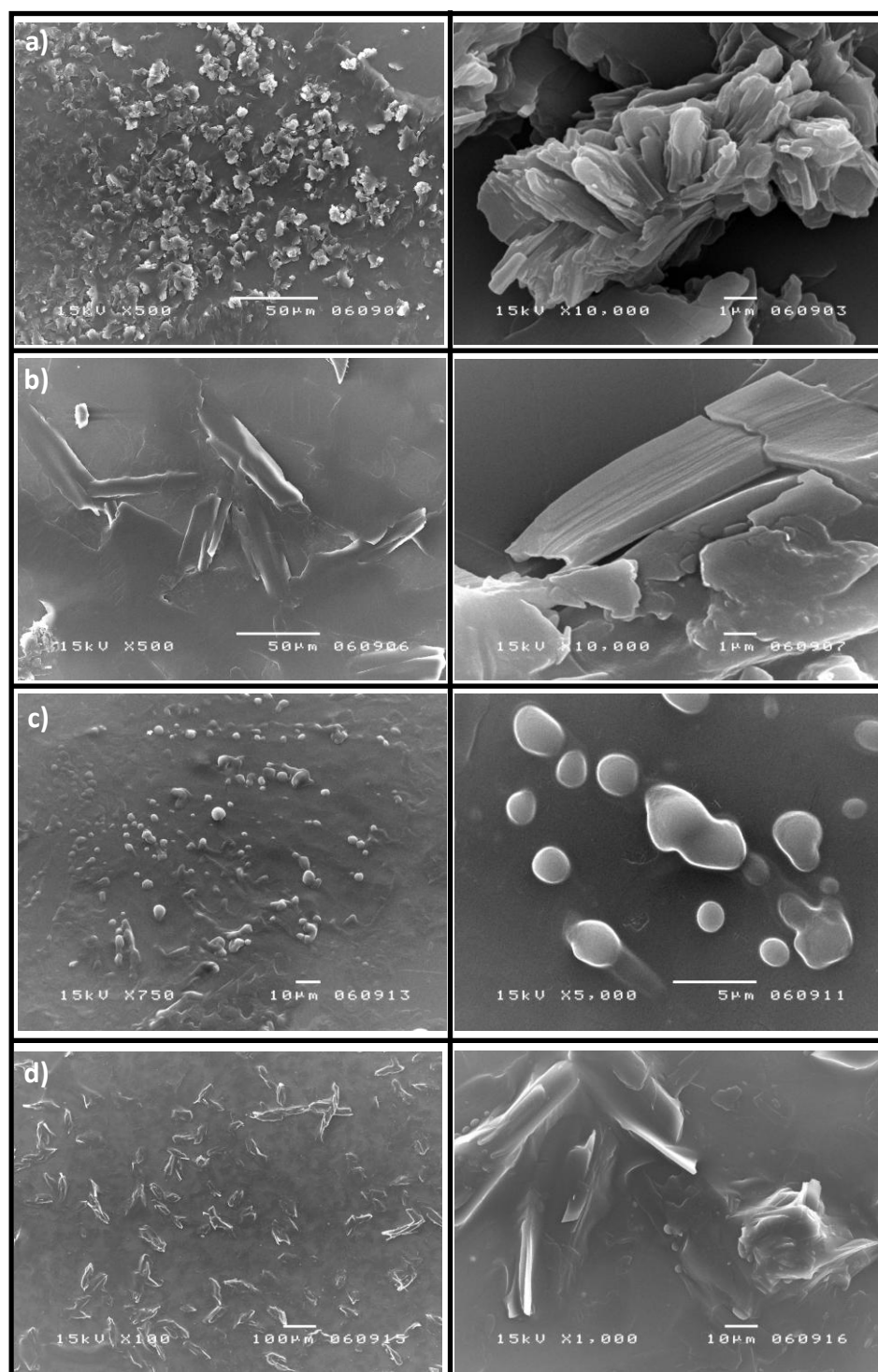


Figure 3.5 SEM images of dry samples on glass substrate prepared from aqueous solutions of PCDA (13 mM, 7.5 mg/mL) in the absence and presence of surfactants (7.5 mg/mL): **a)** PCDA, **b)** with Brij[®] 58 P, **c)** with Triton[®] X-100 and **d)** with Tween[®] 20).

3.1.2 Airbrush painting

The airbrush painting technique [59] is a useful alternative method for dye or ink deposition on material surface especially for the unprintable area such as stationary, large, 3-D, thick or rough surface objects. The airbrush reservoir tank is tolerant to many kind of solvents including organic solvents with allow greater flexibility in ink formulation with or without the use of surfactant. It is also very robust painting system that is easy to operate and maintain. The painting pattern can also be easily created and controlled by masking technique.

The airbrush painting was tested for the deposition of PCDA on surfaces of various types of objects including a clean aluminum lid, Thai coppernickel 1 baht coins, PET bottle, PE sheet, PE plate, white paper (80 g/m²), wood board, white cotton textile and glass slide. A commercial thermochromic leuco dye (orange color, transition temperature 31 °C) was also studied for comparison. Use of the PCDA or leuco dyes with binder (see section 2.1.2 for preparation details) for airbrush painting was found to be viable for surface of all material types tested. Both PCDA and leuco dyes attached well with the surfaces. PCDA ink produced deep to light blue color after UV irradiation while the leuco dye showed its original orange to pink color without UV irradiation (**Figure 3.6**). The blue poly(PCDA) on the surface turned to red color after heating to 85-90 °C. The orange and pink color of leuco dye on the sample surface disappeared and the original color of the substrates appeared above 40 °C. The darker substrate materials led to darker shade of the final appearance. White substrate such as paper (**Figure 3.6 d**) is thus the most suitable substrate for indicator application and colorimetric analyses. These results demonstrated that the airbrush technique is very convenient to be applied in the deposition of the thermochromic dye onto the surface of various materials with retained thermochromic properties ability of the dye materials.

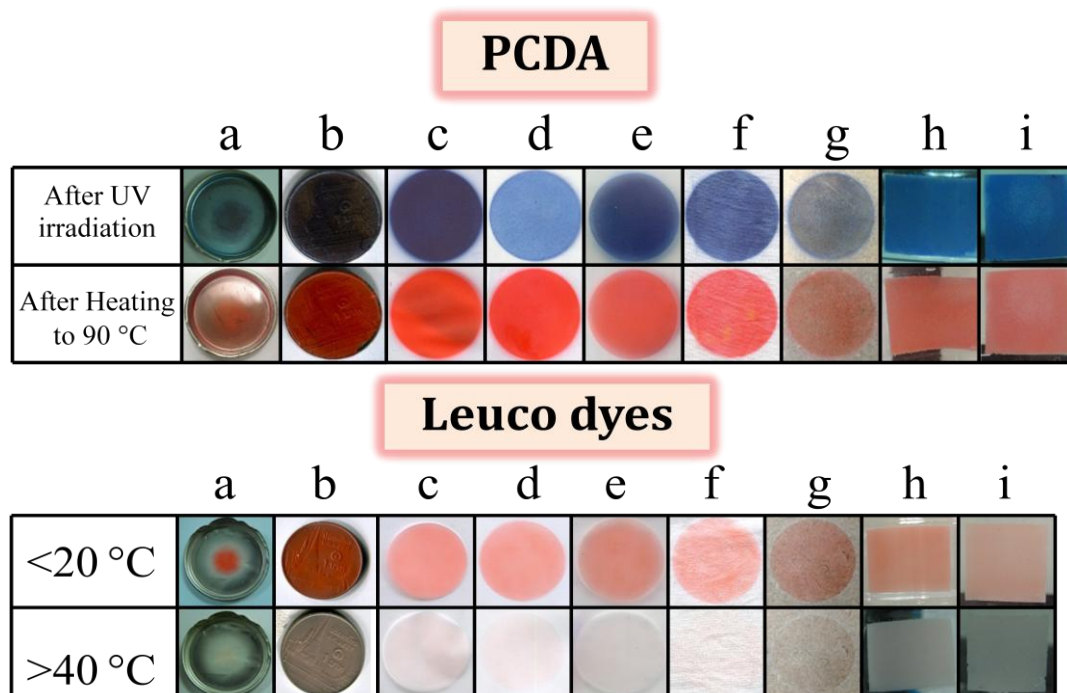


Figure 3.6 Photographic images of PCDA/binder and orange leuco dye/binder solution airbrush-painted on various types of surfaces: **(a)** aluminum lid, **(b)** Thai cupernickel coins, **(c)** PE thin film, **(d)** paper, **(e)** PE plate, **(f)** cotton textile, **(g)** wood board, **(h)** PET bottle, **(i)** glass slide before and after heating.

To demonstrate the benefits of this technique, a multi-component sensing array was fabricated on paper by airbrush painting. The array was designed to contain 3- striped pattern of PCDA/surfactant *i.e.* Brij[®] 58 P, Triton[®] X-100 and Tween[®] 20. The 3-striped pattern (**Figure 3.7**) was conveniently generated by the airbrush painting in conjunction with the ink-jet printer paper feeding system (see section 2.1.3 for experimental details). The PCDA/surfactant array was tested for colorimetric responses toward various solvents *i.e.* water, MeOH, CH₂Cl₂, toluene and THF.

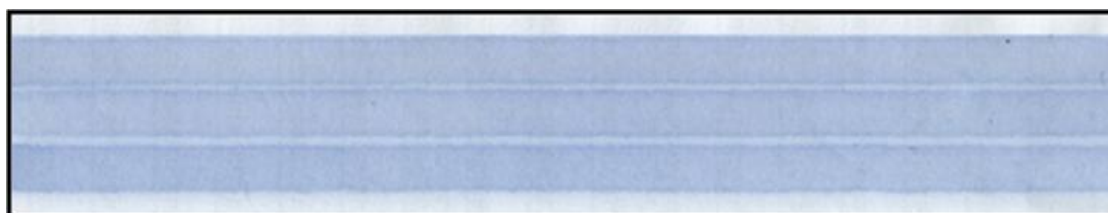


Figure 3.7 Photograph of multi-detector from airbrush painting technique co-operated with ink-jet printing

Upon the solvents exposure, the blue poly(PCDA) printed paper also showed different patterns of blue-to-red solvatochromic color transition depending on the types of solvents (**Figure 3.8**). The results indicate that the combination of PCDA with various surfactants may be used as solvatochromic agents for the fabrication of solvent sensing array by the airbrush painting. The variation of the surfactants gave a tunability of the solvent sensitivity of poly(PCDA). The array platform allowed simultaneous exposure of 3 sensing elements to the solvents. It is also important to mention that the airbrush painting technique can give the images with deeper color than the ink-jet printing technique due to its greater deposition amount of PCDA .

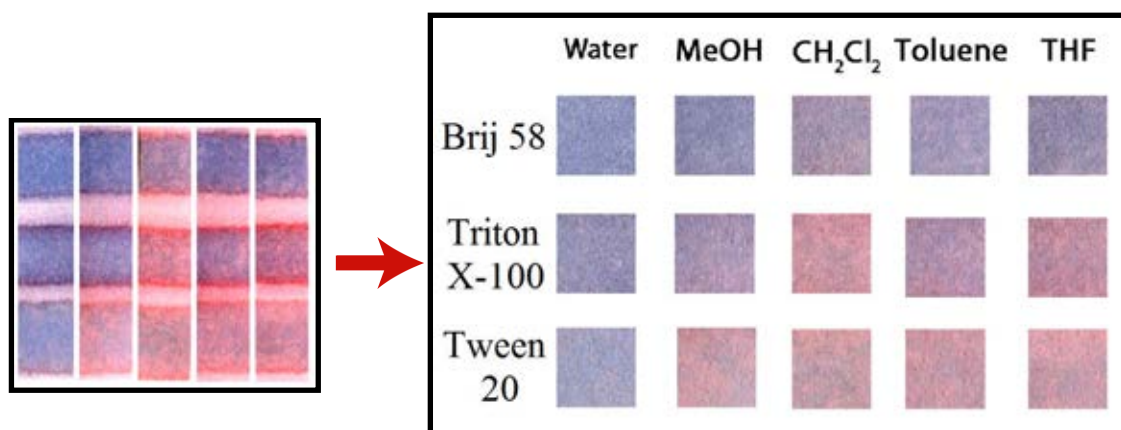


Figure 3.8 Photographic images of UV-irradiated paper printed with PCDA/surfactant after the exposure to water (control) and various organic solvents.

3.1.3 Dip coating

The dip coating technique is an excellent alternative deposition technique on thin and long shape substrates or hard to reach area of small objects. In this work, the dip coating technique was tested for coating of PCDA thermochromic precursor on white polyester threads (see section 2.1.2 for preparation details).

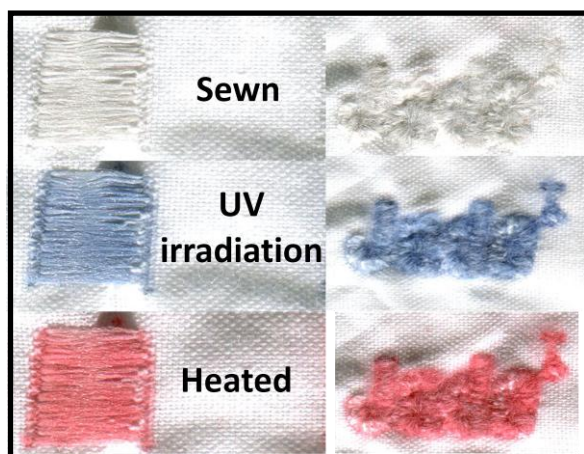


Figure 3.9 Photographic images of PCDA coated polyester thread sewn to white polyester fabric pieces.

The poly(PCDA) coated polyester thread sewn to white polyester fabric pieces was studied for the thermochromism and physical properties. The color images of the coated polyester thread sewn to white polyester fabric pieces are shown in **Figure 3.9**. The images show white thread turned to blue color after UV exposure and turned to red color after heating to 85-90 °C. The sewn thread also withstood against finger rubbing (**Figure C1**). The results demonstrated that the dip coating technique can be applied for the deposition of thermochromic PDA dye onto long and small objects such as thread which may be in turn sewn into logos or brand names of products for anti-counterfeiting purpose.

3.1.4 Paper-based polydiacetylene humidity indicators

The design of humidity indicators made from polydiacetylene was based on the alkanochromism properties of acidic PDAs [15,51-52] and hydroscopic properties of some basic salts. In this work, 10,12-tricosadiynoic acid (TCDA) was used as the monomer for PDA coloring agent while CaCl_2 , MgCl_2 , LiCl , K_2CO_3 and NaOH were tested as the hydroscopic and basic salts. The white color paper of various types were tested as the substrates. The dip coating technique was used for the deposition of all reagents on the substrates (see section 2.1.4 for preparation details).

Fabrication and substrate selection

The substrate selection was performed by testing the water absorbing ability of 5 types of white color papers *i.e.* printing paper (80 grams), drawing paper (80 and 100 grams) and filter paper (whatman No. 1 and No. 3). As shown in **Figure 3.10**, the filter paper (Whatman No. 1 and No. 3) gave the fastest water absorbing rate while the printing and drawing papers absorbed water at much slower rates. The filter paper was thus a substrate of choice for the humidity indicator as it should give the highest moisture sensitivity. In this work, filter paper No. 3 was selected because it is thicker and less flimsy than filter paper No. 1.

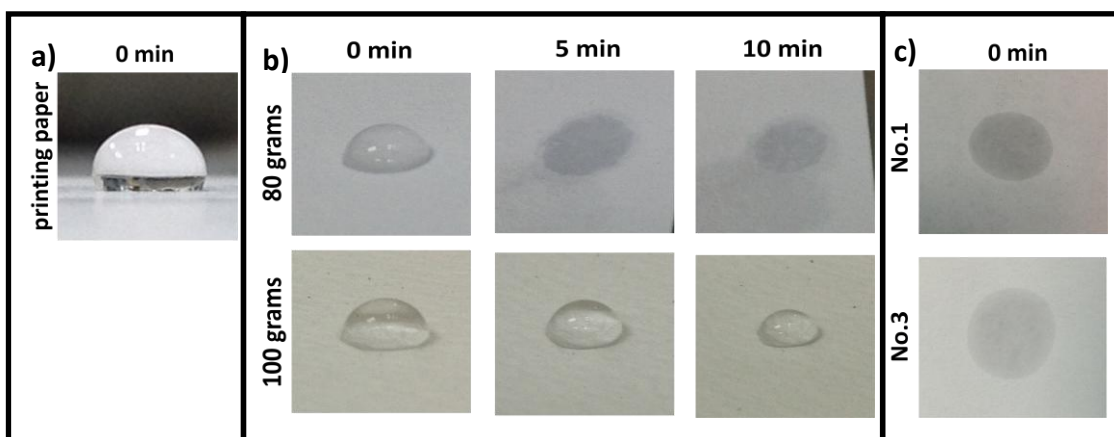
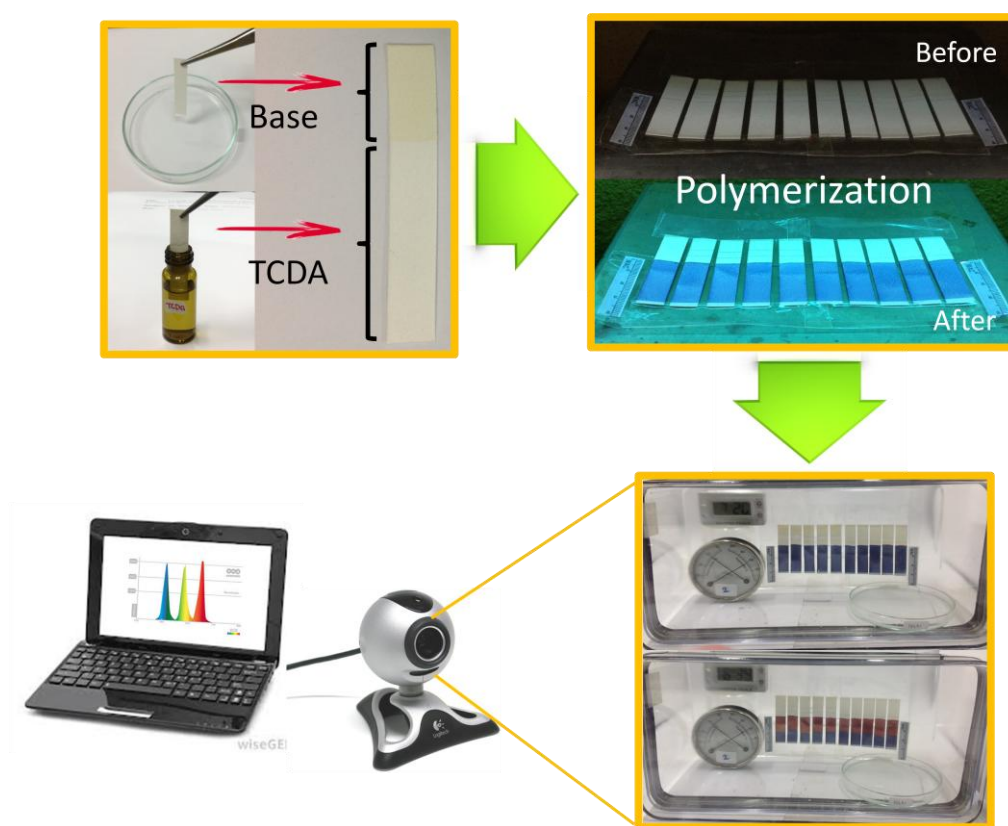


Figure 3.10 Images of water droplet on **a)** printing paper **b)** drawing paper and **c)** filter paper in the water absorbing test.

After the deposition of TCDA and a salt on the filter paper No. 3, the UV irradiation of the coated paper strips gave blue indicators. Five types of the indicators containing no salt and 4 tested salts were incubated in a closed transparent Poly(methyl methacrylate) container with controlled %RH (Scheme 3.1).



Scheme 3.1 Flow chart for preparation and study of humidity indicators.

Selection of hygroscopic and basic salts

In this work, 5 types of salts *i.e.* CaCl_2 , MgCl_2 , LiCl , K_2CO_3 and NaOH were tested as a hygroscopic and basic salt. **Table 3.1** shows percentage of relative air humidity over saturated solutions of the tested salts [55-56]. The lower relative air humidity indicates the higher moisture absorbing capability of the solutions. All of these salts give saturated solutions that can control relative air humidity lower than the 63%RH level recommended by US food and drug administration (FDA) for keeping moisture sensitive foods and drugs [88]. While the saturated NaOH solution seems to be the best choice as a hygroscopic and basic salt because of its highest moisture absorbing capability and basicity. However, it severely damaged the filter

paper causing intense yellowish and deformation, after dipping and drying process, due to its strong basic properties. The indicator fabricated from the saturated NaOH solution was not investigated further (**Figure 3.12**).

Table 3.1 Relative humidity over saturated salt solutions at specified temperatures

Salt	Relative air humidity (%)	At a temperature (°C)
Sodium hydroxide	6	25 °C
Lithium chloride	11	25 °C
Calcium chloride	31	20 °C
Magnesium chloride	33	25 °C
Potassium carbonate	43	25 °C
Sodium bromide	58	25 °C
Sodium chloride	75	25 °C

In the initial test of the indicators, the color transition of the indicators were monitored in a closed container at 75%RH controlled by a saturated NaCl solution. Without the salt, the blue poly(TCDA) on the filter paper did not change its color after moisture exposed for 5 hours while the indicators fabricated with saturated K_2CO_3 solution gave the fastest blue-to-red color transition of poly(TCDA). As the moisture absorbing ability of the saturated K_2CO_3 solution is not as good as those of the other salt solutions, it is likely that the fast color change induce by K_2CO_3 is due to its basicity. The pH measurement confirmed that the saturated solution of K_2CO_3 has the highest pH value (**Figure 3.11**) [62]. The non-basic saturated LiCl solution did not induce the color transition of poly(TCDA) despite being the most hygroscopic. These results indicate that K_2CO_3 has the most suitable hygroscopic and basic properties to be used in inducing the blue-to-red color transition of poly(TCDA) in the humidity indicators.

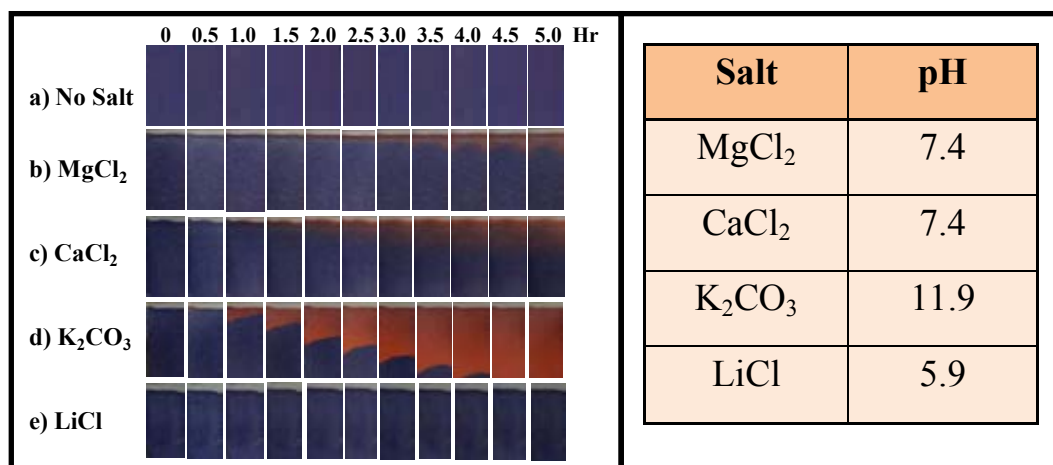


Figure 3.11 Time dependent color image of TCDA zone of the humidity indicators without salt, with MgCl₂, CaCl₂, K₂CO₃ and LiCl incubated in a closed container with 75%RH. The pH values of the saturated salt solutions are shown in the right table.

In the next step, the indicators prepared from TCDA and K₂CO₃ were tested under 63%RH. The color of the indicators gradually turned from blue to red as shown in **Figure 3.13a**. The plot of %R and %B against the incubation time gave the intersection of the two curves at 5 hours (**Figure 3.13b**) which is assigned as the color transition time. To enhance the sensitivity of humidity indicators, a more hygroscopic and basic salt such as NaOH was used in combination with K₂CO₃. The salt zone of the indicators was dip coated with the K₂CO₃:NaOH mixed solution (7.81 molal) having a mole ratio of 4:1, 3:2 and 2:3. In comparison with the indicators coated with K₂CO₃ alone, those coated with the mixed base developed more yellowish color (**Figure 3.12**) due to the effect of the strong base NaOH as mentioned earlier.

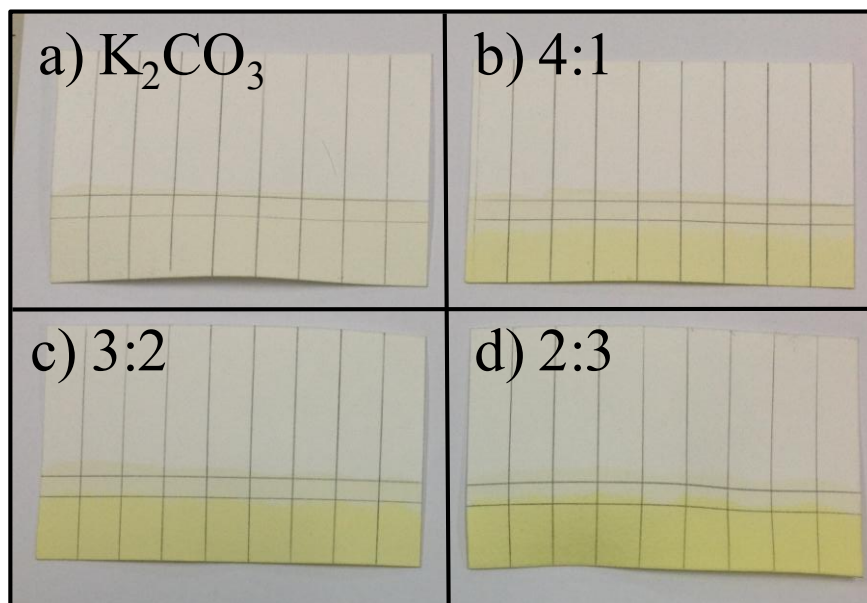


Figure 3.12 Photographic images of the salt zone prepared from 7.81 molal aqueous solution of **a)** K_2CO_3 , and $\text{K}_2\text{CO}_3/\text{NaOH}$ mixed solution with **b)** 4:1, **c)** 3:2, and **d)** 2:3 mole ratio.

Under 63%RH, the indicators prepared from the mixed salts showed similar blue-to-red color transition to those prepared from K_2CO_3 alone but with somewhat difference in sensitivity (compare **Figure 3.14** and **Figure 3.13a**). From the plots of %R and %B, the indicators with 4:1 $\text{K}_2\text{CO}_3/\text{NaOH}$ mole ratio gave the blue-to-red color transition time of less than 4 hours which was faster than those with K_2CO_3 (compare **Figure 3.15a** and **Figure 3.13b**). However, the color transition times of the indicators with 3:2 and 2:3 $\text{K}_2\text{CO}_3/\text{NaOH}$ mole ratio were nearly 9 hours. These longer color transition times indicated the lower moisture absorbing capability of these mixed salts that may be attributed to the unsaturation of the mixed salt solutions used under this experimental design with the control total base molality. Although the sensitivity of the indicators may be enhanced further by using the mixed salts from their saturated solution, it was not investigated due to the undesirable appearance of the salt zone fabricated with high NaOH content. Therefore, the mixed solution of K_2CO_3 and NaOH at 4:1 mole ratio was used in the development of humidity indicator prototypes.

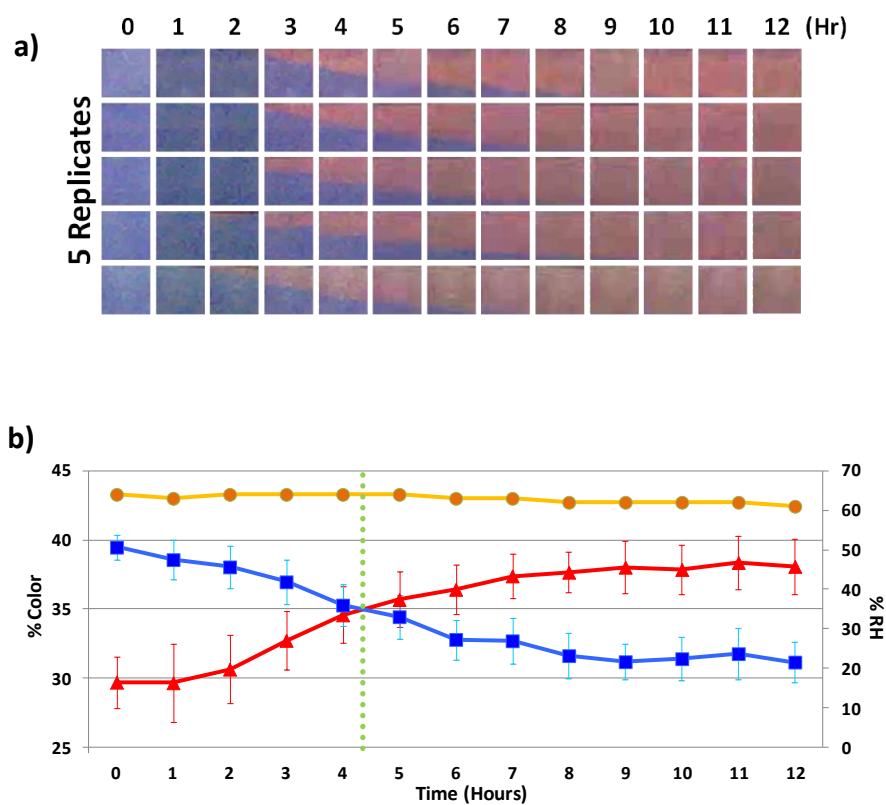


Figure 3.13 a) Photographic images of TCDA zone of the humidity indicators prepared with K_2CO_3 alone at different incubation times, and **b)** Plots of %R (▲) and %B (■) of the TCDA zone in the humidity indicators versus exposure time under controlled %RH (●) by NaBr ($63 \pm 3\%$).

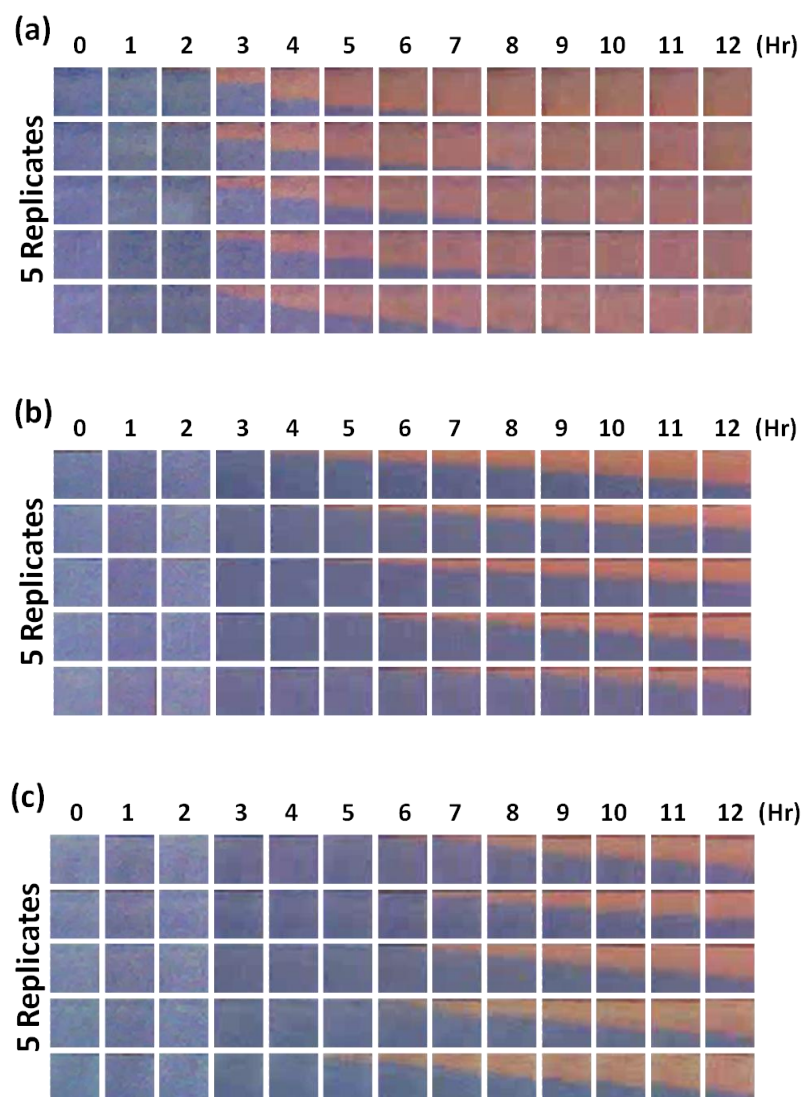


Figure 3.14 Photographic images of TCDA zone of the humidity indicators prepared with a) 4:1 b) 3:2 and c) 2:3 mole ratio of $K_2CO_3/NaOH$ mixed solution (7.81 molal) at different incubation times under $63\pm 3\%RH$.

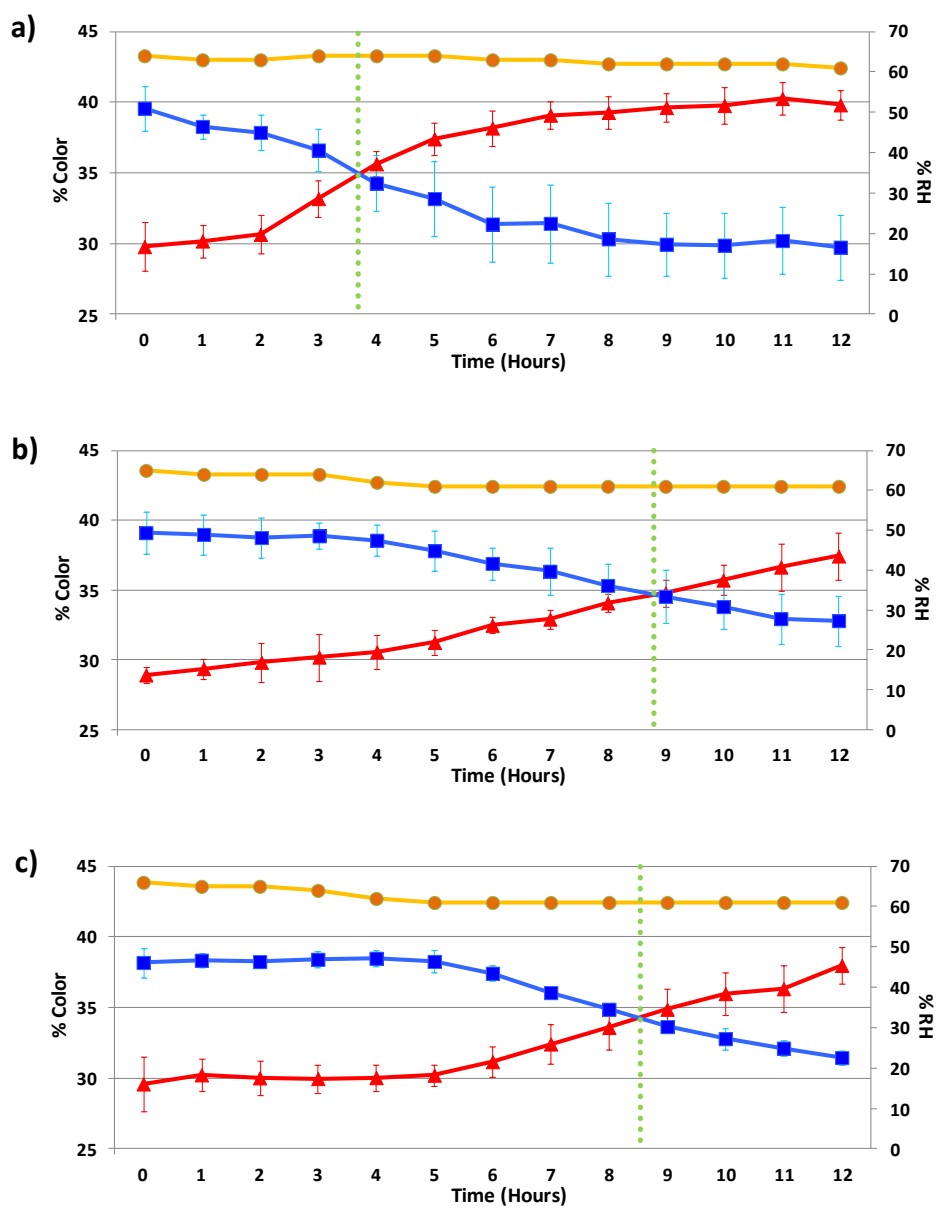


Figure 3.15 Plots of %R (▲) and %B (■) of the TCDA zone in the humidity indicators prepared with **a)** 4:1 **b)** 3:2 and **c)** 2:3 mole ratio of $K_2CO_3/NaOH$ mixed solution (7.81 molal) versus exposure time under controlled %RH (●) by NaBr ($63\pm 3\%$).

Since the sensitivity of the humidity indicators depends on the moisture absorbing ability, the length of K_2CO_3 (50 %w/w) salt zone was increased from 2 to 4 cm to expand the moisture absorbing area and hence enhance the sensitivity of the indicator (**Figure 3.16**).

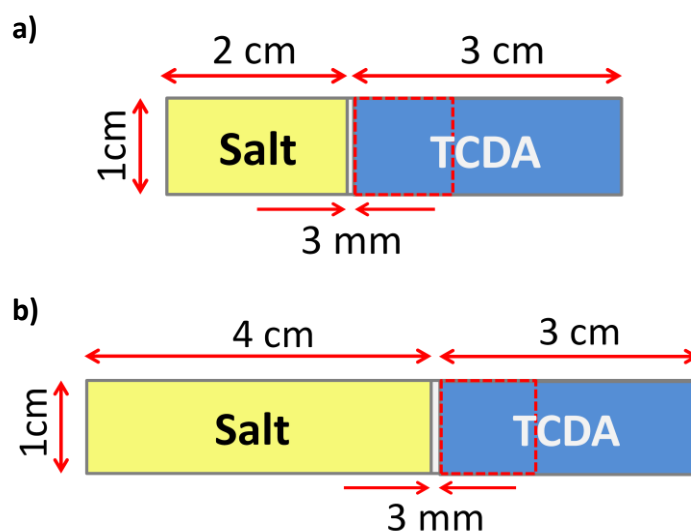


Figure 3.16 Humidity indicators with different zone lengths: **a)** initial design and **b)** expanded salt zone design. The dash square depicts the cropping area for the color analysis.

At 63%RH, the blue PDA zone of the humidity indicators from both preparations turned to red. The plot of %R and %B showed that the color transition time of the indicators having 4 cm salt zone (~4 hours) was shorter than that of the ones with 2 cm salt zone (~5 hours) (**Figure 3.17**). Thus, the increase of salt zone lengths can indeed enhance the sensitivity of the humidity indicators. Consequently, the salt zone length of 4 cm was used in the further development of the humidity indicator prototypes. It is however critical to point out here that the dip coating must be performed with care to avoid the overrunning of TCDA onto the salt zone. The overlapping part between these two zones became insensitive to moisture and remained blue throughout the experimental period (**Figure D12**).

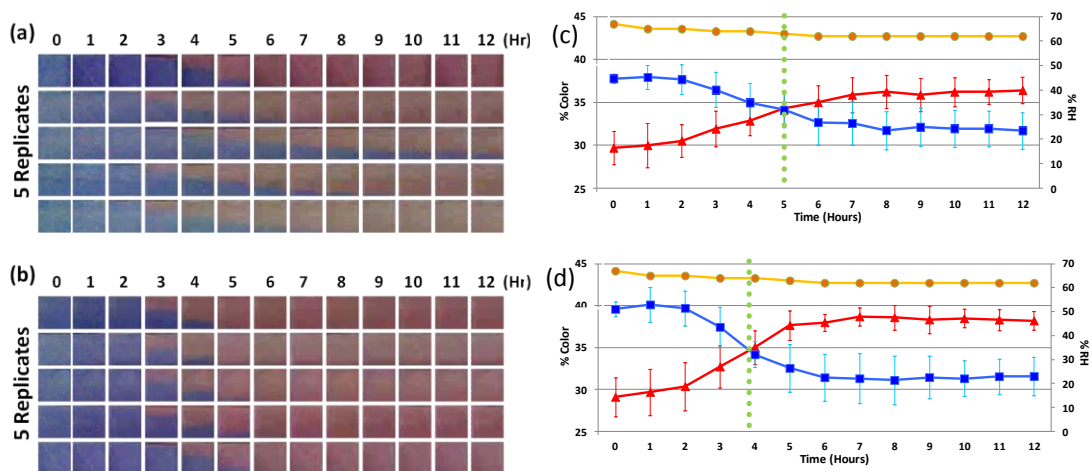


Figure 3.17 Color images of TCDA zone of the humidity indicators prepared with **a)** 2 cm and **b)** 4 cm of K_2CO_3 (50 %w/w) zone and their corresponding plots of %R (\blacktriangle) and %B (\blacksquare). The indicators were incubated under controlled RH of $63 \pm 3\%$ (\bullet).

To further enhance the sensitivity of the humidity indicators, the 4:1 (mole ratio) mixed $K_2CO_3/NaOH$ solution was used to fabricate the 4 cm salt zone. The indicators rapidly turned red within 1 hour at 63%RH (**Figure 3.18**). In conclusion, the combined application of $K_2CO_3/NaOH$ mixed salt and expanded salt zone can cooperatively enhance the sensitivity of the indicators.

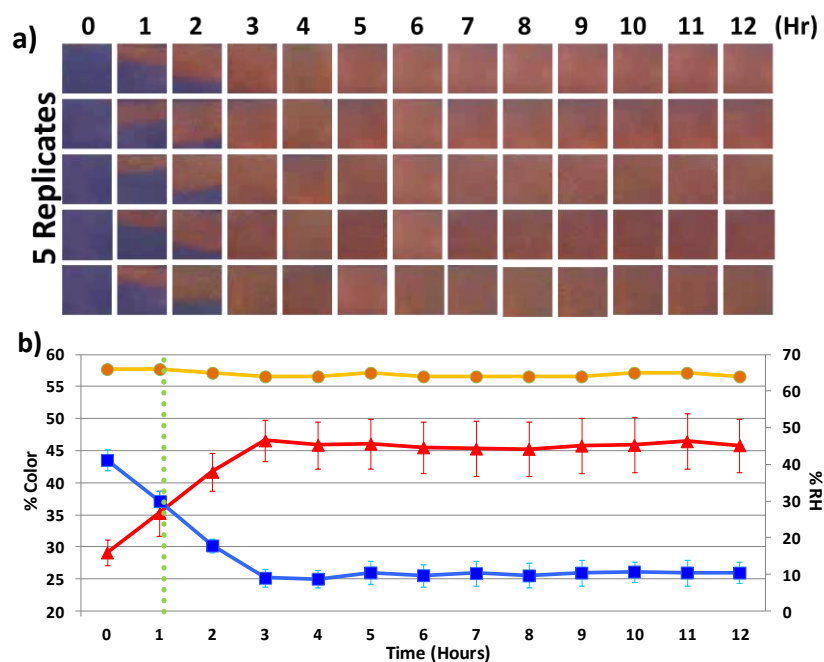


Figure 3.18 a) Color images of TCDA zone of the humidity indicators prepared with 4 cm of $K_2CO_3/NaOH$ (4:1 mol ratio) zone and b) their corresponding plots of %R (▲) and %B (■). The indicators were incubated under controlled RH of $63\pm 3\%$ (●).

Furthermore, the humidity indicators with 4 cm of $K_2CO_3/NaOH$ (4:1 mol ratio) zone also showed the blue-to-red color transition under 36%RH. The color change was however significantly slower than those under 63%RH. The cropped image area ($1\times 1\text{ cm}^2$) of blue TCDA zone did not completely turn to red color even after 24 hours of the incubation time (**Figure 3.19**).

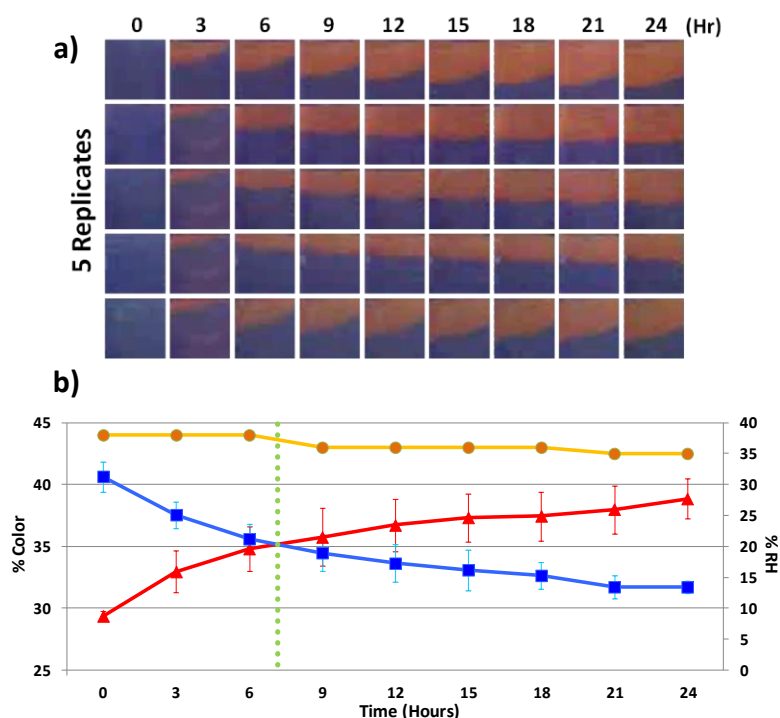


Figure 3.19 a) Color images of TCDA zone of the humidity indicators prepared with 4 cm of $K_2CO_3/NaOH$ (4:1 mol ratio) zone and b) their corresponding plots of %R (▲) and %B (■). The indicators were incubated under controlled RH of $36\pm 2\%$ (●).

Development of humidity indicator prototypes

In the development of humidity indicator prototypes, the scaling patterns are designed to allow the moisture exposure time to be easily justified by simple visualization. To create time scaling patterns, the airbrush painting technique (see section 2.1.3 for preparation details) was selected over the ink-jet printing technique because it is easier to generate the pattern with high color intensity with lower risk of nozzle fouling. The dip coating technique was not used because the pattern generating and controlling by this technique was not so straightforward.

In order to design the time scaling pattern, the humidity indicators prepared with 4 cm of $K_2CO_3/NaOH$ (4:1 mol ratio) zone were tested at 63%RH. The blue TCDA zone of the indicators was monitored by a webcam and the expanding distance of the red color was measured against the millimeter scale marked on its side. The plot of the distance against the moisture exposure time (**Figure 3.20**) was used to assign the time scaling marks on the indicator prototypes. For examples, the marks at 3.0, 8.0, 13.5, 20.5 and 27.5 mm corresponded to the moisture exposure times of 1, 3, 6, 12 and 24 hours.

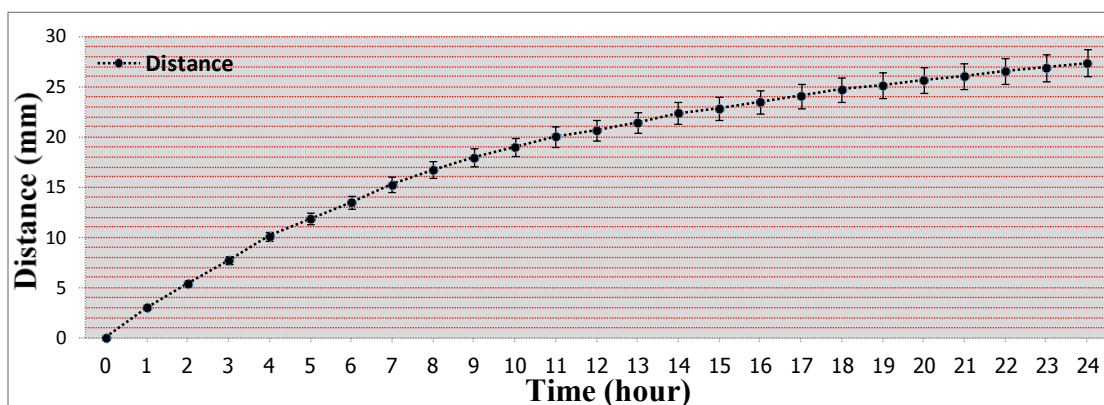


Figure 3.20 Plot of expanding distance of the red color in TCDA zone of humidity indicators versus moisture exposure time at $63\pm 3\%$ RH.

Two patterns of the poly(TCDA) zone of the humidity indicator prototypes were generated by an airbrush painting. The thick lines in one design and the circular dots in the other represent the time scaling marks of 1, 3, 6, 12 and 24 hours. Under the incubation at 63%RH, each blue poly(TCDA) mark turned to red color one by one precisely corresponding to the designed time scales (**Figure 3.21**). The results demonstrated that these periodic patterns could provide a design for humidity indicator prototypes with more explicit time dependence.

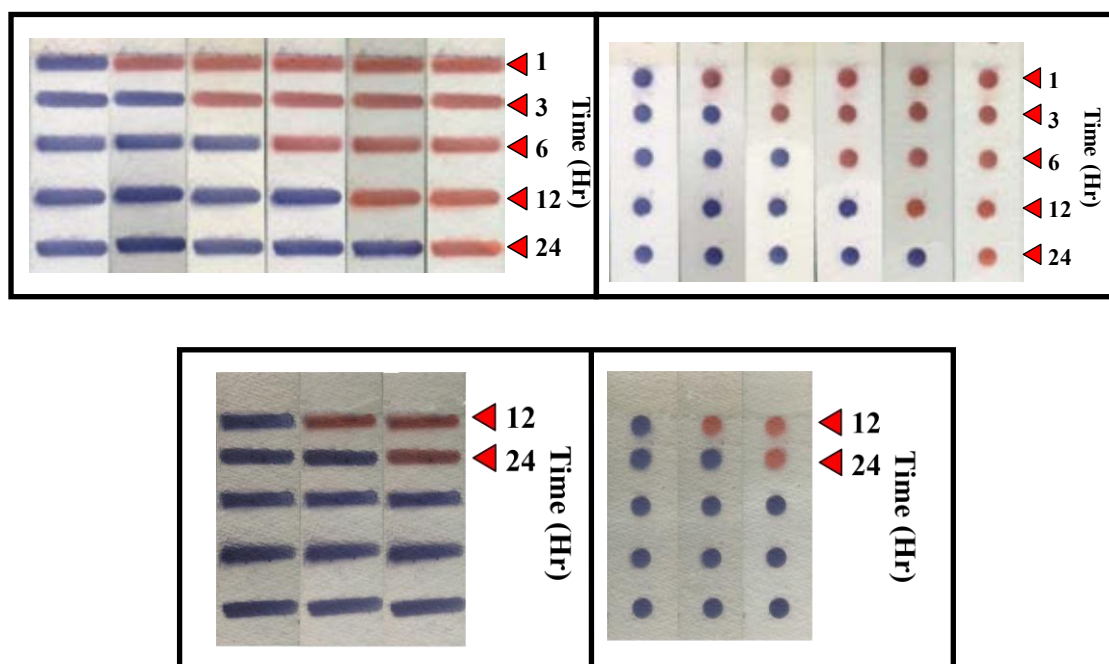


Figure 3.21 Humidity indicator prototypes tested under controlled %RH of $63\pm 3\%$ and $36\pm 2\%$ for 24 hours.

3.2 Techniques for incorporation of leuco dyes into commercial polymers

The incorporation of a thermochromic dye into a commercial polymer is desirable where the applications of the products can cause wear and tear. Three techniques (melt spinning fiber, compression molding and two roll mill) for incorporation of the thermochromic materials into various commercial polymers were studied. Before the processing test, the thermochromic orange Chameleon-T powder with color transition temperature (CTT) of 31°C was characterized by thermal analyses and SEM. The results and discussion of these studies are elaborated in details as follows.

Characterization of leuco dye

A leuco dye is a lactone dye which can reversibly change its color by the protonation and deprotonation process. It has been developed into one of the best known commercially available reversible thermochromic dyes. The control of thermochromic properties usually involve three components *i.e.* a leuco dye, a weak acid and a phase-change medium (PCM) which are microencapsulated within a protective polymeric shell such as melamine. The typical weak acid and PCM used are bisphenol-A and lipids, respectively [67-68]. In this work, the thermal properties of a commercial thermochromic leuco dye (Chameleon-T, orange color, CTT 31°C) were studied by using differential scanning calorimetry (DSC) and thermogravimetric analysis (TGA). The DSC thermogram of the leuco dye exhibited 2 endothermic peaks at 37 °C and 348 °C (**Figure 3.22**) corresponding to the melting temperatures of the PCM and the decomposition temperature of the thermochromic dye components including the encapsulating shell, respectively. The results agreed with the color transition temperature of the Chameleon-T and the decomposition temperature of melamine specified by the vendor [89]. The TGA thermogram (**Figure 3.23**) of Chameleon-T showed the first step weight loss of 3% at 100 °C corresponding to the loss of moisture content in a material. The second step showed another 12% weight loss at 220 °C possibly corresponding to some loss of one or more of the three components (leuco dye, PCM or weak acid). The third step showed additional 60% weight loss at 330 °C which represented the major thermal decomposition of all the components including the polymeric shell. This decomposition temperature is in good agreement with the DSC results.

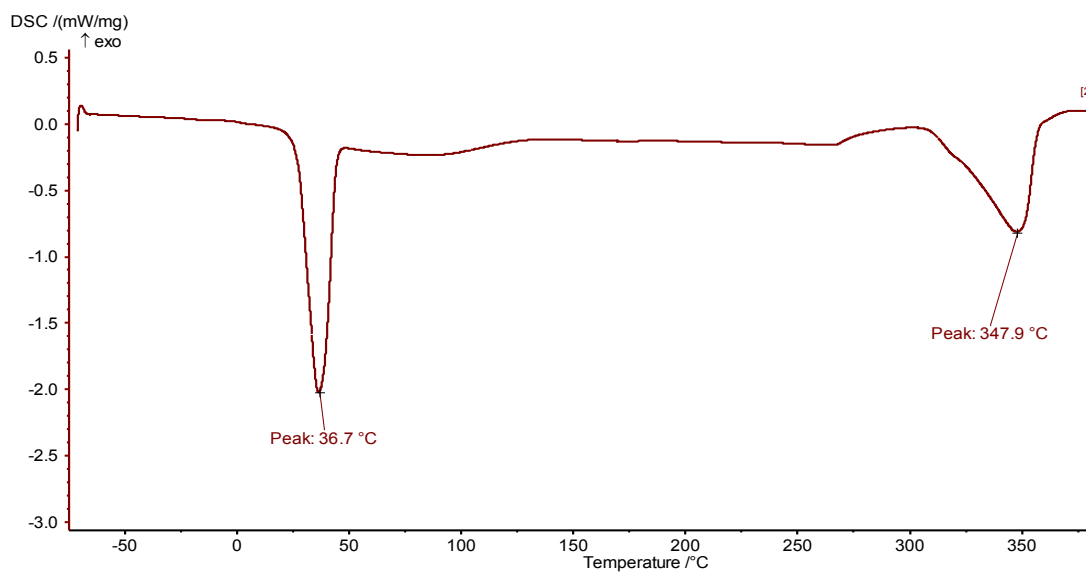


Figure 3.22 DSC thermogram (2nd heating) of commercial thermochromic leuco dye (Chameleon-T).

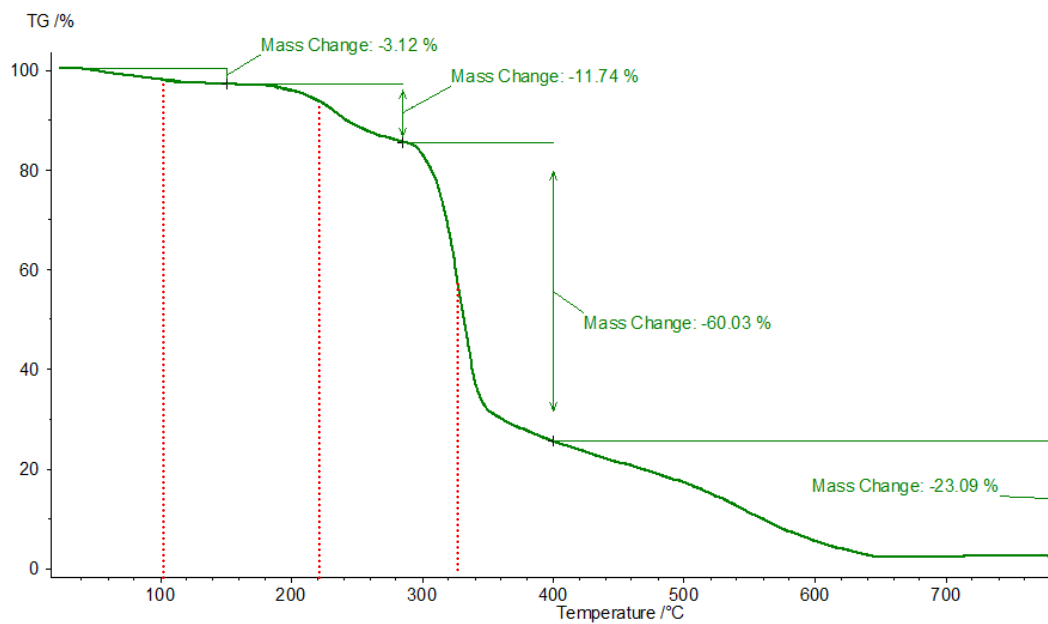


Figure 3.23 TGA thermograms of commercial thermochromic leuco dye (Chameleon-T).

The results from DSC and TGA suggested that this class of commercial thermochromic materials (Chameleon-T powder) should be used under 220 °C to retain their reversible thermochromic properties. To demonstrate this hypothesis, Chameleon-T powder was heated at 220 °C for 5 min in oven. The heating time was selected based on the residual time in the screw extruder of the melt spinning process utilized in the subsequent experiment. As show in **Figure 3.24a**, after the thermochromic was heated, its appearance at 25 °C remained almost the same as that before heating. The thermochromic property of the after heating was evaluated in comparison with the sample before heating by gradual heating from 5 to 40 °C in a test tube immersed in a water bath (see section 2.2.3 for experimental details). The results in **Figure 3.24b** showed almost identical color transition of the material samples before and after heating to 220 °C. It is thus possible to use a thermal process, where the processing temperature is not over 220 °C, such as melt spinning, compression molding and two roll mill for the incorporation of Chameleon-T powder into a commercial polymer.

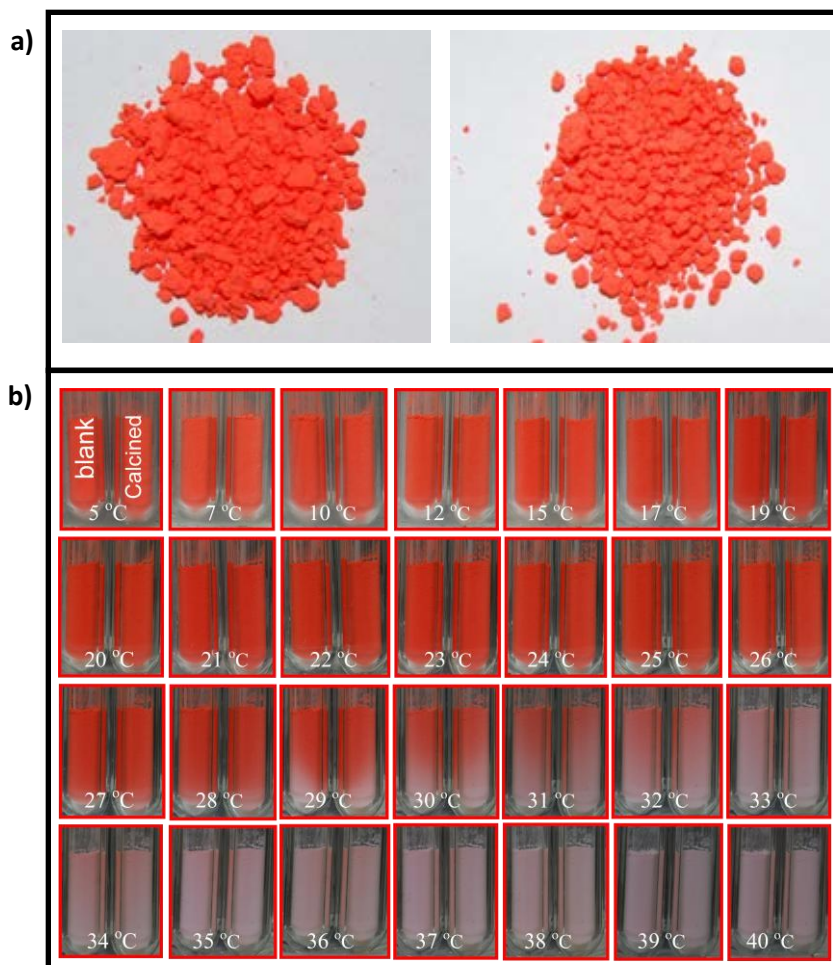


Figure 3.24 Photo images of Chameleon-T powder samples before (left) and after (right) heating to 220 °C recorded **a)** at temperature 25 °C and **b)** during heating from 5 to 40 °C.

Scanning electron microscopy (SEM)

The particle sizes and shapes of the Chameleon-T powder were studied by scanning electron microscopy (SEM). The particles were found to be spherical in shape with diameters below 10 μm (**Figure 3.25**) which are small enough to pass through the 0.3 mm spinnerets and 105 μm filter plate used in the melt spinning process.

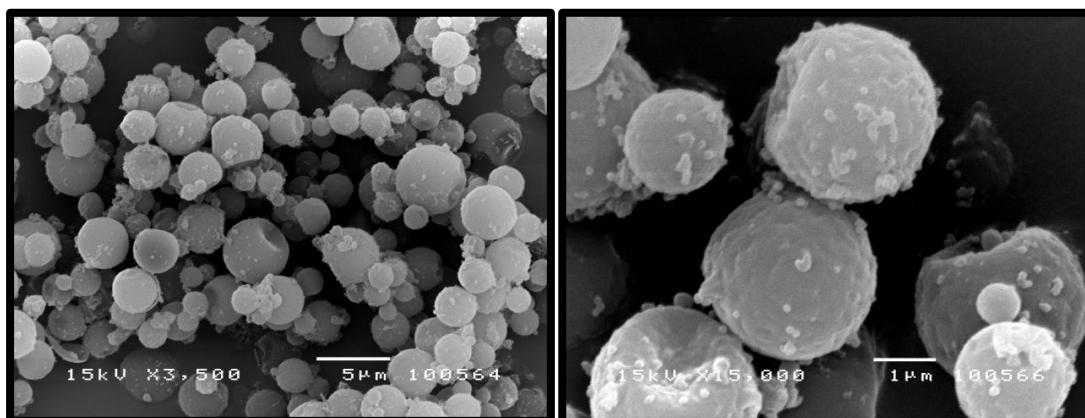


Figure 3.25 SEM images (3,500x and 15,000x) of Chameleon-T powder.

3.2.1 Melt-spinning of polypropylene/leuco dye

The direct incorporation of thermochromic materials into fiber could allow the production of temperature responsive fiber-based products for applications for industrial safety, process control and anti-counterfeit technology. In this work the commercial thermochromic leuco dye, Chameleon-T powder (black color, CTT 28 °C), was used as a model to be incorporated at 1, 2 and 3% w/w into polypropylene (PP, 561R grade, Thai Polypropylene, SCG) by melt-spinning technique. The fiber filament samples were collected and visually inspected. As shown in **Figure 3.26**, the thermochromic property of Chameleon-T powder was retained after the melt spinning processing. The fiber filament with 2% w/w of leuco dye showed the better thermochromic color contrast comparing with the fiber filament with 1% w/w of leuco dye. However, increase of the dye content to 3% w/w did not improve the color contrast. This was due to the loss of the dye from severe clogging of the filter plate (**Figure 3.27**). The clogging implied significant aggregation of the Chameleon-T powder at the higher contents that was evidenced by many small beads found in the

fiber filaments. Additionally, the higher Chameleon-T powder contents, the poorer the strength and smoothness of the fiber filaments became that discouraged their further processing into texture and thread.

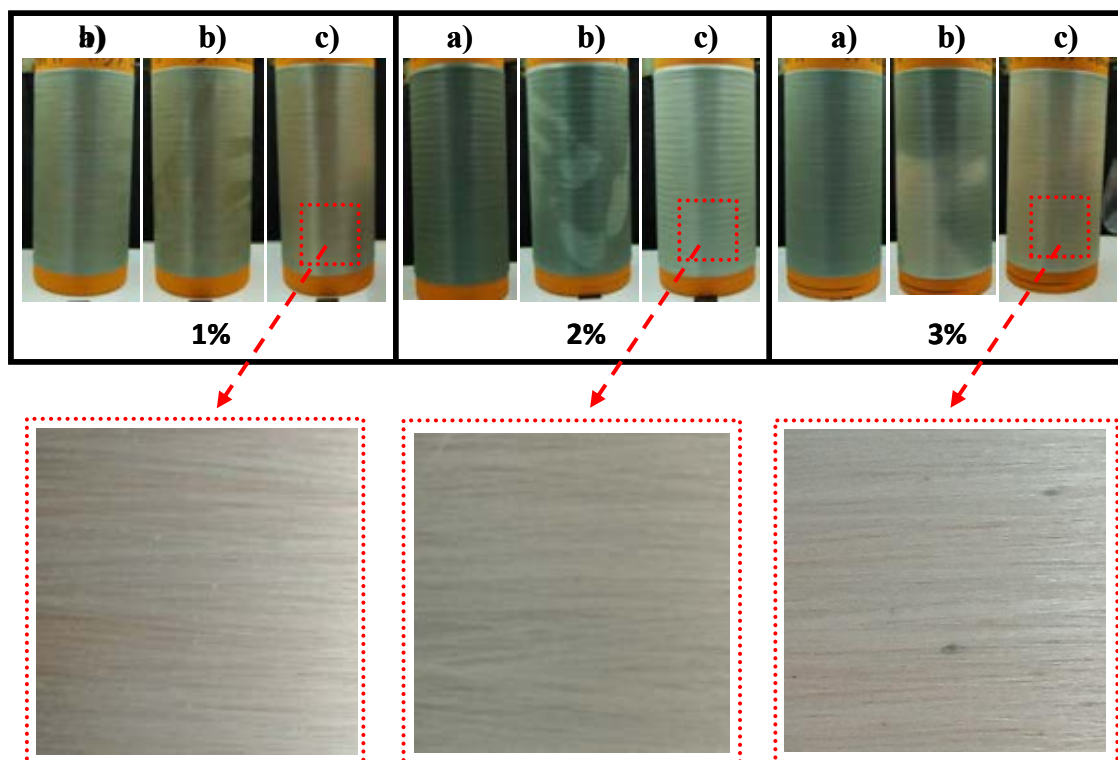


Figure 3.26 Photographs of black Chameleon-T powder (1, 2 and 3% w/w) incorporated polypropylene fiber filament at **a)** 25 °C **b)** body temperature (hand touch) and **c)** warm temperature (blown with a hair dryer). The insets are the closed up pictures showing beads in the fiber filaments with 3% w/w of Chameleon-T powder.

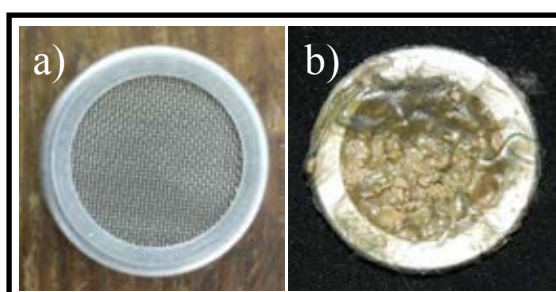


Figure 3.27 Photographs of filter plate (105 μm) **a)** before and **b)** after melt spin processing of PP with % w/w of Chameleon-T powder.

3.2.2 Compression molding of polymer/leuco dye

The compression molding can allow the incorporation of a thermochromic material into a polymer to give 2D-shaped thermochromic objects. These platforms may be attractive for various applications such as toys and temperature warning plates in industry and kitchen. In this work the commercial thermochromic leuco dye, Chameleon-T powder (black color, CCT 29 °C), was used as a model to be incorporated at 3% w/w into polystyrene (PS, PORENE, Thai ABS Co., LTD), polypropylene (PP, 561R grade, Thai Polypropylene, SCG) and low-density polyethylene (LDPE, ExxonMobil™ LDPE LD 100 Series) by compression molding technique. The flat plates (20 cm × 20 cm × 2 mm) were prepared and visually inspected. As shown in **Figure 3.28**, the polymers blended with 3% w/w of Chameleon-T powder gave black plastic plates. These plates showed thermochromic reversibility of Chameleon-T powder with transition temperature around 30 °C. However, the color of the plastic plates was not homogeneous and the plates contained many small cracks on the surface. The appearances of the polymer plates at the temperature above CCT were not clear but rather opaque indicating significant segregation of Chameleon-T powder during the compress molding process. The PS plate appeared yellowish at the temperature above CCT due to its high processing temperature of 250 °C inducing some decomposition of Chameleon-T powder. These results indicate that the incorporation of Chameleon-T powder into polymers by compress molding process still needs significant improvement before it can be used in the real applications. Possibly, polymer compounding is necessary to ensure the good dispersion of Chameleon-T powder and to allow the processing temperature to be below 220 °C.

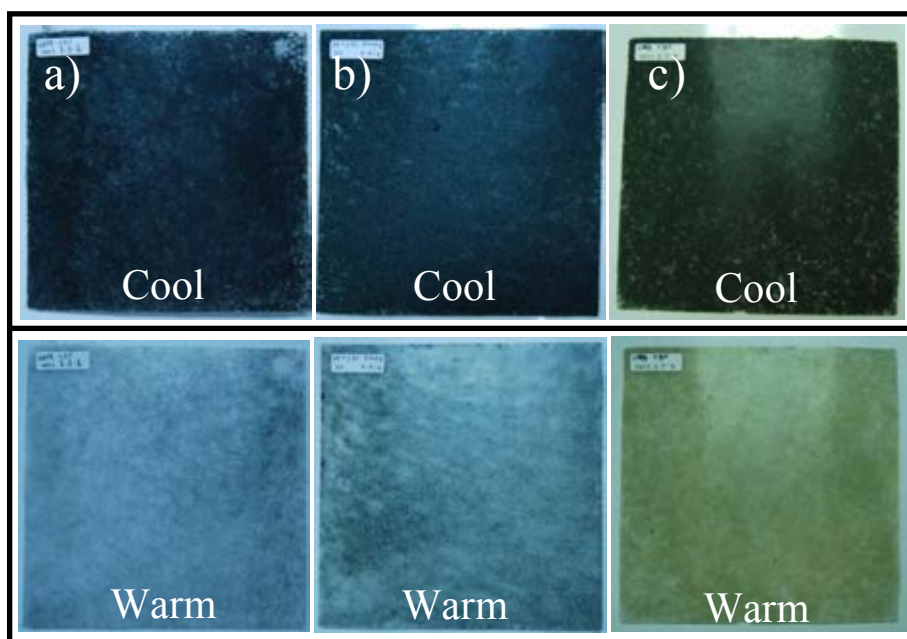


Figure 3.28 Photo images of 3% black Chameleon-T powder incorporated by compressing molding technique with **a)** LDPE at 150 °C, **b)** PP at 210 °C and **c)** PS at 250 °C, the image recorded at 25 °C (up) and warm temperature (blown with a hair dryer) (down).

3.2.3 Two roll mill of rubber/leuco dye

It is also interesting to incorporate the thermochromic materials into elastomer for some applications that require elasticity and temperature responsive properties such as temperature warning sleeves on milk bottles, water hoses and smart rubber tiles. In this work styrene butadiene rubber (SBR, 1502 r) was used as an elastomer model to incorporate with 5% w/w Chameleon-T powder (black color) using a two roll mill compounding process. The rubber compound was compressed into flat plates (12 cm × 12 cm × 5 mm) by a compression molding technique at 95 °C. As shown in **Figure 3.29a**, the SBR plate containing 5% w/w of Chameleon-T powder was black at 25 °C and turned colorless and transparent around 30 °C. However this SBR plate was rather weak that it could be broken easily by hand tearing. To improve the mechanical properties of this SBR plate, the additives such as sulfur (curing agent, 2 phr), N-cyclohexyl-2-benzothiazole sulfonamide (CBS, accelerator, 1.3 phr), stearic (activator, 1 phr) and paraffinic oil (softener, 5 phr) were added during the

compounding process. After the compression molding, the cured SBR plate with the additives appeared in gray color and showed thermochromic reversibility of Chameleon-T powder with CTT around 30 °C. The cured rubber plate also became tougher but its surface was not smooth but contained many small cracks and voids. Furthermore, the cured plate became white opaque above the CTT (**Figure 3.29b**). Again, the incorporation of Chameleon-T powder into rubber by two roll mill process still needs significant improvement before it can be used in the real applications. Possibly, transparent curing agents such as peroxide and better compounding techniques are necessary to ensure the good appearance of the final rubber products.

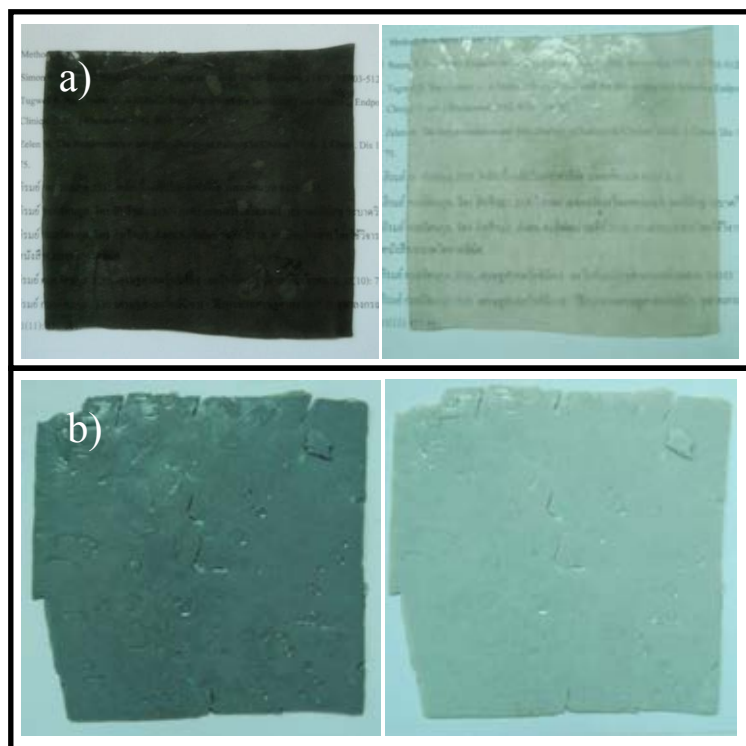


Figure 3.29 Photographs of **a)** SBR plate containing 5% black Chameleon-T powder and **b)** cured SBR plate containing 5% black Chameleon-T powder at 25 °C (left), and at above 30 °C (blown with a hair dryer, right).

CHAPTER IV

CONCLUSION

In conclusion, ink-jet printing, airbrush painting and dip coating techniques can be used to fabricate diacetylene monomers (PCDA and TCDA) onto surface of various solid materials. The conversion of the monomers on the solid surface can be achieved by UV irradiation that produces blue PDA coating with retained blue-to-red chromism properties. In the ink-jet printing technique, a nonionic surfactant was required for the diacetylene ink formulation and it can affect the color transition points in chromism of the PDA. In general, the surfactant increased the chromism sensitivity of the PDA. The airbrush painting technique allowed the deposition of both diacetylene and leuco dyes with or without the use of surfactants on surfaces of various materials. While retaining the desired chromic properties of the dyes, the airbrush painting also gave more intense color images on the surface than those produced by the ink-jet printing. Although the airbrush painting required manual operation and brought about more dye loss, it was more convenient to be used in the early development stage due to its greater operating flexibility and hassle-free dye formulation in comparison with the ink-jet technique. The dip coating was however the most simple dye deposition technique to be used in the earliest step for the development of indicators. It was successfully used to deposit the diacetylene lipids (TCDA and PCDA), from their solutions in CH_2Cl_2 , onto the surface of polyester (PET) thread and filter paper strips. The diacetylene deposited by the dip coating technique was also polymerized by UV irradiation to give the corresponding blue PDA with retained blue-to-red color transition properties that the coating on the filter paper was readily developed into humidity indicators. The most sensitive humidity indicators consisted of two dip coating zones i.e. $\text{K}_2\text{CO}_3/\text{NaOH}$ (4:1 mole ratio) and TCDA. The humidity sensing is operated by the moisture absorption of the salts followed by the diffusion of hydroxide ion which in turn induces alkalinochromism of poly(TCDA). The moisture sensitivity of the indicators is thus also highly depended on the amount of the salts deposited on the filter paper. To develop the time-humidity

indicator prototypes, the airbrush painting was used in the subsequent step to generate the designed time-scale patterns of the TCDA deposition. The blue poly(TCDA) marks in the indicator prototypes exhibited blue-to-red color transition one by one precisely corresponding to the designed time scales of 1-24 hours at 63%RH. Additionally, this moisture indicator can perform at 36%RH. The time-humidity indicator prototypes developed in this thesis work should find immediate applications where the excessive environmental moisture is concerned.

For the incorporation of thermochromic leuco dyes into commercial polymers, 3 techniques i.e. melt spinning, compression molding and two roll mill processes. The results indicated that these 3 techniques could be used to incorporate the commercial thermochromic Chameleon-T powder into several commercial polymers with retained reversible thermochromic properties provided that the processing temperatures were below its decomposition temperature of 220 °C. In the melt spinning process, only 2% of Chameleon-T powder could be incorporated into PP fiber filaments. The higher Chameleon-T powder contents weaken the fiber strength, increased fiber surface roughness and caused clogging of the filter plate for the spinneret that discouraged their further processing into texture and thread. The compression molding process allowed the incorporation of 3% Chameleon-T powder into LDPE, PP and PS plastic plates. Good thermochromic reversibility of Chameleon-T powder with transition temperature around 30 °C were observed for LDPE and PP but not PS due to the high processing temperature of PS (250 °C). However, the colors of the plastic plates were not homogeneous and their surface contained many small cracks on the surface. The appearances of the polymer plates at the temperature above CCT were opaque indicating significant segregation of Chameleon-T powder during the compression molding process. The two roll mill combined with the compression molding process allowed the incorporation of 5% w/w of Chameleon-T powder into SBR rubber plates. Without the curing agents, the rubber plates showed good optical and thermochromic properties but weak mechanical properties while adding sulfur curing agents could improve the mechanical properties but somewhat adversely affected the final appearance. Therefore, further investigation is required to optimize these incorporation techniques before they can be used in preparation of real temperature sensing plastic products.

REFERENCES

- [1] McQuade, D. T.; Pullen, A. E.; Swager, T. M. Conjugated polymer-based chemical sensors. *Chem. Rev.* 100 (2000): 2537-2574.
- [2] Ahn, D. J.; Lee, S.; Kim, J. M. Rational design of conjugated polymer supramolecules with tunable colorimetric responses. *Adv. Funct. Mater.* 19 (2009): 1483-1496.
- [3] Kim, J. M.; Lee, J. S.; Choi, H.; Sohn, D.; Ahn, D. J. Rational design and in-situ FTIR analyses of colorimetrically reversible polydiacetylene supramolecules. *Macromolecules* 38 (2005): 9366-9376.
- [4] Tajima, K.; Aida, T. Controlled polymerizations with constrained geometries *Chem. Commun.* 24 (2000): 2399-2412.
- [5] Baughman, R. H.; Yee, K. C. Solid-state polymerization of linear and cyclic acetylenes *J. Polym. Sci. Macromol. Rev.* 13 (1978): 219-239.
- [6] Enkelmann, V. Structural aspects of the topochemical polymerization of diacetylenes *Adv. Polym. Sci.* 63 (1984) 91-136.
- [7] Potisatityuenyong, A.; Rojanathanes, R.; Tumcharern, G.; Sukwattanasinitt, M. Electronic absorption spectroscopy probed side-chain movement in chromic transitions of polydiacetylene vesicles. *Langmuir* 24 (2008): 4461-4463.
- [8] Wacharasindhu, S.; Montha, S.; Boonyiseng, J.; Potisatityuenyong, A.; Phollookin, C.; Tumcharern, G.; Sukwattanasinitt, M. Tuning of thermochromic properties of polydiacetylene toward universal temperature sensing materials through amido hydrogen bonding. *Macromolecules* 43 (2010): 716-724.
- [9] Phollookin, C.; Wacharasindhu, S.; Ajavakom, A.; Tumcharern, G.; Ampornpun, S.; Eaidkong, T.; Sukwattanasinitt, M. Tuning down of color transition temperature of thermochromically reversible bisdiynamide polydiacetylenes. *Macromolecules* 43 (2010): 7540-7548.

- [10] Song, J.; Cheng, Q.; Kopta, S.; Stevens, R. C. Modulating artificial membrane morphology: pH-induced chromatic transition and nanostructural transformation of a bolaamphiphilic conjugated polymer from blue helical ribbons to red Nanofibers. *J. Amer. Chem. Soc.* 123 (2001): 3205-3213.
- [11] Shimizu, T.; Masuda, M.; Minamikawa, H. Supramolecular nanotube architectures based on amphiphilic molecules. *Chem. Rev.* 105 (2005): 1401-1443.
- [12] Park, K. H.; Lee, J. S.; Park, H.; Oh, E. H.; Kim, J. M. Vancomycin-induced morphological transformation of self-assembled amphiphilic diacetylene supramolecules. *Chem. Commun.* 4 (2007): 410-412.
- [13] Okada, S.; Peng, S.; Spevak, W.; Charych, D. Color and chromism of polydiacetylene vesicles. *Acc. Chem. Res.* 31 (1998): 229-239.
- [14] Frankel, D. A.; O'Brien, D. F. Supramolecular assemblies of diacetylenic aldonamides. *J. Amer. Chem. Soc.* 116 (1994): 10057-10069.
- [15] Jonas, U.; Shah, K.; Norvez, S.; Charych, D. H. Reversible color switching and unusual solution polymerization of hydrazide-modified diacetylene lipids. *J. Amer. Chem. Soc.* 121 (1999): 4580-4588.
- [16] Charych, D. H.; Nagy, J. O.; Spevak, W.; Bednarski, M. D. Direct colorimetric detection of a receptor-ligand interaction by a polymerized bilayer assembly. *Science* 261 (1993): 585-588.
- [17] Van den Heuvel, M.; Lowik, D.; van Hest, J. C. M. Self-assembly and polymerization of diacetylene-containing peptide amphiphiles in aqueous solution. *Biomacromolecules* 9 (2008): 2727-2734.
- [18] Champaiboon, T.; Tumcharern, G.; Potisatityuenyong, A.; Wacharasindhu, S.; Sukwattanasinitt, M. A polydiacetylene multilayer film for naked eye detection of aromatic compounds. *Sensor. Actuat-B.* 139 (2009): 532-537.
- [19] Chen, X.; Yoon, J. A thermally reversible temperature sensor based on polydiacetylene: Synthesis and thermochromic properties. *Dyes. Pigments.* 89 (2011): 194-198.
- [20] Eo, S. H.; Song, S.; Yoon, B.; Kim, J. M., A microfluidic conjugated-polymer sensor chip. *Adv. Mater.* 20 (2008): 1690-1694.

- [21] Martinez, A. W.; Phillips, S. T.; Carrilho, E.; Thomas, S. W.; Sindi, H.; Whitesides, G. M. Simple telemedicine for developing regions: Camera phones and paper-based microfluidic devices for real-time, off-site diagnosis. *Anal. Chem.* 80 (2008): 3699-3707.
- [22] Apilux, A.; Dungchai, W.; Siangproh, W.; Praphairaksit, N.; Henry, C. S.; Chailapakul, O., Lab-on-paper with dual electrochemical/colorimetric detection for simultaneous determination of gold and iron. *Anal. Chem.* 82 (2010): 1727-1732.
- [23] Pumtang, S.; Siripornnoppakhun, W.; Sukwattanasinitt, M.; Ajavakom, A. Solvent colorimetric paper-based polydiacetylene sensors from diacetylene lipids. *J. Colloid Interface Sci.* 364 (2011): 366-372.
- [24] Thongmalai, W.; Eaidkong, T.; Ampornpun, S.; Mungkarndee, R.; Tumcharern, G.; Sukwattanasinitt, M.; Wacharasindhu, S., Polydiacetylenes carrying amino groups for colorimetric detection and identification of anionic surfactants. *J. Mater. Chem.* 21 (2011): 16391-16397.
- [25] Eaidkong, T.; Mungkarndee, R.; Phollookin, C.; Tumcharern, G.; Sukwattanasinitt, M.; Wacharasindhu, S. Polydiacetylene paper-based colorimetric sensor array for vapor phase detection and identification of volatile organic compounds. *J. Mater. Chem.* 22 (2012): 5970-5977.
- [26] Jung, Y. K.; Park, H. G.; Kim, J. M. Polydiacetylene (PDA)-based colorimetric detection of biotin-streptavidin interactions. *Biosensors Bioelectronics* 21 (2006): 1536-1544.
- [27] http://www.nobelprize.org/nobel_prizes/physics/laureates/2009/press.html (accessed Jun 7, 2012).
- [28] Friedman, S.; Kolusheva, S.; Volinsky, R.; Zeiri, L.; Schrader, T.; Jelinek, R. Lipid/polydiacetylene films for colorimetric protein surface-charge analysis. *Anal. Chem.* 80 (2008): 7804-7811.
- [29] Volinsky, R.; Kliger, M.; Sheynis, T.; Kolusheva, S.; Jelinek, R. Glass-supported lipid/polydiacetylene films for colour sensing of membrane-active compounds. *Biosensors Bioelectronics* 22 (2007): 3247-3251.

- [30] Reppy, M.A.; Pindzola, B.A. Biosensing with polydiacetylene materials: structures, optical properties and applications *Chem. Commun.* (2007) 4137-4338.
- [31] Yoon, J.; Chae, S.; Kim, J. Colorimetric sensors for volatile organic compounds (VOCs) based on conjugated polymer-embedded electrospun fibers *J. Am. Chem. Soc.* 129 (2007) 3038-3039.
- [32] Rangin, M.; Basu, A., Lipopolysaccharide identification with functionalized polydiacetylene liposome sensors. *J. Am. Chem. Soc.* 126 (2004): 5038-5039.
- [33] Yoon, B.; Lee, S.; Kim, J. M. Recent conceptual and technological advances in polydiacetylene-based supramolecular chemosensors. *Chem. Soc. Rev.* 38 (2009): 1958-1968.
- [34] Su, Y. L.; Li, J. R.; Jiang, L., Chromatic immunoassay based on polydiacetylene vesicles. *Colloids Surf.B.* 38 (2004): 29-33.
- [35] http://en.wikipedia.org/wiki/RGB_color_model (accessed April 17, 2013).
- [36] Kuriyama, K.; Kikuchi, H.; and Kajiyama, T. Chromatic Phase of Polydiacetylene Langmuir-Blodgett Film. *Langmuir* 14 (1998): 1130-1138.
- [37] Fujita, N.; Sakamoto, Y.; Shirakawa, M.; Ojima, M.; Fujii, A.; Ozaki, M.; Shinkai, S., Polydiacetylene nanofibers created in low-molecular-weight gels by post modification: Control of blue and red phases by the odd-even effect in alkyl chains. *J. Am. Chem. Soc.* 129 (2007): 4134-4135.
- [38] Ampornpun, S.; Montha, S.; Tumcharern, G.; Vchirawongkwin, V.; Sukwattanasinitt, M.; Wacharasindhu, S. Odd-even and hydrophobicity effects of diacetylene alkyl chains on thermochromic reversibility of symmetrical and unsymmetrical diyndiamide polydiacetylenes. *Macromolecules* 45 (2012): 9038-9045.
- [39] Chanakul, A.; Traiphol, N.; Traiphol, R. Controlling the reversible thermochromism of polydiacetylene/zinc oxide nanocomposites by varying alkyl chain length. *J. Colloid Interface Sci.* 389 (2013): 106-114.

- [40] Kanetake, T.; Tokura, Y.; Koda, T. Photo and thermochromism in vacuum deposited polydiacetylene films. *Solid State Commun.* 56 (1985): 803-807.
- [41] Tokura, Y. Photochromism and photoinduced bond-structure change in the conjugated polymer polydiacetylene. *Phys. Rev. B.* 36 (1987): 2913-2915.
- [42] Wenzel, M.; Atkinson, G. H.; Chromatic Properties of Polydiacetylene Films. *J. Am. Chem. Soc.* 111 (1989): 6123-6121.
- [43] Peng, J. C. Photochromism and its mechanism polydiacetylene crystals. *Acta Physica Sinica* 6 (1997): 140-150.
- [44] Huo, Q.; Russell, K. C.; Leblanc, R. M. Chromatic studies of a polymerizable diacetylene hydrogen bonding self-assembly: A "self-folding" process to explain the chromatic changes of polydiacetylenes. *Langmuir* 15 (1999): 3972-3980.
- [45] Song, J.; Cisar, J. S.; Bertozzi, C. R. Functional self-assembling bolaamphiphilic polydiacetylenes as colorimetric sensor scaffolds. *J. Am. Chem. Soc.* 126 (2004): 8459-8465.
- [46] Yuan, W. F.; Jiang, G. Y.; Song, Y. L.; Jiang, L. Micropatterning of polydiacetylene based on a photoinduced chromatic transition and mechanism study. *J. Appl. Pol. Sci.* 103 (2007): 942-946.
- [47] Sung, X. M.; Chen, T.; Huang, S. Q.; Cai, F. J.; Chen, X. L.; Yang, Z. B.; Li, L.; Cao, H.; Lu, Y. F.; Peng, H. S., UV-Induced chromatism of polydiacetylenic assemblies. *J. Phys. Chem. B* 114 (2010): 2379-2382.
- [48] Yoon, J.; Jung, Y. S.; Kim, J. M. A Combinatorial approach for colorimetric differentiation of organic solvents based on conjugated polymer embedded electrospun Fibers. *Adv. Funct. Mater.* 19 (2009): 209-214.
- [49] Jiang, H.; Wang, Y. L.; Ye, Q.; Zou, G.; Su, W.; Zhang, Q. J. Polydiacetylene-based colorimetric sensor microarray for volatile organic compounds. *Sensors Actuat-B.* 143 (2010): 789-794.
- [50] Wu, S.; Zhang, Q. J.; Bubeck, C. Solvent effects on structure, morphology, and photophysical properties of an azo chromophore-functionalized polydiacetylene. *Macromolecules* 43 (2010): 6142-6151.

- [51] Cheng, Q.; Stevens, C. Charge-induced chromatic transition of amino acid-derivatized polydiacetylene liposomes. *Langmuir* 14 (1998): 1974.
- [52] Charoenthai, N.; Pattanatornchai, T.; Wacharasinidhu, S.; Sukwattanasinitt, M.; Traiphol, R., Roles of head group architecture and side chain length on colorimetric response of polydiacetylene vesicles to temperature, ethanol and pH. *J. Colloid Interface Sci.* 360 (2011): 565-573.
- [54] Li, L. S.; Stupp, S. I., Two-dimensional supramolecular assemblies of a polydiacetylene .2. Morphology, structure, and chromic transitions. *Macromolecules* 30 (1997): 5313-5320.
- [55] Louis, B. R. Saturated salt solutions for static control of relative humiditybetween 5° and 40° C. *Anal. chem.* 32(1960): 1375-1376.
- [56] Robinson, R. A. Standard solution for humidity control at 25 °C.
- [56] Yoon, B.; Ham, D. Y.; Yarimaga, O.; An, H.; Lee, C. W. Inkjet printing of conjugated polymer precursors on paper substrates for colorimetric sensing and flexible electrothermochromic display. *Adv. Mater.* 23(2011): 5492-5497.
- [57] Yoon, B.; Shin, H.; Yarimaga, O.; Ham, D. Y.; Kim, J.; Park, I. S.; Kim, J. M. An inkjet-printable microemulsion system for colorimetric polydiacetylene supramolecules on paper substrates. *J. Mater. Chem.* 22 (2012): 8680-8686
- [58] Yoon, B.; Shin, H.; Kang, E. M.; Cho, D. W.; Kim, J. M. Inkjet-compatible single-component polydiacetylene precursors for thermochromic paper sensors. *Appl. Mater. Interfaces.* 5 (2013): 4527-4535.
- [59] Grazia, A. D.; Mikhael, M.; Stojanovska, N.; Reedy, B.; Tahtouh, M. Diacetylene copolymers for fingerprint development. *Forensic Science International.* 216 (2012): 189-197. (Airbrush)
- [60] Lee, J.; Seo, S.; Kim, J. Colorimetric detection of warfare gases by polydiacetylenes toward equipment-free detection. *Adv. Funct. Mater.* 22 (2012): 1632-1638.

- [61] Kauffman, J. S.; Ellerbrock, B. M.; Stevens, K. A.; Brown, P. J.; Hanks, T. W. Preparation, characterization, and sensing behavior of polydiacetylene liposomes embedded in alginate fibers. *Appl. Matter. Interface*. 1 (2009): 1287-1291.
- [62] Potisatityuenyong, A.; Tumcharern, G.; Dubas, S.; Sukwattanasinitt, M. Layer-by-layer assembly of intact polydiacetylene vesicles with retained chromic properties. *J. Colloid Interface Sci.* 304 (2006): 45-51.
- [63] Champaiboon, T.; Tumcharern, G.; Potisatityuenyong, A.; Watcharosindhu, S.; Sukwattanasinitt, M. A polydiacetylene multilayer film for naked eye detection of aromatic compounds. *Sens. Actuators, B*. 139 (2009): 532-537.
- [64] Marla, V. T.; Shambaugh, R. L.; Papavassiliou, D. V. Online measurement of fiber diameter and temperature in the melt-spinning and melt-blowing processes. *Ind. Eng. Chem. Res.* 48 (2009): 8736-8744.
- [65] Chen, P.; Afshari, M.; Cuculo, J. A.; Kotek, R. Direct formation and characterization of a unique precursor morphology in the melt-spinning of polyesters. *Macromolecules*. 41 (2009): 5437-5441.
- [66] Magdassi, S.; Moshe, M. B. Patterning of organic nanoparticles by ink-jet printing of microemulsions. *Langmuir*. 19 (2003): 939-942
- [67] Nelson, G. Application of microencapsulation in textiles. *Int. J. Pharmaceut.* 242 (2002): 55-62.
- [68] Malherbe, I.; Sanderson, R. D.; Smit, E. Reversibly thermochromic micro-fibres by coaxial electrospinning. *Polymer*. 51 (2010): 5037-5043.
- [69] Ngampeungpis, W. Preparation of multi-purposed paper indicators from diacetylene lipids. Degree of Doctor of Philosophy Program in Petrochemistry. Chulalongkorn University (2012).
- [70] Gou, M.; Guo, G.; Zhang, J.; Men, K.; Song, J.; Luo, F.; Zhao, X.; Qian, Z.; and Wei, Y. Time-temperature chromatic sensor based on polydiacetylene (PDA) vesicle and amphiphilic copolymer. *Sens. Actuators, B* 150 (2010): 406-411.

- [71] Thongmalai, W.; Eaidkong, T.; Ampornpun, S.; Mungkarndee, R.; Tumcharern, G.; Sukwattanasinitt, M.; and Wacharasindhu, S. Polydiacetylenes carrying amino groups for colorimetric detection and identification of anionic surfactants. *J. Mater. Chem.* 21 (2011): 16391-16397.
- [72] Kim, J. M.; Lee, Y. B.; Chae, S. K.; and Ahn D. J. Patterned color and fluorescent images with polydiacetylene supramolecules embedded in poly(vinyl alcohol) films. *Adv. Funct. Mater.* 16 (2006): 2103-2109.
- [73] Pattanatornchai, T.; Charoenthai, N.; Wacharasindhu, S.; Sukwattanasinitt, M.; and Traiphol, R. Control over the color transition behavior of polydiacetylene vesicles using different alcohols. *J. Colloid Interface Sci.* 391 (2013): 45-53.
- [74] Gou, M.; Gou, G.; Zhang, J.; Men, K.; Song, J.; Lou, F.; Zhao, X.; Qian, Z.; Wei, Y. Time-temperature chromatic sensor based on polydiacetylene (PDA) vesicle and amphiphilic copolymer. *Sensor Actuat B-Chem.* 150 (2010): 406-411.
- [75] Liu, F.; Urban, M. W. Recent advances and challenges in designing stimuli-responsive polymers. *Prog. Polym. Sci.* 35 (2010): 3-23.
- [76] MacLaren, D. C.; White, M. A. Competition between dye-developer and solvent-developer interactions in a reversible thermochromic system. *J. Mater. Chem.* 13 (2003): 1701-1704.
- [77] Yoon, J.; Kim, J. M. Fabrication of conjugated polymer supramolecules in electrospun micro/nanofibers. *Macromol Chem. Phys.* 209 (2008): 2194-2203.
- [78] Jiang, H.; Wang, Y.; Ye, Q.; Zou, G.; Su, W.; Zhang, Q. Polydiacetylene-based colorimetric sensor microarray for volatile organic compounds. *Sensor Actuat B-Chem.* 143 (2010): 789-794.
- [79] Chen, X.; Yoon, J. A thermally reversible temperature sensor based on polydiacetylene: synthesis and thermochromic properties. *Dyes Pigment.* 89 (2011): 194-198.
- [80] Gentile, M., Appliance windows coated with thermochromic polymer dispersed liquid crystal, U.S. Patent US 2001/6294258.

- [81] <http://www.fibre2fashion.com/industry-article/9/804/thermochromic-colors-in-textiles2.asp> [2013, august 8]
- [82] <http://en.wikipedia.org/wiki/Humidity> [2013, august 8]
- [83] <http://hyperphysics.phy-astr.gsu.edu/hbase/kinetic/relhum.html> [2013, august 8]
- [84] http://en.wikipedia.org/wiki/Inkjet_printing [2013, august 8]
- [85] <http://en.wikipedia.org/wiki/Airbrush> [2013, august 8]
- [86] [http://en.wikipedia.org/wiki/Spinning_\(polymers\)](http://en.wikipedia.org/wiki/Spinning_(polymers)) [2013, august 8]
- [87] http://en.wikipedia.org/wiki/Rubber_technology [2013, august 8]
- [88] <http://www.fda.gov/> [2013, august 8]
- [89] <http://polychrom.co.kr/> [2013, august 8]

APPENDICES

APPENDIX A

INK-JET PRINTING

Table A1 RGB values of PCDA/ Brij[®] 58 P indicators at UV exposure times (3 independent experiments)

Time (min)	Sample 1				Sample 2				Sample 3			
	R	G	B	sum	R	G	B	sum	R	G	B	sum
0.5	203	212	237	652	204	213	238	655	206	214	237	657
1.0	201	209	234	644	200	207	232	639	203	211	236	650
1.5	200	207	233	640	200	206	233	639	200	206	232	638
2.0	195	200	228	623	199	203	231	633	198	203	229	630
2.5	196	200	227	623	198	201	229	628	198	202	228	628
3.0	195	201	228	624	198	200	228	626	197	202	228	627
3.5	197	199	226	622	198	199	227	624	197	200	226	623
4.0	195	196	222	613	198	199	227	624	197	200	226	623
4.5	197	196	224	617	200	200	227	627	197	198	225	620
5.0	197	197	224	618	200	199	226	625	200	201	228	629

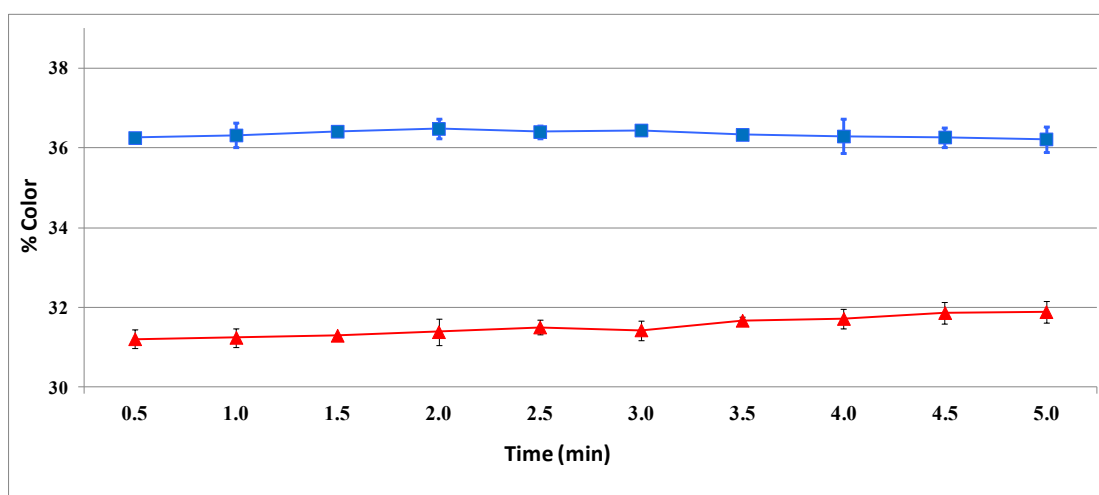


Figure A1 Plots of %RGB value of 3 independent PCDA/ Brij[®] 58 P indicators against UV exposure times to determine the optimized time for exposure of PCDA

Table A2 RGB values of PCDA/ Triton[®] X-100 indicators at UV exposure times (3 independent experiments)

Time (min)	Sample 1				Sample 2				Sample 3			
	R	G	B	sum	R	G	B	sum	R	G	B	sum
0.5	204	215	241	660	206	217	243	666	205	217	241	663
1.0	198	208	235	641	200	210	237	647	201	211	237	649
1.5	191	199	225	615	198	206	232	636	198	206	231	635
2.0	194	201	228	623	197	205	231	633	197	204	231	632
2.5	193	199	225	617	195	200	227	622	195	201	228	624
3.0	195	199	225	619	196	200	227	623	195	200	227	622
3.5	195	198	224	617	195	199	226	620	194	198	225	617
4.0	191	194	220	605	194	196	224	614	194	198	224	616
4.5	192	194	219	605	195	196	223	614	193	195	223	611
5.0	195	196	221	612	195	196	222	613	195	197	222	614

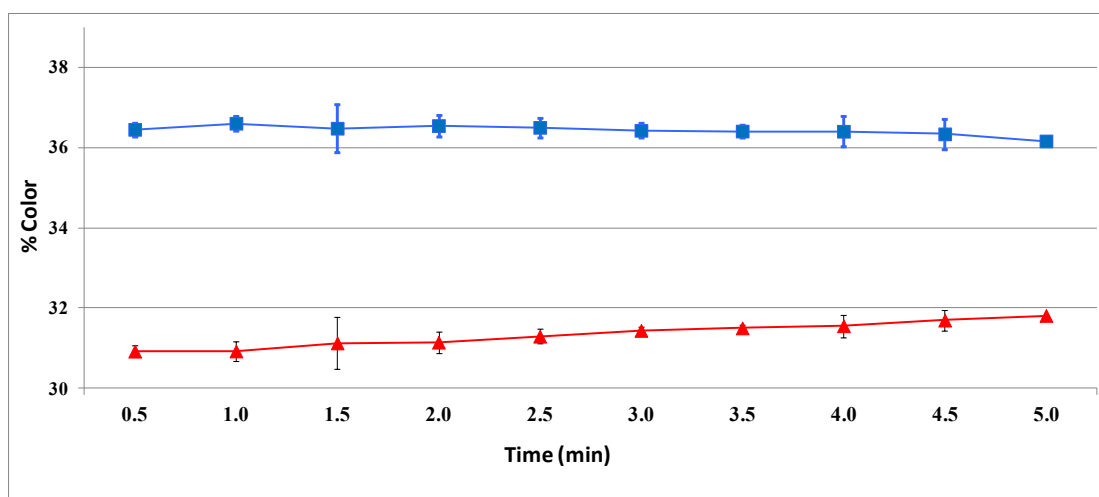


Figure A2 Plots of %RGB value of 3 independent PCDA/Triton[®] X-100 indicators against UV exposure times to determine the optimized time for exposure of PCDA

Table A3 RGB values of PCDA/ Tween[®] 20 indicators at UV exposure times (3 independent experiments)

Time (min)	Sample 1				Sample 2				Sample 3			
	R	G	B	sum	R	G	B	sum	R	G	B	sum
0.5	189	200	228	617	187	199	228	614	187	197	228	612
1.0	185	194	226	605	187	197	228	612	183	194	228	605
1.5	184	192	224	600	182	191	223	596	181	189	225	595
2.0	182	189	222	593	180	187	220	587	177	185	221	583
2.5	181	186	219	586	179	184	217	580	176	182	217	575
3.0	180	184	216	580	179	184	216	579	177	182	217	576
3.5	181	184	217	582	180	184	216	580	177	181	217	575
4.0	181	183	216	580	179	182	214	575	176	180	216	572
4.5	180	182	215	577	177	181	214	572	177	179	214	570
5.0	179	178	211	568	178	179	213	570	177	179	213	569

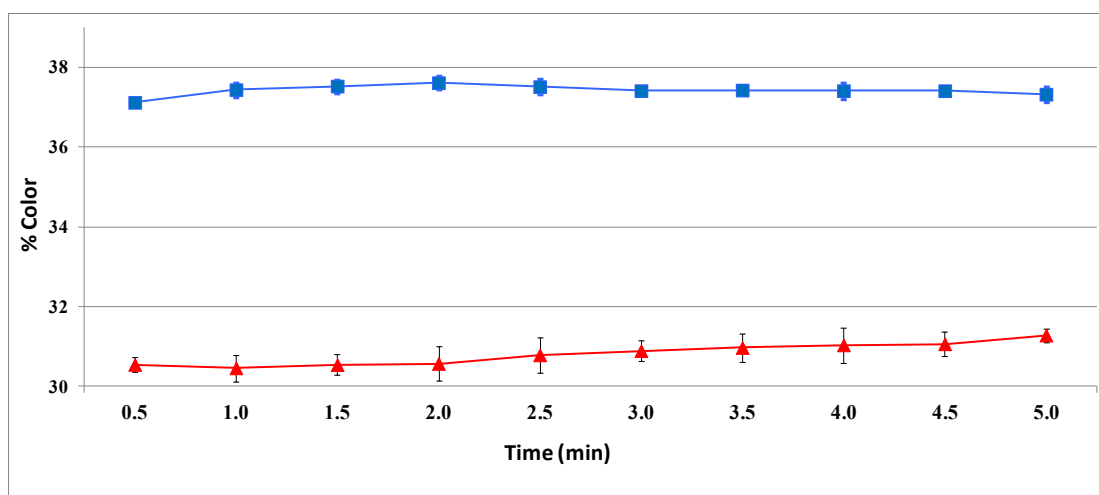


Figure A3 Plots of %RGB value of 3 independent PCDA/ Tween[®] 20 indicators against UV exposure times to determine the optimized time for exposure of PCDA

APPENDIX B

AIRBRUSH PAINTING

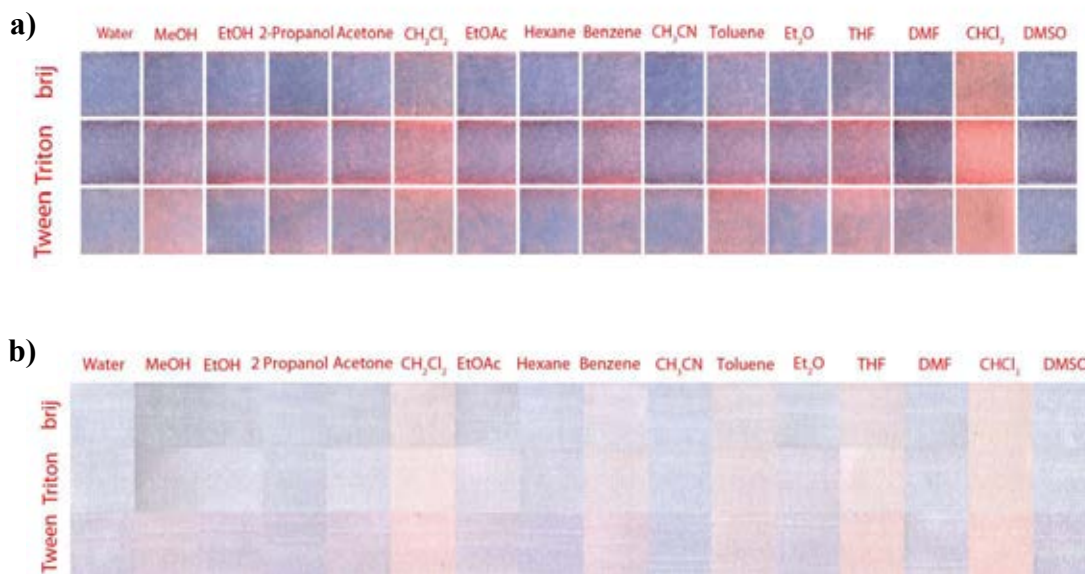


Figure B1 Cropped photographic images of solvent sensing arrays fabricated by **a)** airbrush painting and **b)** ink-jet printing technique of PCDA incorporated with Brij[®] 58 P, Triton[®] X-100 and Tween[®] 20 after the exposure to water (control) and 14 organic solvents.

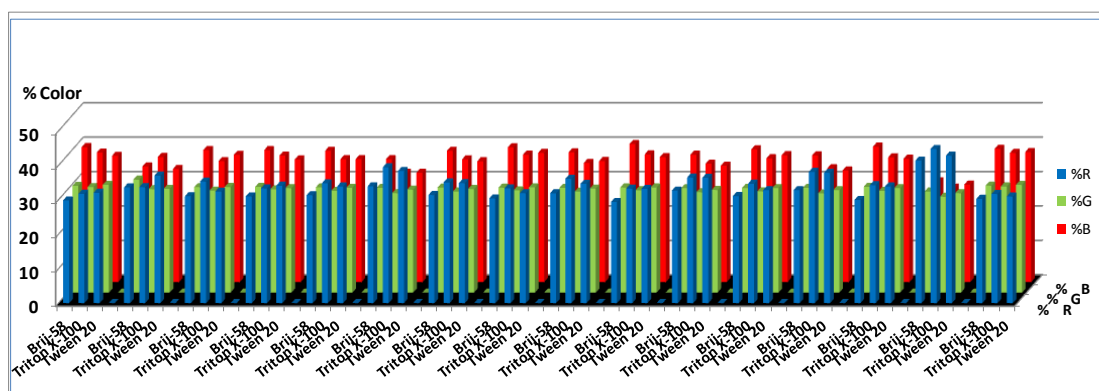


Figure B2 RGB histogram of colorimetric responses of PCDA incorporated with Brij[®] 58 P, Triton[®] X-100 and Tween[®] 20 in the presence of water (control) and 14 organic solvents.

APPENDIX C
DIP COATING

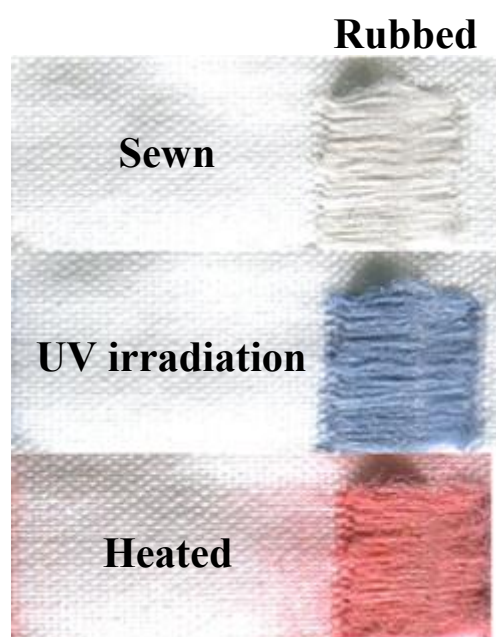


Figure C1 Photo image of rubbing on polyester thread sewn to white polyester fabric pieces.

APPENDIX D

PAPER-BASED POLYDIACETYLENE HUMIDITY INDICATORS

Table D1 RGB values of TCDA indicators without base after exposure at 63% RH for 24 hours (5 independent experiments)

Time (Hr)	1				2				3				4				5			
	R	G	B	Sum	R	G	B	Sum	R	G	B	Sum	R	G	B	Sum	R	G	B	Sum
0	60	57	99	216	61	59	101	221	64	61	100	225	60	59	99	218	59	59	98	216
3	63	58	96	217	62	59	98	219	66	62	97	225	64	61	95	220	61	60	94	215
6	66	58	99	223	66	61	102	229	70	65	101	236	67	62	100	229	63	60	99	222
9	65	58	102	225	65	58	102	225	68	60	102	230	66	59	99	224	64	57	100	221
12	64	55	96	215	65	55	96	216	68	59	95	222	66	56	94	216	63	56	93	212
15	64	56	95	215	66	55	97	218	69	58	97	224	67	57	95	219	63	56	96	215
18	66	56	94	216	65	56	93	214	68	60	95	223	67	57	93	217	64	56	95	215
21	66	54	96	216	66	54	95	215	70	57	97	224	67	56	93	216	65	55	92	212
24	67	61	100	228	67	60	100	227	72	63	100	235	70	61	98	229	67	59	97	223

Table D2 RGB values of TCDA humidity indicators prepared with K_2CO_3 alone at different incubation time under 63% RH for 24 hours (5 independent experiments)

Time (Hr)	1				2				3				4				5			
	R	G	B	Sum	R	G	B	Sum	R	G	B	Sum	R	G	B	Sum	R	G	B	Sum
0	120	122	152	394	109	111	147	367	109	113	147	369	108	114	148	370	111	118	146	375
1	112	112	134	358	105	102	135	342	100	101	126	327	95	103	126	324	106	110	128	344
2	111	111	132	354	100	101	127	328	98	99	125	322	102	101	122	325	105	109	127	341
3	124	114	138	376	113	103	131	347	112	103	128	343	112	105	129	346	119	112	129	360
4	134	117	136	387	125	106	129	360	123	106	126	355	121	107	127	355	130	116	128	374
5	134	112	129	375	126	102	121	349	122	102	119	343	122	103	120	345	129	111	122	362
6	133	113	120	366	126	103	113	342	123	103	111	337	122	104	112	338	129	112	114	355
7	141	113	124	378	133	104	117	354	131	103	113	347	131	104	115	350	134	112	117	363
8	138	114	118	370	133	105	108	346	129	104	108	341	129	105	110	344	133	112	112	357
9	141	115	115	371	135	105	109	349	129	104	107	340	130	105	107	342	133	112	110	355
10	142	117	119	378	137	106	110	353	131	105	109	345	131	107	110	348	134	113	112	359
11	145	114	122	381	139	103	111	353	132	103	111	346	135	104	111	350	136	111	114	361
12	141	115	115	371	135	104	107	346	128	103	106	337	130	105	107	342	132	111	110	353

Table D3 RGB values of TCDA humidity indicators prepared with 4:1 mole ratio of $K_2CO_3/NaOH$ mixed solution at different incubation time under 63% RH for 24 hours (5 independent experiments)

Time (Hr)	1				2				3				4				5			
	R	G	B	Sum	R	G	B	Sum	R	G	B	Sum	R	G	B	Sum	R	G	B	Sum
0	100	105	135	340	102	105	136	343	105	108	142	355	109	109	143	361	110	114	143	367
1	102	110	132	344	106	111	130	347	105	109	133	347	99	102	128	329	102	105	129	336
2	101	106	125	332	102	104	123	329	107	110	131	348	98	101	125	324	102	103	126	331
3	119	109	127	355	120	107	125	352	119	109	134	362	112	104	131	347	119	107	133	359
4	133	110	119	362	132	110	122	364	130	113	131	374	127	107	126	360	131	111	130	372
5	131	100	112	343	130	100	110	340	128	102	116	346	125	100	119	344	132	106	122	360
6	132	102	111	345	130	101	101	332	126	103	106	335	126	102	111	339	132	107	114	353
7	138	102	101	341	137	102	105	344	135	103	113	351	134	102	113	349	140	107	114	361
8	137	103	96	336	134	104	100	338	134	104	107	345	132	103	107	342	139	109	112	360
9	137	104	96	337	136	104	100	340	135	105	105	345	135	103	106	344	141	109	110	360
10	137	104	96	337	136	104	101	341	138	106	106	350	137	104	106	347	144	110	111	365
11	139	101	98	338	140	101	102	343	140	104	107	351	140	103	109	352	146	108	113	367
12	137	104	96	337	135	103	98	336	137	105	105	347	137	104	105	346	142	110	110	362

Table D4 RGB values of TCDA humidity indicators prepared with 3:2 mole ratio of $K_2CO_3/NaOH$ mixed solution at different incubation time under 63% RH for 24 hours (5 independent experiments)

Time (Hr)	1				2				3				4				5			
	R	G	B	Sum	R	G	B	Sum	R	G	B	Sum	R	G	B	Sum	R	G	B	Sum
0	107	112	139	358	109	117	143	369	105	120	147	372	108	120	148	376	107	124	148	379
1	105	117	138	360	108	115	141	364	108	115	145	368	110	115	146	371	109	120	147	376
2	108	111	139	358	107	119	143	369	112	118	146	376	115	118	148	381	115	121	148	384
3	92	97	123	312	99	102	126	327	98	100	126	324	98	100	127	325	103	103	129	335
4	98	98	122	318	100	102	126	328	98	101	127	326	99	102	127	328	105	102	129	336
5	102	101	120	323	104	103	123	330	101	100	124	325	101	102	126	329	106	103	129	338
6	106	98	116	320	107	101	118	326	104	98	122	324	104	99	121	324	106	101	122	329
7	108	100	115	323	111	104	120	335	107	100	119	326	109	102	122	333	110	103	126	339
8	114	101	112	327	116	104	118	338	114	101	118	333	113	103	120	336	112	102	122	336
9	119	102	109	330	118	104	116	338	116	102	116	334	116	102	115	333	113	103	122	338
10	123	102	108	333	121	104	114	339	120	102	114	336	121	102	114	337	116	103	119	338
11	129	103	107	339	122	104	112	338	124	104	112	340	129	103	111	343	120	104	119	343
12	137	105	108	350	131	106	117	354	130	103	114	347	131	103	114	348	125	103	120	348

Table D5 RGB values of TCDA humidity indicators prepared with 2:3 mole ratio of $K_2CO_3/NaOH$ mixed solution at different incubation time under 63% RH for 24 hours (5 independent experiments)

Time (Hr)	1				2				3				4				5			
	R	G	B	Sum	R	G	B	Sum	R	G	B	Sum	R	G	B	Sum	R	G	B	Sum
0	116	122	146	384	112	119	143	374	113	122	143	378	107	119	140	366	103	118	139	360
1	108	112	137	357	109	109	134	352	109	112	136	357	104	111	134	349	103	110	135	348
2	115	120	144	379	114	118	144	376	115	120	143	378	110	118	143	371	108	118	142	368
3	102	103	127	332	97	100	125	322	98	102	124	324	97	105	125	327	96	107	127	330
4	103	104	129	336	99	101	127	327	100	103	126	329	99	106	127	332	97	108	129	334
5	103	104	128	335	99	102	126	327	99	104	125	328	100	106	129	335	102	109	129	340
6	104	101	123	328	99	98	122	319	99	101	120	320	102	105	123	330	104	107	122	333
7	110	103	121	334	105	101	122	328	106	105	121	332	110	109	121	340	113	111	120	344
8	114	105	120	339	111	103	119	333	113	106	118	337	115	111	120	346	121	114	119	354
9	118	104	114	336	115	105	116	336	117	106	115	338	121	109	114	344	124	113	115	352
10	123	105	115	343	119	103	114	336	123	105	111	339	126	111	111	348	129	114	114	357
11	127	107	113	347	124	105	113	342	127	107	111	345	121	113	110	344	132	116	111	359
12	135	107	114	356	132	105	113	350	136	107	111	354	137	113	112	362	141	116	114	371

Table D6 RGB values of TCDA humidity indicators prepared with 2 cm of K_2CO_3 (50 %w/w) solution at different incubation time under 63% RH for 12 hours (5 independent experiments)

Time (Hr)	1				2				3				4				5			
	R	G	B	Sum	R	G	B	Sum	R	G	B	Sum	R	G	B	Sum	R	G	B	Sum
0	118	120	158	396	131	141	157	429	130	143	159	432	120	137	161	418	126	144	160	430
1	113	117	153	383	126	132	156	414	130	137	159	426	124	138	160	422	133	146	164	443
2	119	116	150	385	127	130	154	411	131	136	159	426	126	137	160	423	134	145	163	442
3	124	114	142	380	133	128	146	407	130	132	154	416	130	134	154	418	141	144	156	441
4	129	115	131	375	134	128	140	402	129	132	145	406	133	133	146	412	141	145	147	433
5	142	119	133	394	143	128	138	409	136	131	147	414	141	133	144	418	151	145	147	443
6	141	117	121	379	142	128	128	398	134	132	138	404	141	133	135	409	150	144	139	433
7	147	118	124	389	150	128	132	410	140	131	140	411	149	133	136	418	157	144	143	444
8	147	118	121	386	150	128	126	404	140	131	133	404	148	134	131	413	156	144	138	438
9	146	116	122	384	141	127	126	394	140	131	135	406	148	133	132	413	154	143	138	435
10	146	117	123	386	148	128	127	403	143	131	135	409	151	134	132	417	156	144	139	439
11	146	118	122	386	148	128	128	404	144	131	136	411	150	133	132	415	155	143	137	435
12	147	117	122	386	150	129	128	407	145	132	133	410	151	135	131	417	157	144	139	440

Table D7 RGB values of TCDA humidity indicators prepared with 4 cm of K_2CO_3 (50 %w/w) solution at different incubation time under 63% RH for 12 hours (5 independent experiments)

Time (Hr)	1				2				3				4				5			
	R	G	B	Sum	R	G	B	Sum	R	G	B	Sum	R	G	B	Sum	R	G	B	Sum
0	101	111	147	359	118	128	152	398	112	123	150	385	108	114	149	371	113	118	153	384
1	95	100	136	331	112	115	146	373	110	112	146	368	104	103	141	348	111	111	150	372
2	99	100	135	334	119	116	146	381	112	111	146	369	107	104	142	353	112	110	149	371
3	113	101	127	341	128	117	137	382	123	113	140	376	117	103	133	353	113	108	143	364
4	133	117	123	373	133	117	123	373	130	114	126	370	125	106	122	353	121	110	132	363
5	140	107	111	358	147	121	128	396	149	117	126	392	141	108	122	371	138	113	131	382
6	137	106	106	349	143	121	121	385	144	117	125	386	141	110	113	364	142	115	120	377
7	142	106	107	355	147	122	123	392	150	118	125	393	147	108	114	369	148	115	125	388
8	139	107	106	352	149	121	122	392	148	118	122	388	145	111	112	368	146	114	124	384
9	137	106	108	351	144	120	122	386	146	119	122	387	143	108	114	365	149	114	124	387
10	141	107	110	358	149	122	123	394	147	119	122	388	146	110	116	372	147	115	123	385
11	140	108	111	359	144	122	124	390	147	118	121	386	149	109	117	375	146	114	125	385
12	140	108	111	359	146	121	125	392	148	119	123	390	146	110	116	372	146	116	125	387

Table D8 RGB values of TCDA humidity indicators prepared with 4 cm of $K_2CO_3/NaOH$ (4:1 mole ratio) at different incubation time under 63% RH for 12 hours (5 independent experiments)

Time (Hr)	1				2				3				4				5			
	R	G	B	Sum	R	G	B	Sum	R	G	B	Sum	R	G	B	Sum	R	G	B	Sum
0	75	71	115	261	80	72	117	269	80	71	116	267	77	74	116	267	71	72	109	252
1	102	76	102	280	101	75	101	277	95	77	103	275	87	69	97	253	89	74	96	259
2	125	80	88	293	126	82	88	296	123	85	90	298	116	76	85	277	112	83	85	280
3	144	83	75	302	142	85	78	305	142	87	76	305	129	78	72	279	132	85	71	288
4	146	90	76	312	140	86	78	304	141	88	76	305	127	79	72	278	131	91	71	293
5	148	91	83	322	140	84	79	303	140	85	77	302	128	73	74	275	130	83	74	287
6	156	99	83	338	145	91	83	319	143	93	82	318	132	81	74	287	138	90	79	307
7	156	98	85	339	148	92	84	324	145	94	85	324	132	80	75	287	135	91	80	306
8	159	101	85	345	149	95	85	329	147	96	85	328	137	83	75	295	135	94	80	309
9	157	96	84	337	145	90	85	320	146	91	84	321	132	77	75	284	136	88	78	302
10	151	92	83	326	143	85	81	309	139	89	79	307	128	73	75	276	131	83	76	290
11	155	92	83	330	144	84	83	311	143	88	81	312	130	73	74	277	136	83	75	294
12	152	94	82	328	144	86	83	313	141	89	80	310	129	75	75	279	133	86	76	295

Table D9 RGB values of TCDA humidity indicators prepared with 4 cm of $K_2CO_3/NaOH$ (4:1 mole ratio) at different incubation time under 36% RH for 24 hours (5 independent experiments)

Time (Hr)	1				2				3				4				5			
	R	G	B	Sum	R	G	B	Sum	R	G	B	Sum	R	G	B	Sum	R	G	B	Sum
0	104	103	139	346	103	102	145	350	102	103	140	345	102	107	146	355	104	111	143	358
3	121	104	128	353	116	99	131	346	114	101	130	345	110	102	135	347	112	107	129	348
6	130	105	122	357	123	100	124	347	120	102	125	347	118	105	130	353	123	110	127	360
9	139	109	119	367	130	103	124	357	126	106	125	357	123	108	129	360	129	113	127	369
12	141	110	117	368	136	104	121	361	130	105	122	357	127	107	128	362	132	112	122	366
15	142	109	114	365	135	102	116	353	131	104	119	354	129	105	125	359	133	111	120	364
18	145	115	117	377	139	107	118	364	135	106	120	361	134	108	124	366	132	111	118	361
21	149	119	116	384	148	112	119	379	139	110	119	368	139	112	123	374	139	116	119	374
24	151	113	116	380	142	106	117	365	141	107	118	366	141	106	119	366	143	112	116	371

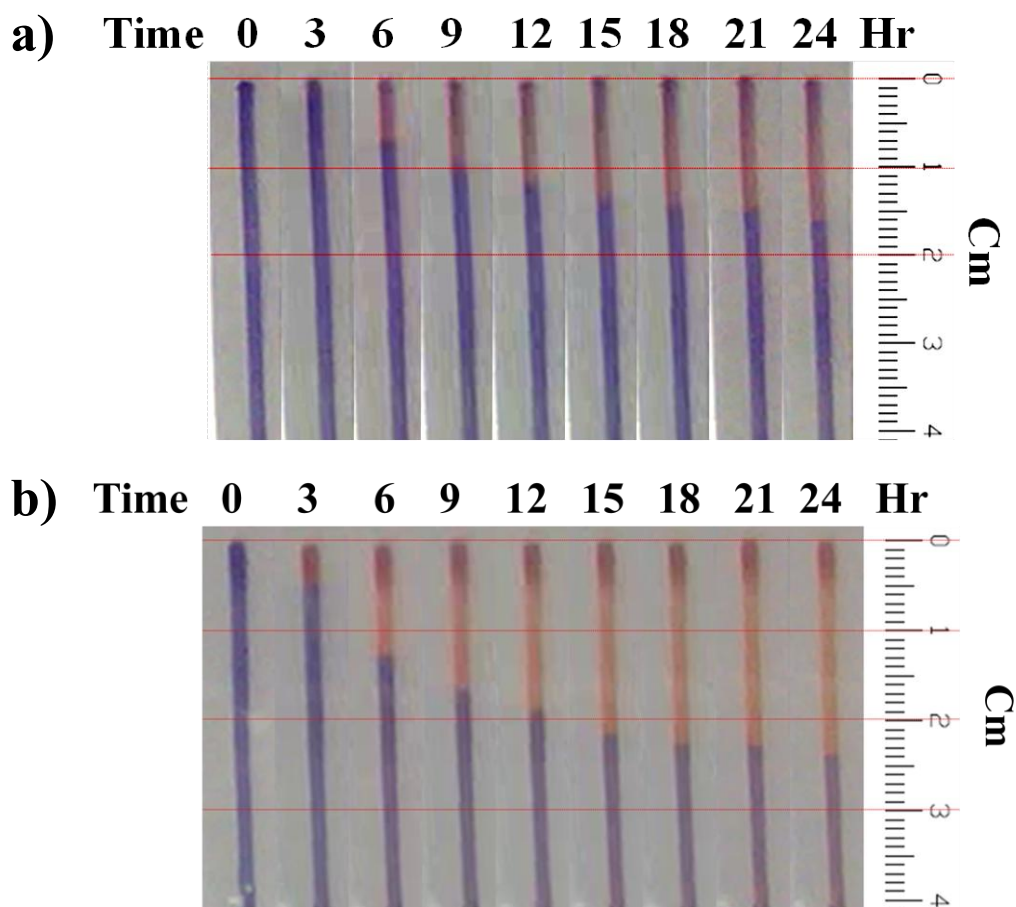


Figure D10 the photo image of TCDA humidity indicators prepared with K_2CO_3 alone deposit on **a)** filter paper Whatman No.1 and **b)** filter paper whatman No.3 of (5 independent experiments) at different incubation time under 63% RH for 24 hours.

The thickness of filter paper involve for surface area for contact with moisture, stable shape and affect to high hygroscopic of paper as show as **Figure D10**.

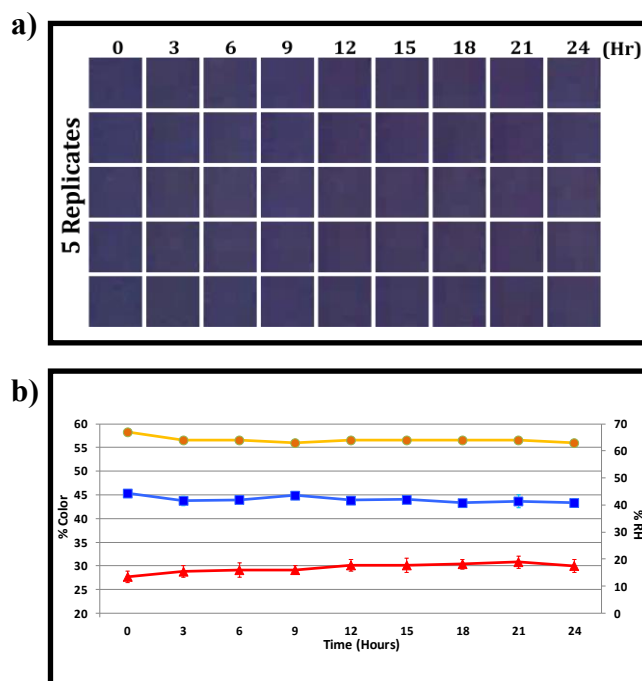


Figure D11 a) Color image of TCDA zone of the humidity indicators prepared without b) their corresponding plots of %R (▲) and %B (■). The indicators were incubated under controlled %RH of $63 \pm 3\%$ (●) for 24 hours.

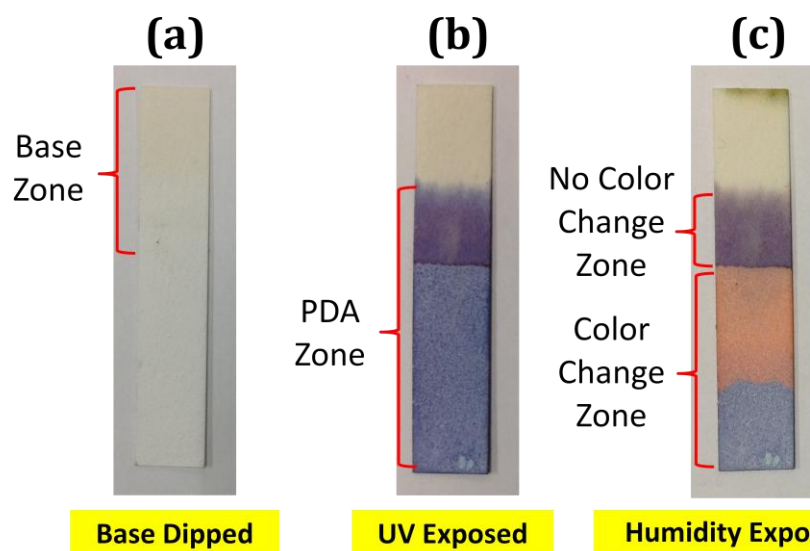


Figure D12 Image of indicators fabricated by dip coating of TCDA and $K_2CO_3:NaOH$ mole ratio (4:1) **a)** before **b)** after exposed to UV lamp for 1 minute and **c)** after exposed to ambient humidity.

APPENDIX E
MELT-SPINNING OF POLYPROPYLENE/PCDA

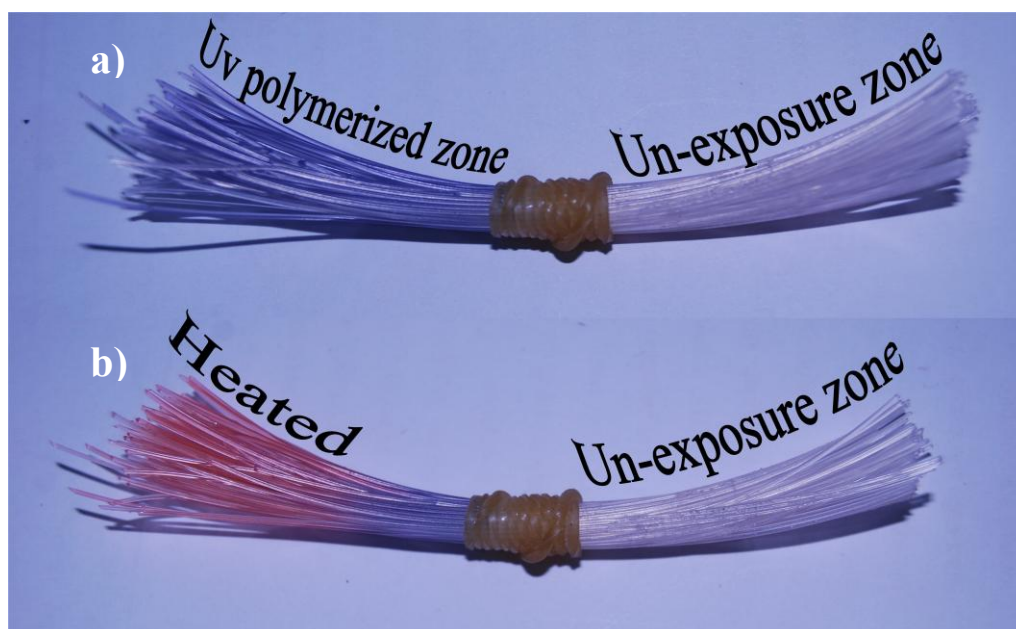


Figure E1. Photo image of multi-filament of PP + 0.5 % PCDA **a)** after UV irradiated **b)** after heated.

APPENDIX F

AWARD



Figure F1 Winning the 2nd award from 5th Sci & Tech initiative and Sustainability Award by The Thai Institute of Chemical Engineering and Applied Chemistry, SCG Chemicals and Dow Chemical (From left to right : Mr. Jettapong Klaharn, Mr. Natdanai Suta, Mr. Pracharat Sa-ngadsup and Mr. Watcharin Ngampeungpis) (“System for real time monitoring of environmental parameters via optical responses”)

VITAE

Mr. Jadetapong Klahan was born on August 8th, 1985 in Nakhonratchasima, Thailand. He received a Diploma's Degree majoring in Petrochemical form Faculty of Industrial Technology, Rayong Technical College in 2006. He graduated with Bachelor's Degree of Engineering, majoring in polymer engineering from Faculty of Engineering, Rajamangala University of Technology Thanyaburi in 2009. He has been graduate student in polymer science under supervision of Assoc. Prof. Dr. Mongkol Sukwattanasinitt and Assist. Prof. Dr. Boonchoat Paosawatyanong. He had presented his research in Pure and Applied Chemistry International Conference (PACCON 2013). He was graduated with a master degree in Program of Petrochemistry and Polymer Science, Faculty of Science, Chulalongkorn University in 2013. His current address is 1680 Mittraparp 15th Road, Muang, Nakhonratchasima, 30000.